INVESTIGATIONS OF P WAVE ARRIVALS AT LASA

MICHAEL A. CHINNERY

UNCLASSIFIED
Security Classification

DOCUMENT CONTROL DATA - R & D

(Security classification of title, body of abstract and indexing annotation must be entered when the overall report is classified)

1. ORIGINATING ACTIVITY (Corporate author)

Brown University
Department of Geological Sciences
Providence, RI 02912

2a. REPORT SECURITY CLASSIFICATION

UNCLASSIFIED

2b. GROUP

3. REPORT TITLE

INVESTIGATIONS OF P-WAVE ARRIVALS AT LASA

4. DESCRIPTIVE NOTES (Type of report and inclusive dates)

Scientific.....Final

5. AUTHOR(S) (First name, middle initial, last name)

Michael A. Chinnery

6. REPORT DATE	7a. TOTAL NO. OF PAGES	7b. NO. OF REFS
31 August 1971	85	18

8a. CONTRACT OR GRANT NO	9a. ORIGINATOR'S REPORT NUMBER(S)
F44620-68-C-0082	
b. PROJECT NO. 8652	
c. 62701D	9b. OTHER REPORT NO(S) (Any other numbers that may be assigned this report)
d.	

10. DISTRIBUTION STATEMENT

Approved for public release;
distribution unlimited.

11. SUPPLEMENTARY NOTES	12. SPONSORING MILITARY ACTIVITY
TECH, OTHER	AF Office of Scientific Research (NPG) 1400 Wilson Boulevard Arlington, VA 22209

13. ABSTRACT

The arrivals of P-waves at the Large Aperture Seismic Array (LASA) from over 3000 earthquakes at various azimuths and distances have been studied. From each set of arrival times a variety of parameters related to the travel time curve are determined. This report consists primarily of a summary of the principal features of these parameters, as functions of epicentral distance and azimuth.

DD FORM 1 NOV 68 1473

UNCLASSIFIED
Security Classification

14. KEY WORDS	LINK A		LINK B		LINK C	
	ROLE	WT	ROLE	WT	ROLE	WT
Seismic Arrays						
LASA						
Apparent velocities						
Travel time anomalies						

INVESTIGATIONS OF P-WAVE ARRIVALS AT LASA

Final Technical Report

Task A

Project: Seismology and Acoustic Gravity Waves

Period Ending: 31 July 1971

Contract No: F44620-68-C-0082

Amendment/Modification No: P002

ARPA Order No: 292-68, Amendment No. 49

Program Code No: 8F10

Contractor: Brown University

Date of Contract: 1 August 1968

Amount of Contract: $123,108

Project Scientist: Michael A. Chinnery
401/863-3338

ABSTRACT

The arrivals of P-waves at the Large Aperture Seismic Array (LASA) from over 3000 earthquakes at various azimuths and distances have been studied. From each set of arrival times a variety of parameters related to the travel time curve are determined. This report consists primarily of a summary of the principal features of these parameters, as functions of epicentral distance and azimuth.

TABLE OF CONTENTS

INTRODUCTION

Investigations of the arrival times of P-waves at the Large Aperture Seismic Array (LASA) at Billings, Montana, have been carried out by the principal investigator during the period October, 1965 to July, 1971, under several ARPA contracts. These studies were unusual in that a very large quantity of high-quality data were obtained. Portions of these data, together with interpretations, have been published (see References), but inevitably much remains that cannot be interpreted at present. The purpose of this report is to catalogue as many as possible of the observations that have been made.

Since many similar studies using various arrays have appeared, and continue to appear, in the literature, it is worthwhile to emphasize the uniqueness of the present set of data. The quality of the data is primarily due to the physical size (about 200 km aperture) of the LASA array, and to the availability of recordings that permit the relative timing of arrivals to .05 seconds or better. This immediately suggests that it should be possible to determine $dT/d\Delta$ from these arrivals with a precision of better than 0.1 seconds/degree, and the observed scatter in the determinations agrees with this conclusion. In fact, the observed scatter is between 3 and 10 times smaller than those of most other published studies.

The high quantity of data is partly due to the sensitivity of the array, and partly due to its location. The array lies in such a position that most of the circum-Pacific belt of seismic activity lies within two rather small azimuth ranges

from the array (see Section 2). The array is therefore particularly suited to observations of the variation of travel-time parameters with epicentral distance. It is unfortunate that the azimuthal distribution of events is much less complete. One important result of the large number of earthquakes studied is that it has become possible to apply strong criteria in the selection of data. The data shown in this report represent only about 70% of those obtained; the rest were eliminated as being somewhat less reliable for a variety of reasons.

One unexpected problem that results from the high quality of the present data is that considerable fine structure becomes apparent. This is shown not only by the distance variation of $dT/d\Delta$, but also in the differences between observations along different azimuths. Unfortunately it is not possible to provide a convincing explanation for most of these features. On the other hand, smoothing (or averaging) of the data does not seem justified in view of the small amount of scatter. This leads to certain ambiguities in the interpretation of the data.

This report concentrates, therefore, on an exposition of the data, and the methods by which they were obtained. Very few comments on the possible meanings of the results are included.

I. ANALYSIS OF THE DATA

The data used in this study consists of the first arrivals of P-waves at the Large Aperture Seismic Array (LASA) in Billings, Montana. These arrivals were determined visually from the 16 mm film records of the short period instruments at the array. In particular, the arrivals were recorded for the center seismometer in each of the sub-arrays in the E and F rings, and the center sub-array AO. The locations of these sub-arrays are shown in Figure 1, and their coordinates with respect to a N-S E-W coordinate system centered on the sub-array AO are shown in Table 1.

The recording of a typical earthquake (one of magnitude 4.4 in the Aleutian Islands) is shown in Figure 2a. The lack of coherence of the waveforms beyond the first half-cycle is clearly indicated. For this reason, timing methods that involved correlation of the waveform across the array were tested and eliminated early in the study. Ideally, the "knee" of the onset should be timed, but this was found to be difficult for all but the largest events. As a compromise, all arrival measurements were made on the first peak (or trough) of the arrival. For all the events included in this report, it was possible to time this point with a precision of 0.05 seconds or better. The relative times of arrival with respect to AO were therefore subject to a maximum error of ±0.05 seconds, and in most cases the estimated error is about one half of this.

Many events were not recorded at all nine seismometers, due to equipment failure, excessive noise level, and so on. It was

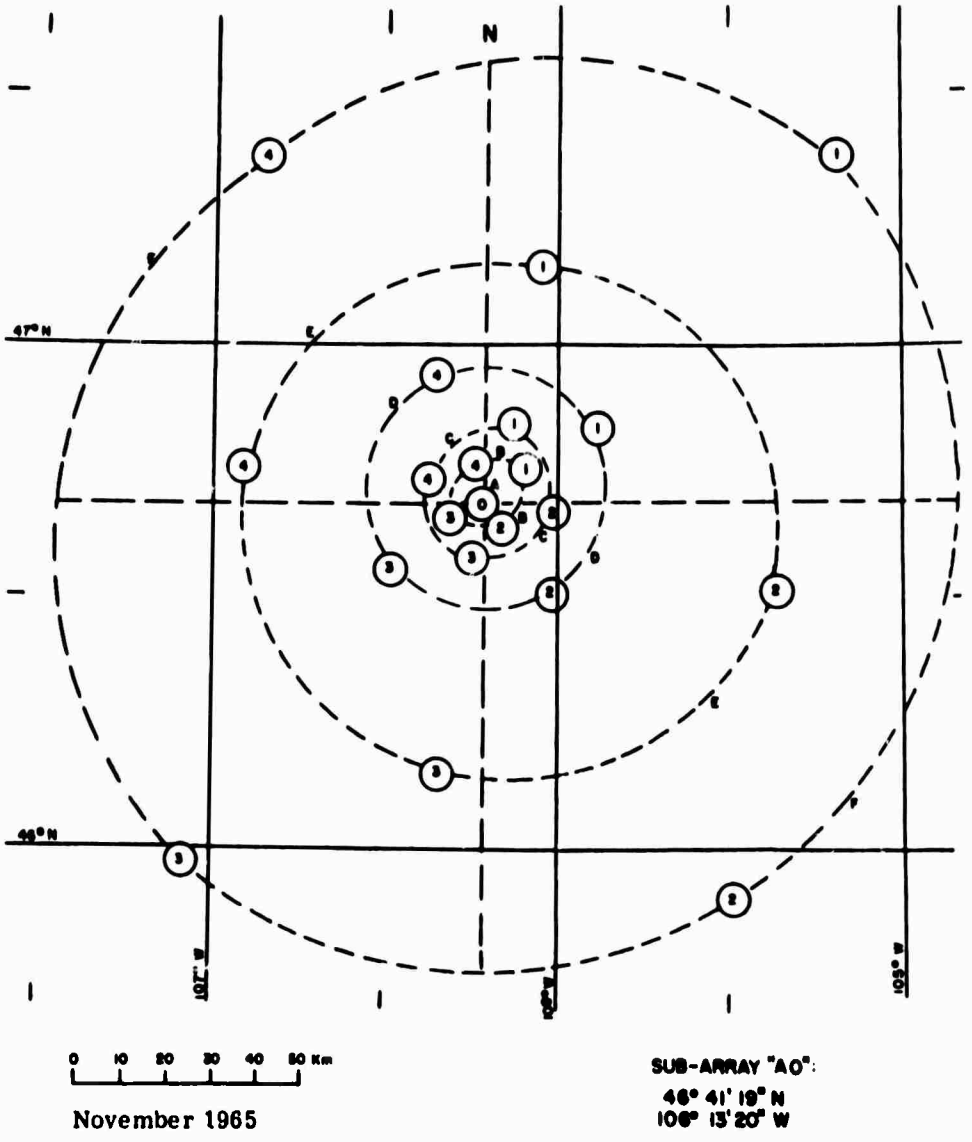

Fig. 1: Location and Geometry of the Large Aperture Seismic Array (LASA), near Billings, Montana.

Table 1: Station Coordinates, in km. The x axis points due East, and the y axis points due North.

Subarray	x	y
A0	0	0
B1	12.596	52.727
B2	65.810	-19.109
B3	-8.649	-59.927
B4	-53.054	8.262
F1	78.157	76.360
F2	57.159	-86.343
F3	-66.609	-79.209
F4	-54.449	80.574

found in the course of the study that the $dT/d\Delta$ values for these events showed a significantly larger scatter than for those recorded at all the sites. For this reason, incompletely recorded events have not been included in this study.

The basic data for each event therefore consists of a set of eight times, relative to AO. These times were processed on the IBM 360 computer at Brown University to extract a variety of information. One page of printed output was obtained for each event, and a typical output is shown in Figure 2b, for the event shown in Figure 2a. The various items on this output are described briefly below:

a) Using the USCGS epicenter, the azimuth and distance of the event were calculated, using a sub-program that includes the effect of ellipticity.

b) The distance was corrected for the effect of focal depth, by extrapolating the ray path back to the earth's surface. This correction is small for events at teleseismic distances with focal depths less than about 200 km. It can be estimated accurately enough for the present purposes on the basis of a standard crust and upper mantle structure. The Jeffreys-Bullen structure was used, and the corrections for various focal depths and distances are given in Figure 3. Earthquakes deeper than 200 km were not used in this study.

c) The $dT/d\Delta$ corresponding to any given model is determined for the corrected distance, and listed as "calculated slope." In this case, the model A (Chinnery, 1969) was used as a standard.

WWNT 16N1: Region: Andreanof Islands, Aleutian Islands

Location: Lat 51.3N Long 176.5W

Origin Time: 00 25 51 Focal Depth: 58 km

Magnitude: 4.4

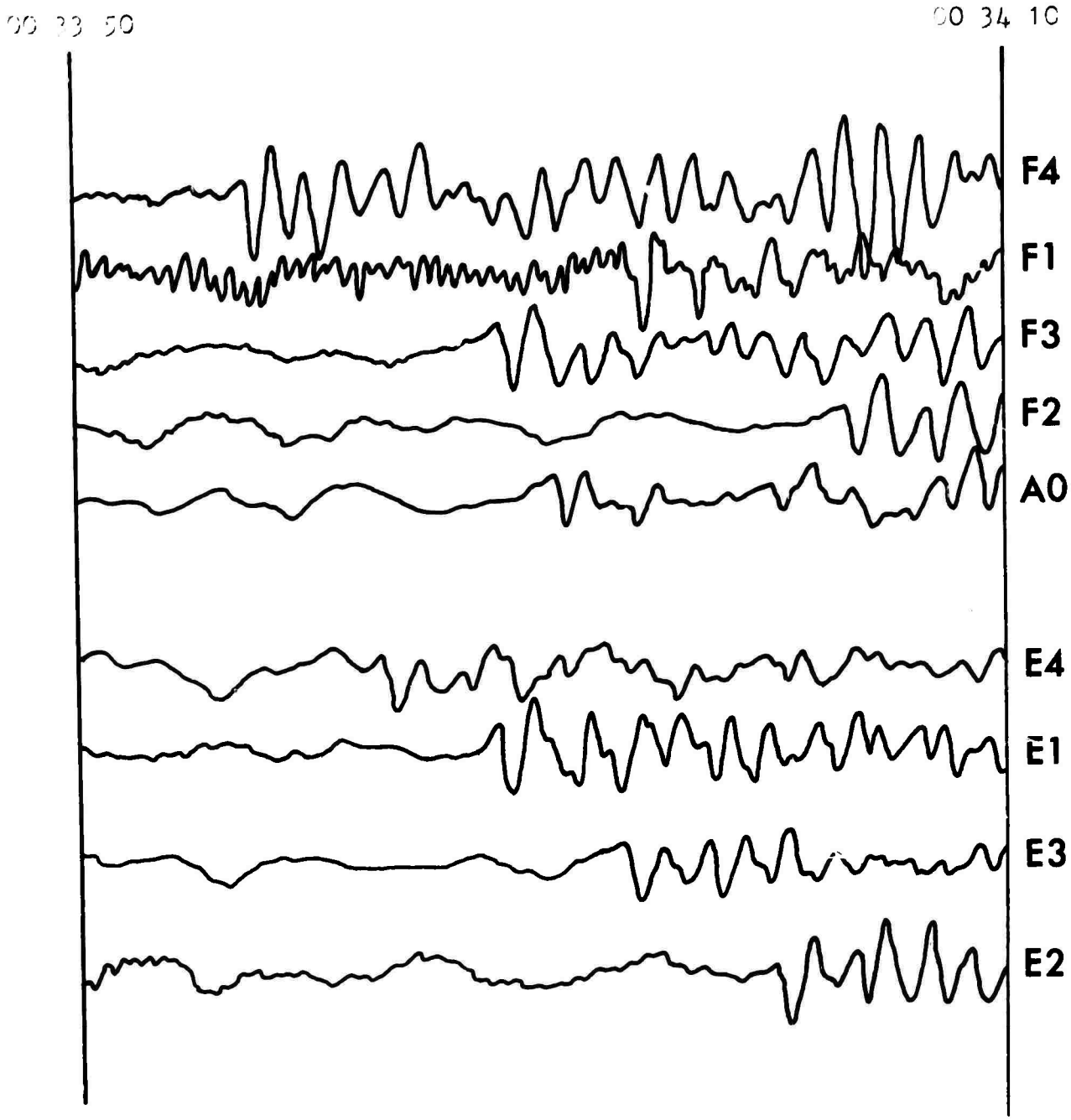

Fig. 2a

EVENT 18N1

Latitude= 51.30 Longitude= -176.50
Azimuth= 302.89 Distance= 44.73 Depth= 50 Corrected Distance= 45.1

Model A calculated slope= 7.861 secs/deg

Plane Wave Fit
Observed azimuth= 301.12 degrees
True - observed azimuth= 1.77 degrees
Travel time 1st derivative= 7.93 secs/deg
Standard deviation= 0.168 secs

First Degree Polynomial Fit
Travel-time 1st derivative= 7.92 secs/deg
Standard deviation= 0.176 secs

Second Degree Polynomial Fit
Travel-time 1st derivative= 7.94 secs/deg
Travel-time 2nd derivative= -0.68 secs/deg/deg
Calculated - observed slope= -0.08 secs/deg
Standard deviation= 0.152 secs

Fig. 2b

Third Degree Fit with P Fixed
Travel time 1st derivative= 7.94 secs/deg
Travel-time 2nd derivative= -0.66 secs/deg/deg
Travel-time 3rd derivative= -0.410 secs/deg/deg/deg
Standard deviation= 0.151 secs

Third Degree Polynomial Fit
Travel-time 1st derivative= 8.19 secs/deg
Travel-time 2nd derivative= -0.63 secs/deg/deg
Travel-time 3rd derivative= -2.744 secs/deg/deg/deg
Standard deviation= 0.143 secs

Station	Obs Time	Delay	Delta	Residuals Plane	1st	2nd	3rdF	3rd	Calc Time	Station Corr
AC	10.60	0.0	0.0	0.0	0.12	0.04	0.04	0.04	0.00	0.00
E1	9.36	-1.24	-0.16	0.07	-0.17	-0.10	-0.10	-0.14	-1.28	-0.04
E2	15.27	4.67	0.59	0.06	-0.12	-0.14	-0.15	-0.08	4.63	-0.04
E3	12.11	1.51	0.23	0.17	0.17	0.24	0.24	0.29	1.79	0.28
E4	6.92	-3.68	-0.44	0.14	0.06	0.07	0.08	0.01	-3.47	0.21
F1	12.53	1.93	0.22	0.03	-0.33	-0.26	-0.26	-0.21	1.71	-0.22
F2	17.00	6.40	0.85	0.27	0.23	0.09	0.05	0.03	6.68	0.28
F3	9.50	-1.10	-0.12	-0.05	0.06	0.14	0.13	0.10	-0.91	0.19
F4	4.00	-6.60	-0.70	0.01	0.11	-0.05	-0.01	0.00	-6.05	0.05

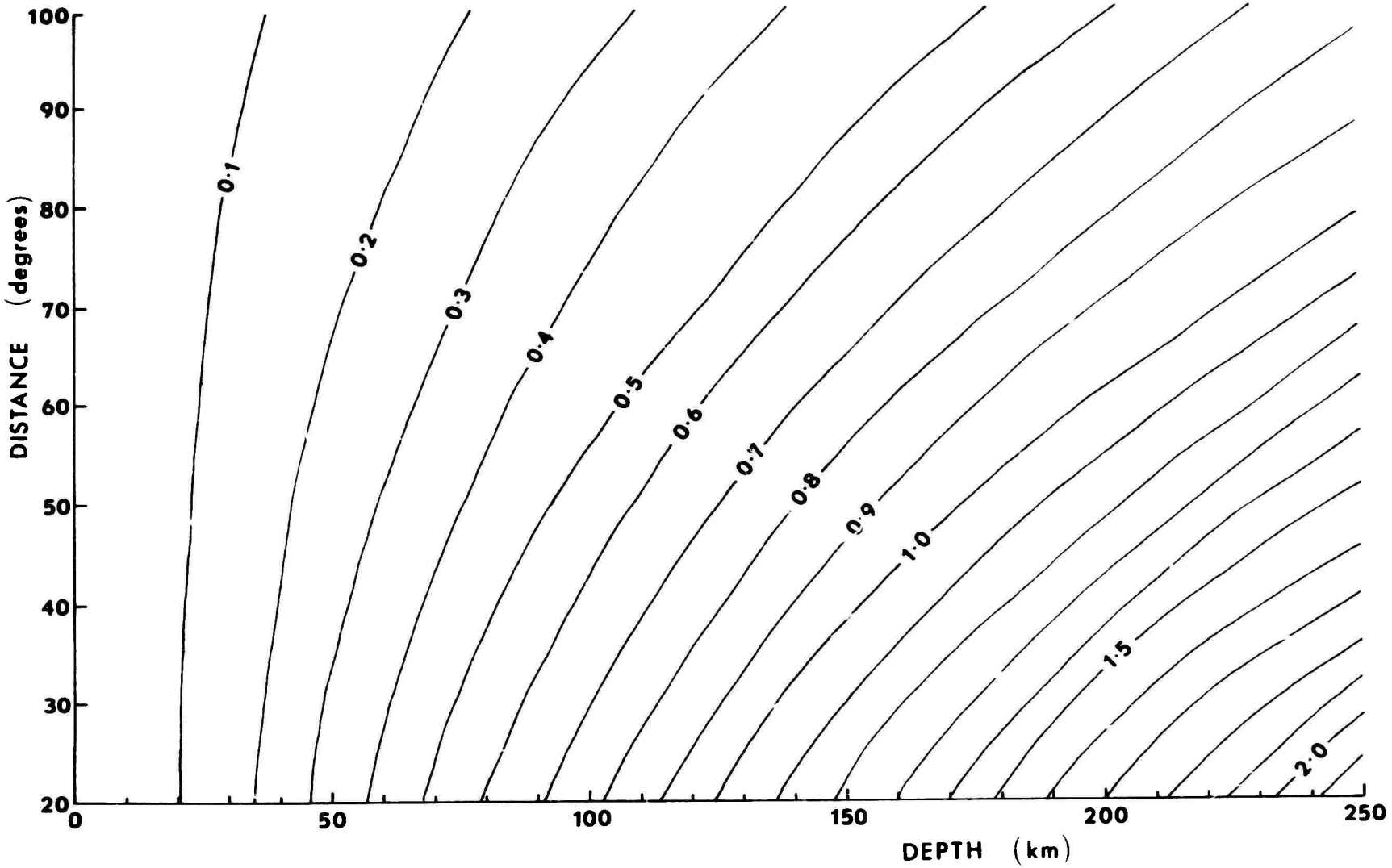

Fig. 3: Distance corrections for a standard Jeffreys-Bullen structure, as functions of epicentral distance and focal depth.

This facilitates the comparison of this particular event with other results.

d) A plane wave is first fitted to the wavefront. If the arrival time (relative to AO) is T_i at a site with coordinates x_i, y_i (again, relative to AO), the data are fitted to an equation of the form:

$$T_i + a x_i + b y_i = 0 \qquad (1)$$

The coefficients a and b were determined by a least squares process, and from them the apparent azimuth and a first estimate of $dT/d\Delta$ could be obtained. These results are listed under the heading "plane wave fit." The agreement between the apparent and true azimuths was in general very good. This point is discussed further later in this report.

e) Because of the comparatively large aperture of the array, about 200 km, it was necessary to include the possibility of curvature of the wavefront in the vertical plane containing the azimuth to the source. A simple and effective way of doing this is to project the positions of the sub-arrays onto this plane, and replace the coordinates x_i, y_i by a single variable δ_i, the distance of the ith sub-array from AO along the azimuth towards the event. In this calculation, the "true" azimuth was used. Now T_i may be regarded as a function of δ_i alone, and first, second and third order relations may be written as:

$$T_i - T_0 + a\delta_i = 0 \qquad (2)$$

$$T_i - T_o + b\delta_i + c\delta_i^2 = 0 \qquad (3)$$

$$T_i - T_o + d\delta_i + e\delta_i^2 + f\delta_i^3 = 0 \qquad (4)$$

where a-f are constant coefficients, and T_o is included so that the equations are not constrained to pass through AO.

Equations 2, 3 and 4 were fitted to the observed times by least squares, and it is clear that the first, second and third derivatives of the travel time curve may be determined from the coefficients a-f. The results are listed under first, second and third degree polynomial fit, on the output sheet. In addition, an equation of the form of 4, but with d constrained to be equal to b, was used. The latter fit was found to give the least scatter in estimates of the second derivative.

f) At the foot of the page, the observed times, the δ_i, and the residuals from the various fits are listed. In addition, the times predicted by the model and the apparent station correction are included.

g) Also printed out are the differences between the true and observed azimuths, and between the observed and calculated $dT/d\Delta$, together with the standard deviation of the various polynomial fits.

II. DISTRIBUTION OF EVENTS

Over three thousand events have been processed in the above manner. This covers the operation of the array from its inception, in October, 1965, through the end of 1968. These events are distributed at a variety of azimuths and distances from the array, as shown in Figure 4. It should be noted that only those earthquakes that gave an amplitude of greater than 5 millimicrons at the array have been included. This means that there is a considerable variation in magnitude of the events considered, and accounts for the scarcity of data at distances greater than about 100°.

It is clear from Figure 4 that most of the events recorded lie within two azimuth ranges. A large number of events were recorded from the northwest of the array (azimuth range 290 to 330), and a slightly smaller number were recorded from the south (azimuth range 140° to 170°). In these two ranges of azimuth it has been possible to study the variation of $dT/d\Delta$ with distance, in some detail. Information is available at some other azimuths, but the coverage is much less complete.

It should be noted, too, that the earthquakes are not well distributed in azimuth. One of the interesting results of this study is that there are significant azimuthal variations in the observed quantities. However, the gaps in azimuthal coverage make it difficult to study these azimuthal variations in detail (see section 8).

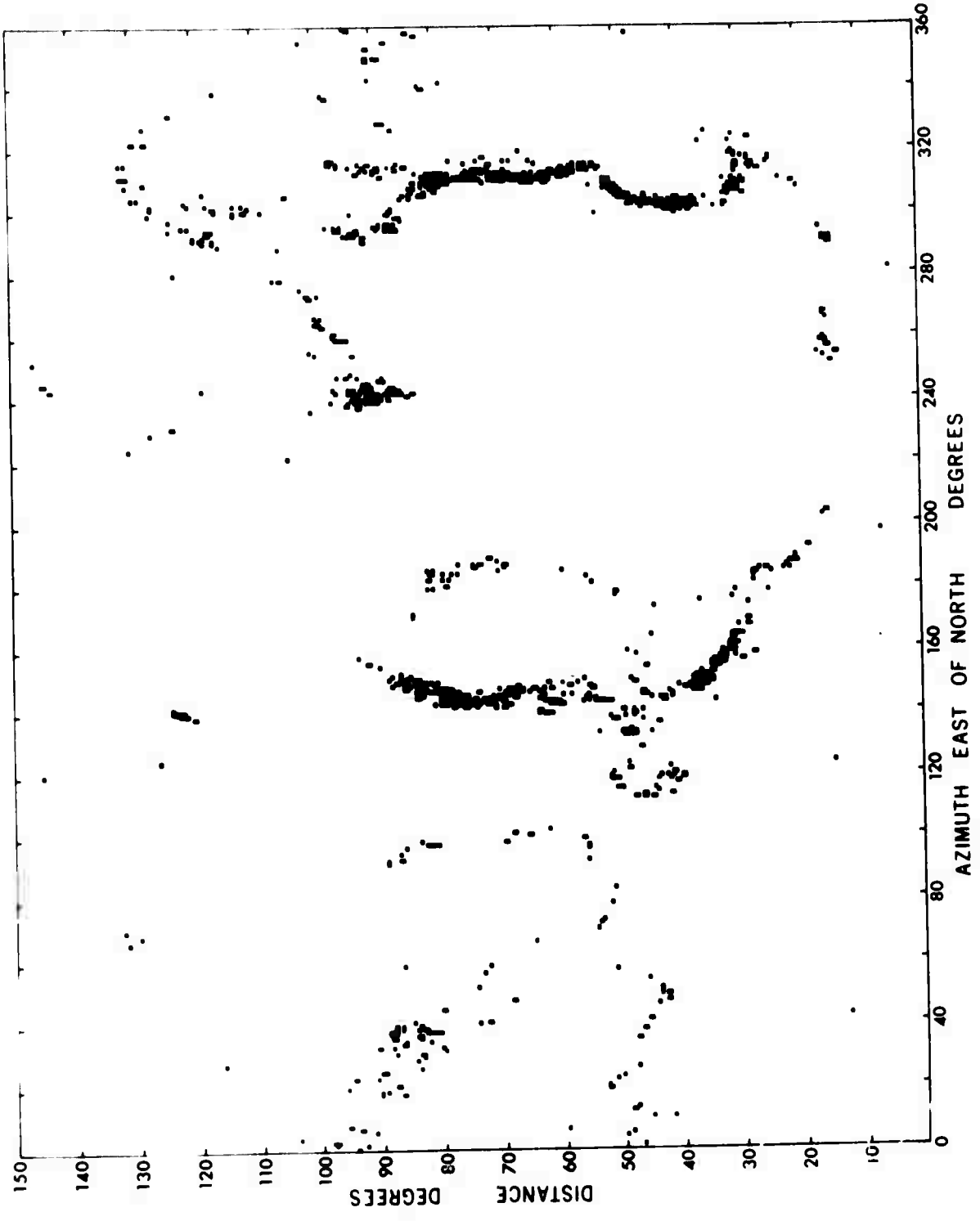

Fig. 4: Distribution of events studied.

III. OBSERVATIONS OF $dT/d\Delta$

In this section we show the raw $dT/d\Delta$ data, obtained as described above. The particular value plotted is the derivative resulting from the second degree polynomial fit (Figure 2b). It should be emphasized that none of these data have been corrected for source or array structure. The nature of these corrections will be considered later.

In order to minimize the effects of the array, the data are presented in a series of azimuth ranges. The differences between these azimuth ranges are considered in section 8. Some comments are made on unusual features in each azimuth range.

a. Azimuth Range 290-330 (Figures 5 and 6)

This azimuth range contains the most complete coverage as a function of distance. The scatter of the data is, in general, quite small, of the order of 0.1 seconds/degree. In two regions, one between 33 and 38 degrees and one between 84 and 88 degrees, the scatter is significantly larger than this. As we shall see in sections 7 and 8, there are reasons for proposing that the first of these is the result of mantle structure, and the second is due to source effects. The interpretation of this azimuth range is taken up in detail in section 7.

b. Azimuth Range 330-60 (Figures 7 and 8)

The distribution of events in this azimuth range is much poorer than above. The data at distances beyond 75 degrees show little dependence on azimuth. They do, however, show a distinctly

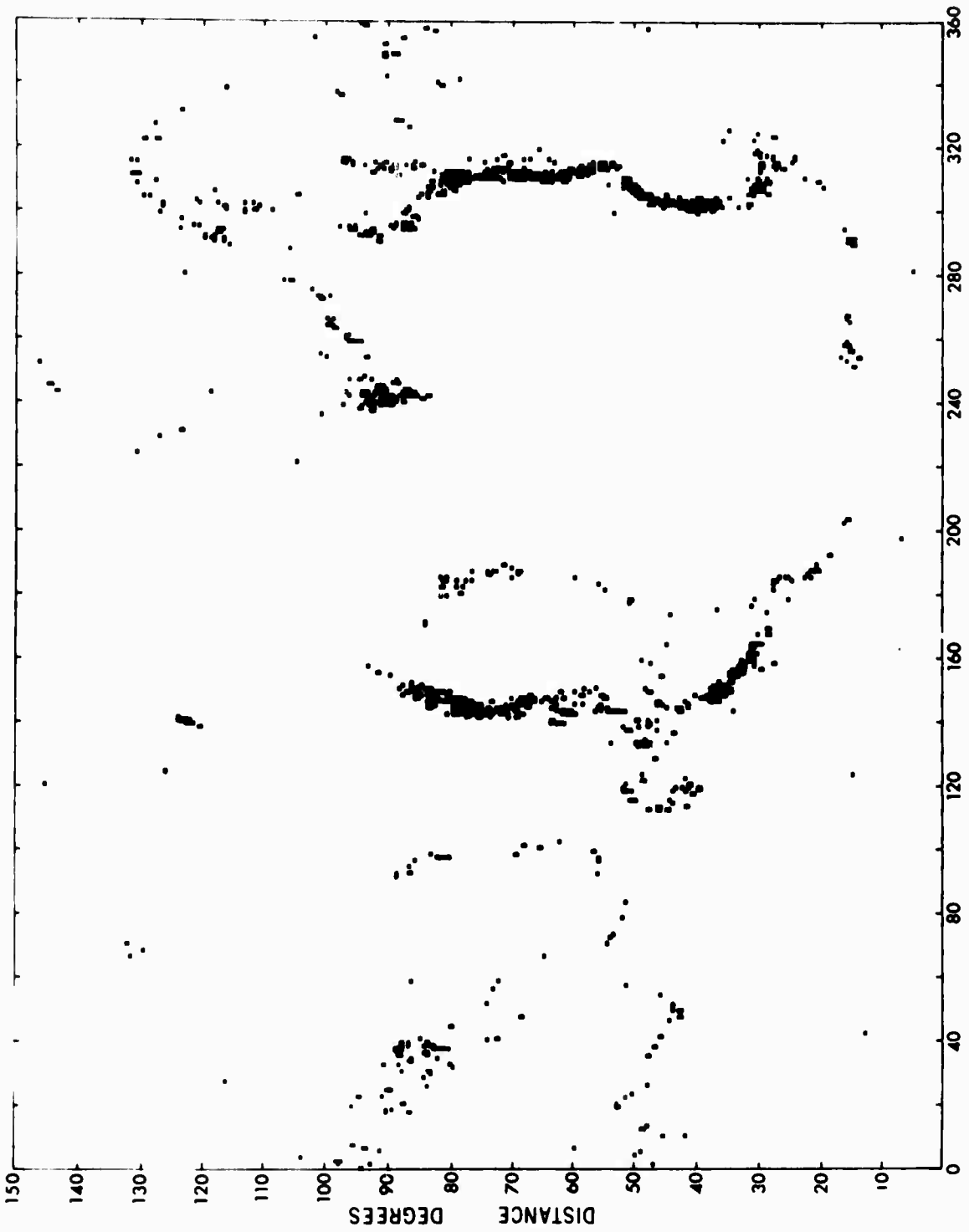

Fig. 4: Distribution of events studied.

III. OBSERVATIONS OF $dT/d\Delta$

In this section we show the raw $dT/d\Delta$ data, obtained as described above. The particular value plotted is the derivative resulting from the second degree polynomial fit (Figure 2b). It should be emphasized that none of these data have been corrected for source or array structure. The nature of these corrections will be considered later.

In order to minimize the effects of the array, the data are presented in a series of azimuth ranges. The differences between these azimuth ranges are considered in section 8. Some comments are made on unusual features in each azimuth range.

a. Azimuth Range 290-330 (Figures 5 and 6)

This azimuth range contains the most complete coverage as a function of distance. The scatter of the data is, in general, quite small, of the order of 0.1 seconds/degree. In two regions, one between 33 and 38 degrees and one between 84 and 88 degrees, the scatter is significantly larger than this. As we shall see in sections 7 and 8, there are reasons for proposing that the first of these is the result of mantle structure, and the second is due to source effects. The interpretation of this azimuth range is taken up in detail in section 7.

b. Azimuth Range 330-60 (Figures 7 and 8)

The distribution of events in this azimuth range is much poorer than above. The data at distances beyond 75 degrees show little dependence on azimuth. They do, however, show a distinctly

different behavior from those along the 290-330 direction. In the distance range 43 to 50 degrees, events from an azimuth of 330-60 depart strongly from those at an azimuth of 20 to 60 degrees. This may be the result of source structure, but the data are sufficiently sparse that it is hard to investigate the problem further at present.

c. Azimuth Range 60-130 (Figures 9 and 10)

These data too are quite sparse. This does seem to be a significant difference between events at 110-130 and those at 60-110, in the distance range 45 to 60 degrees.

d. Azimuth Range 130-170 (Figures 11 and 12)

Good coverage is obtained in this azimuth range. Some of the apparent scatter in this diagram may be due to errors in epicentral location. The pronounced difference between the shape of this curve and that for the azimuth range 290-330 is discussed in section 8.

e. Azimuth Range 170-290 (Figures 13 and 14)

These events are very poorly distributed in distance.

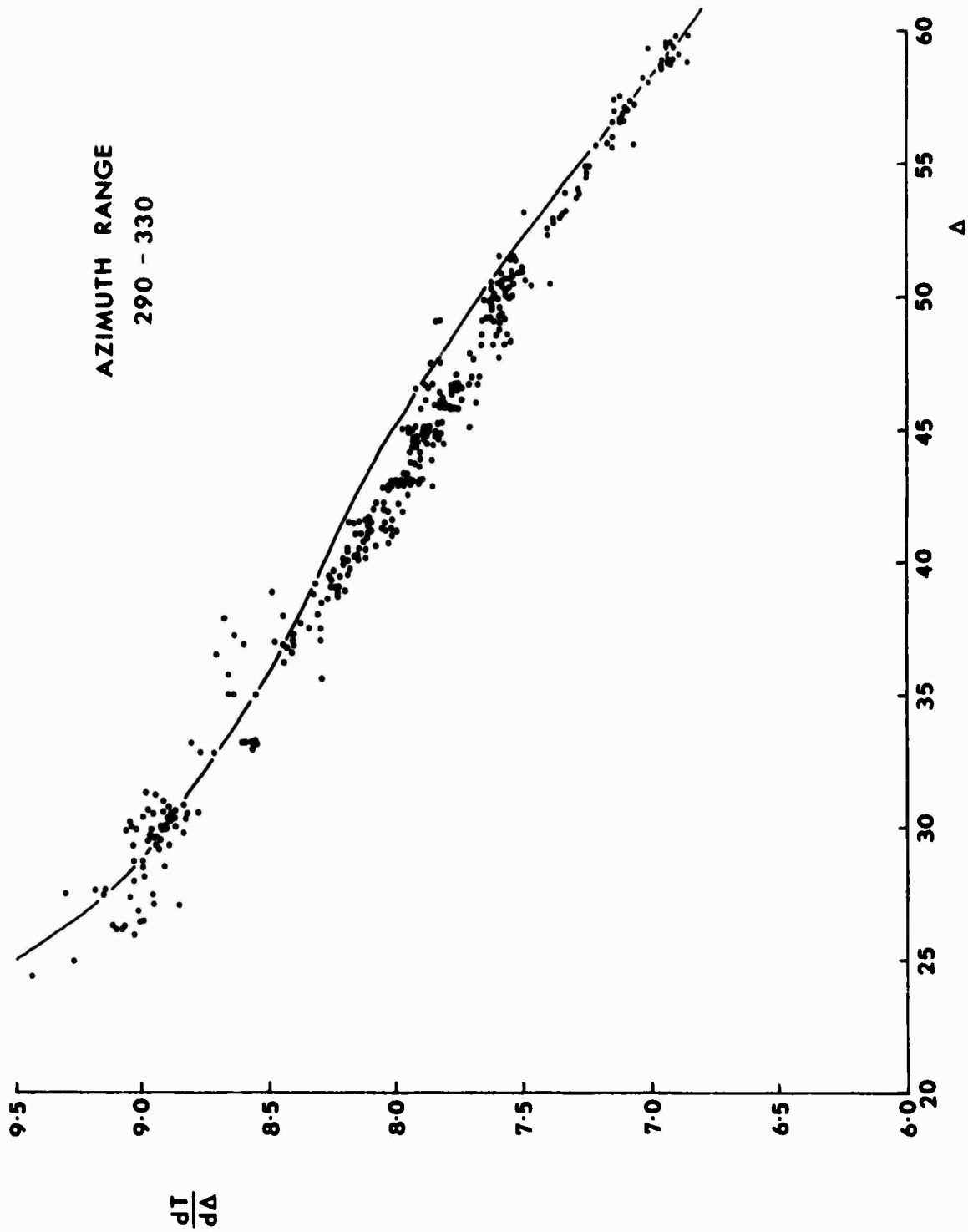
AZIMUTH RANGE
290 - 330
dT/dΔ
Δ
9·5
9·0
8·5
8·0
7·5
7·0
6·5
6·0
20
25
30
35
40
45
50
55
60

Fig. 5

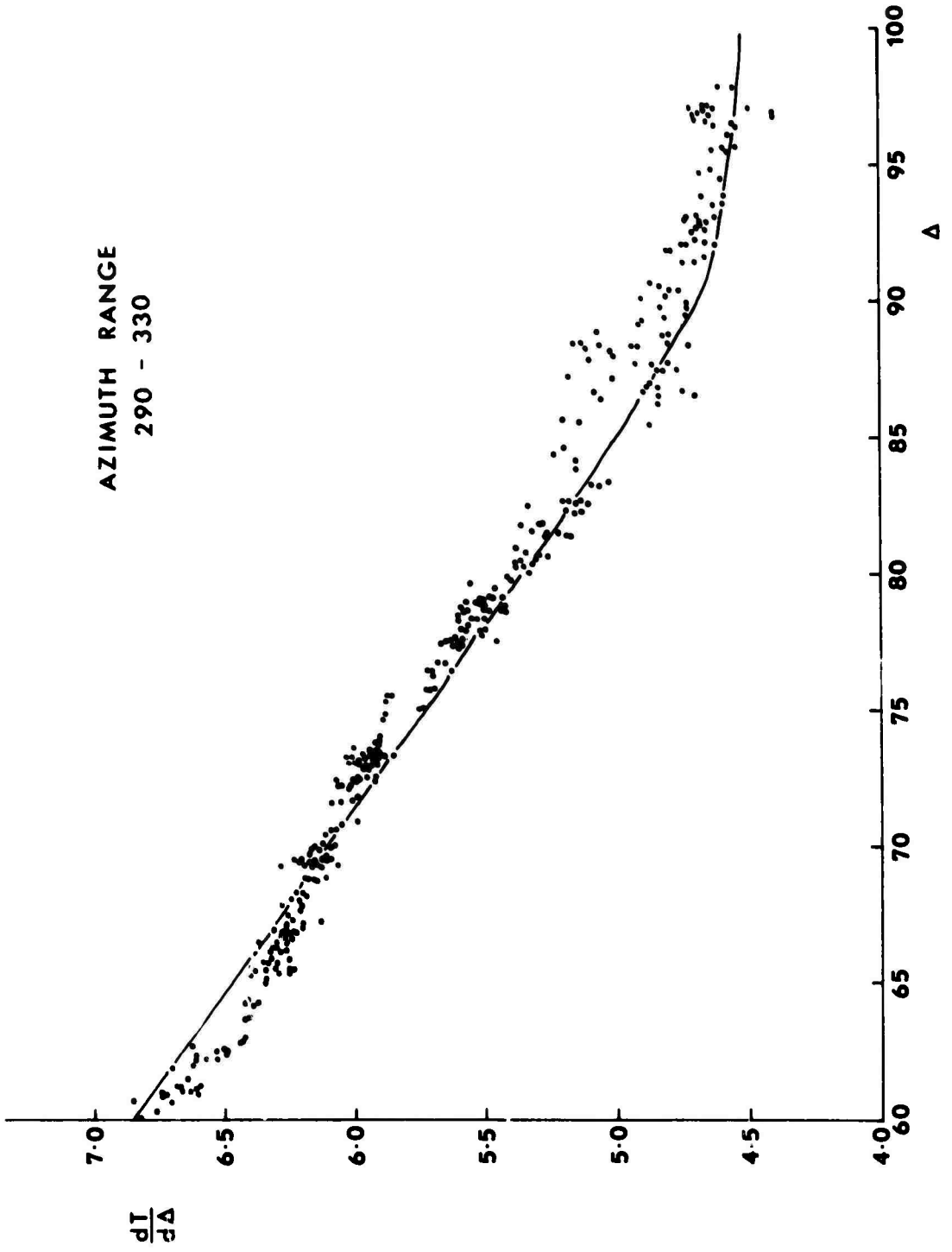
AZIMUTH RANGE
290 - 330
dT/dΔ
Δ
7·0
6·5
6·0
5·5
5·0
4·5
4·0
60
65
70
75
80
85
90
95
100

Fig. 6

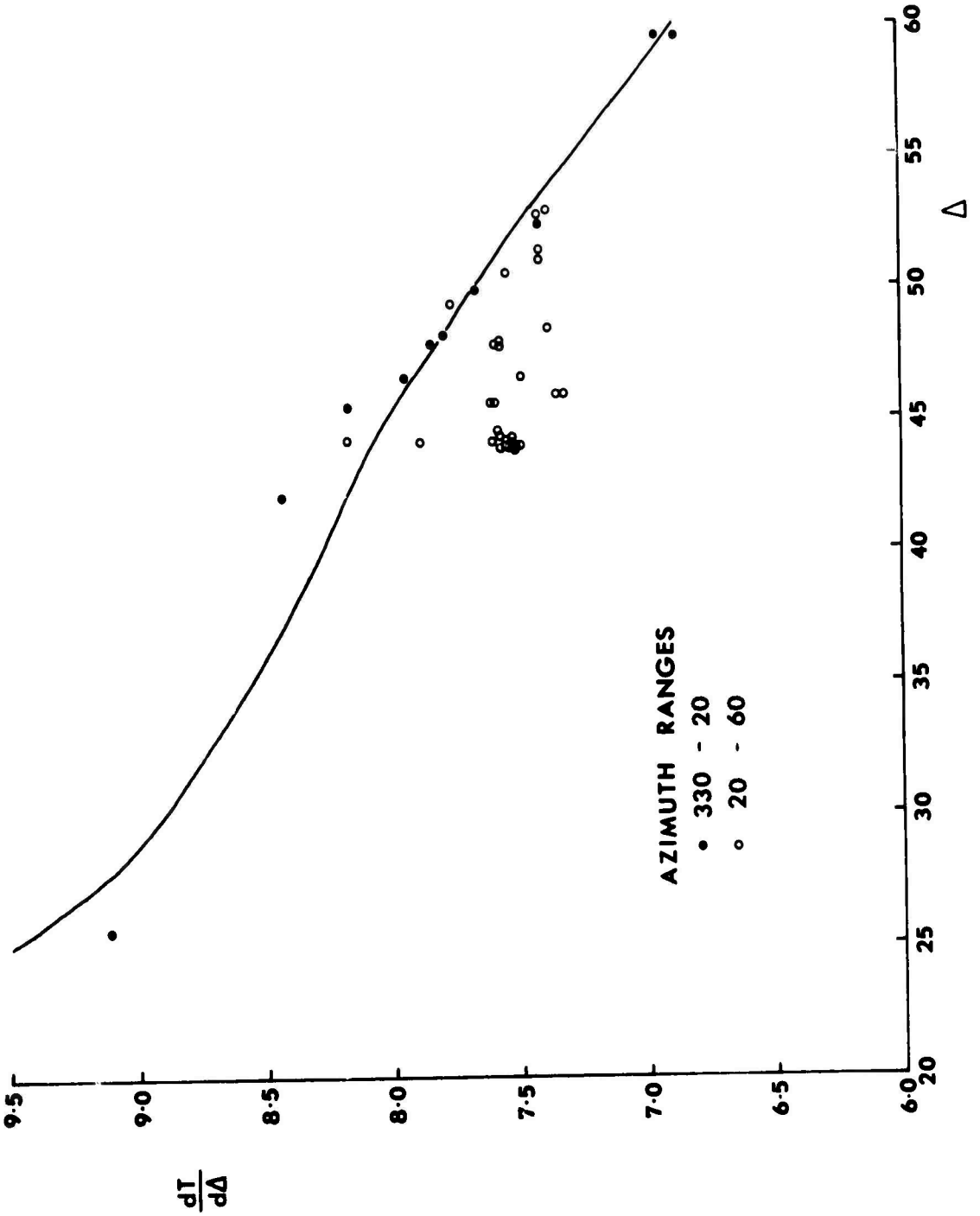
9·5
9·0
8·5
8·0
7·5
7·0
6·5
6·0
dT/dΔ
20
25
30
35
40
45
50
55
60
Δ
AZIMUTH RANGES
• 330 - 20
○ 20 - 60

Fig. 7

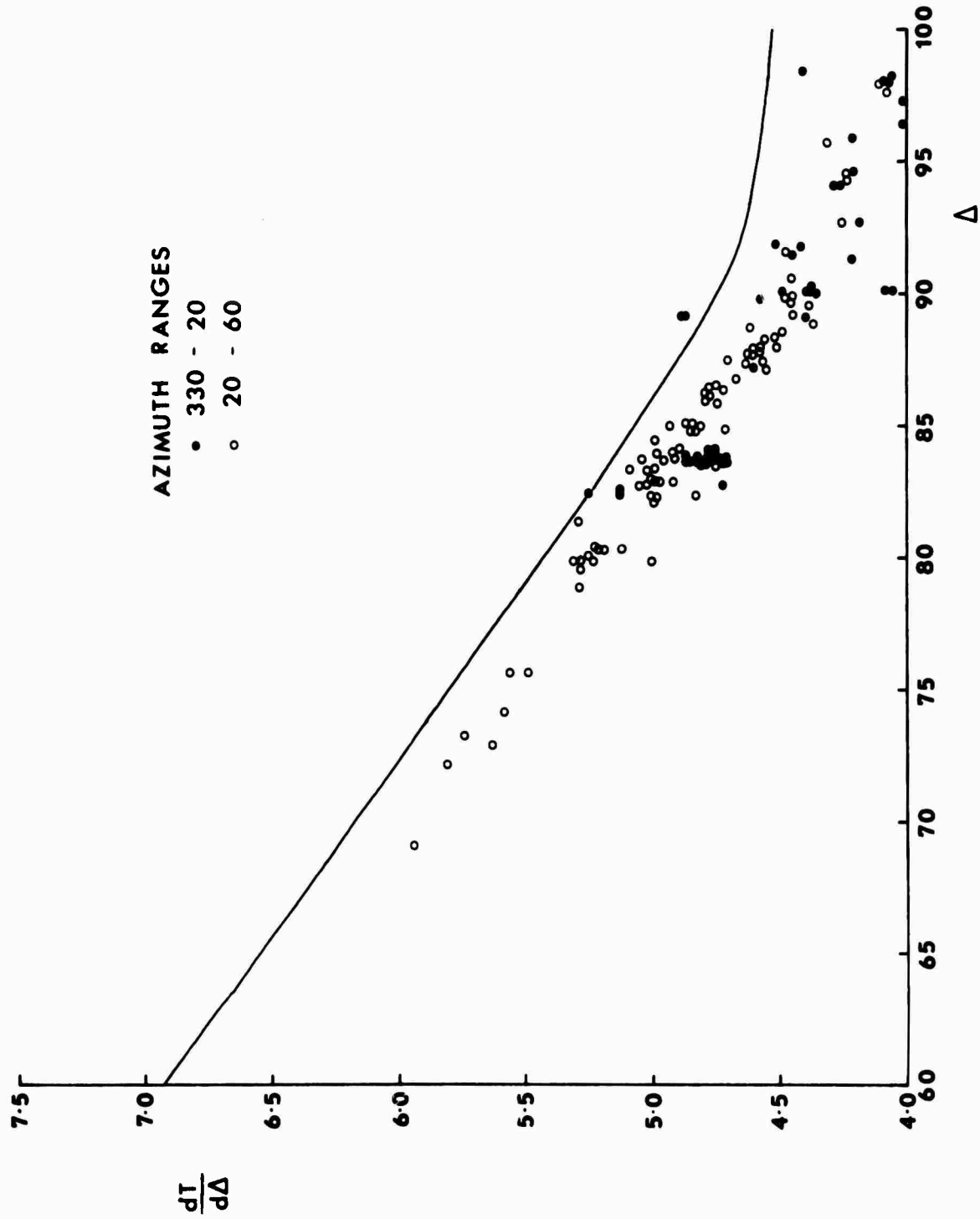
AZIMUTH RANGES
• 330 - 20
○ 20 - 60
dT/dΔ
Δ
7·5
7·0
6·5
6·0
5·5
5·0
4·5
4·0
60
65
70
75
80
85
90
95
100

Fig. 8

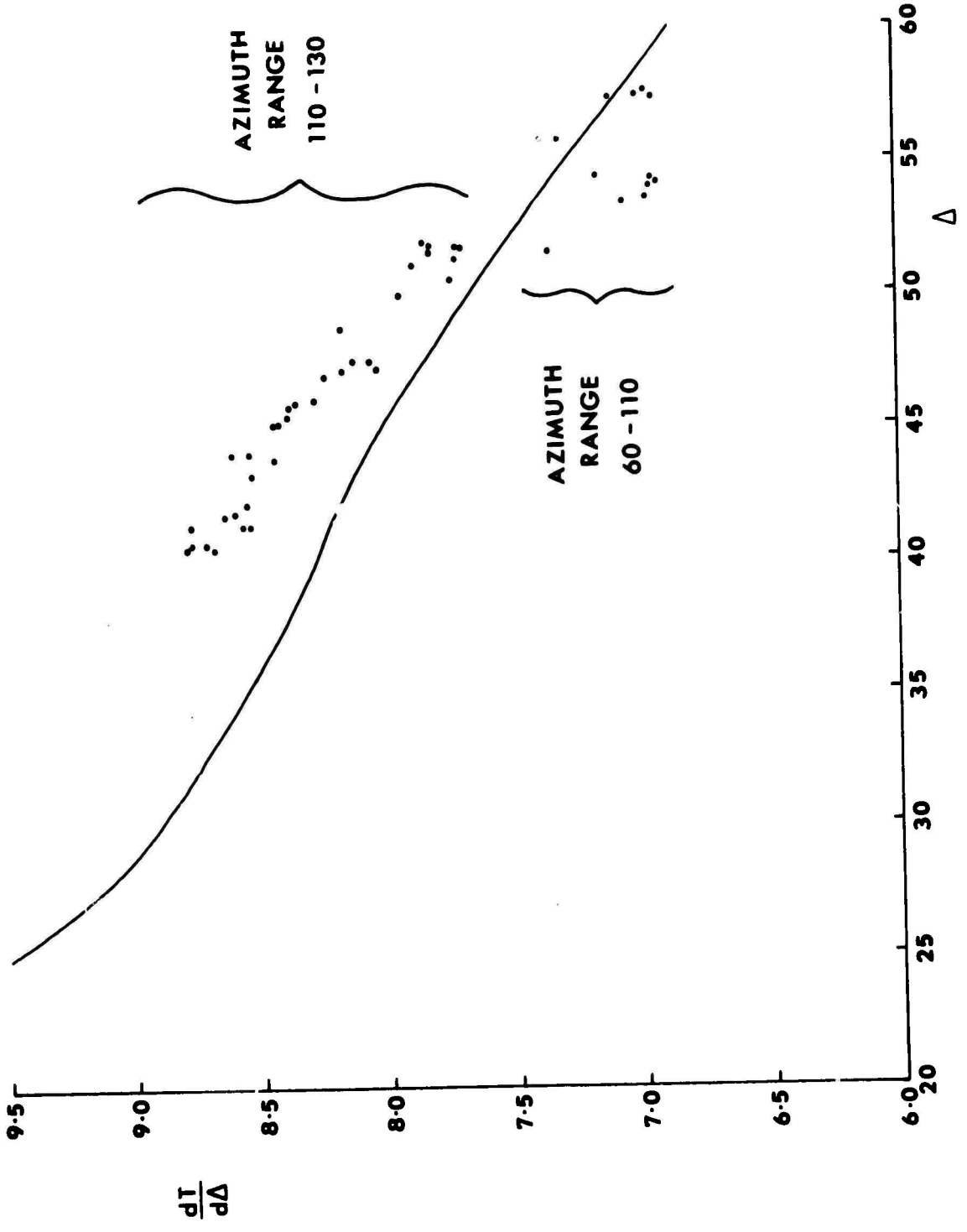
AZIMUTH
RANGE
110 - 130
AZIMUTH
RANGE
60 - 110
dT/dΔ
Δ
9·5
9·0
8·5
8·0
7·5
7·0
6·5
6·0
20
25
30
35
40
45
50
55
60

Fig. 9

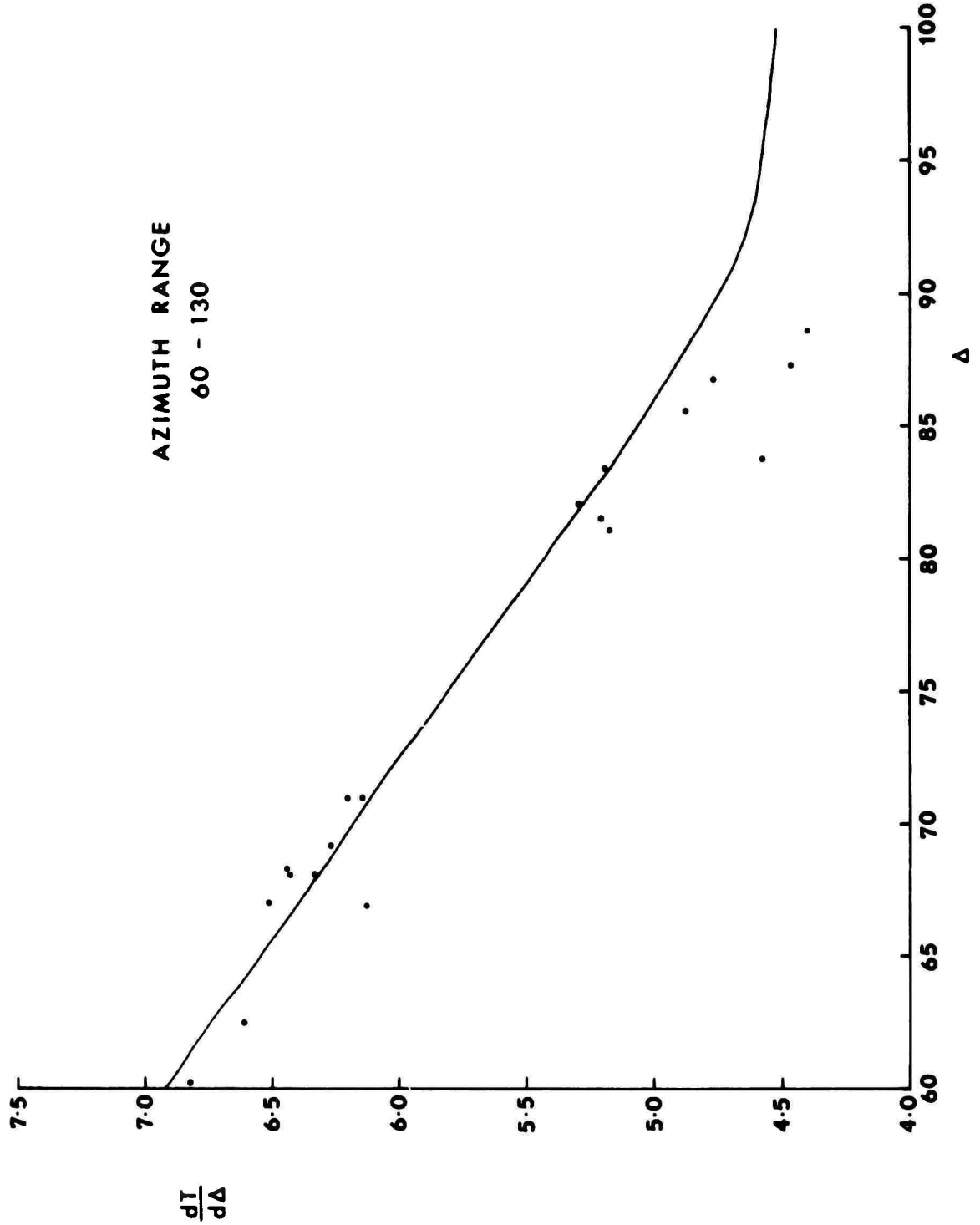
AZIMUTH RANGE
60 - 130
dT/dΔ
Δ
7·5
7·0
6·5
6·0
5·5
5·0
4·5
4·0
60
65
70
75
80
85
90
95
100

Fig. 10

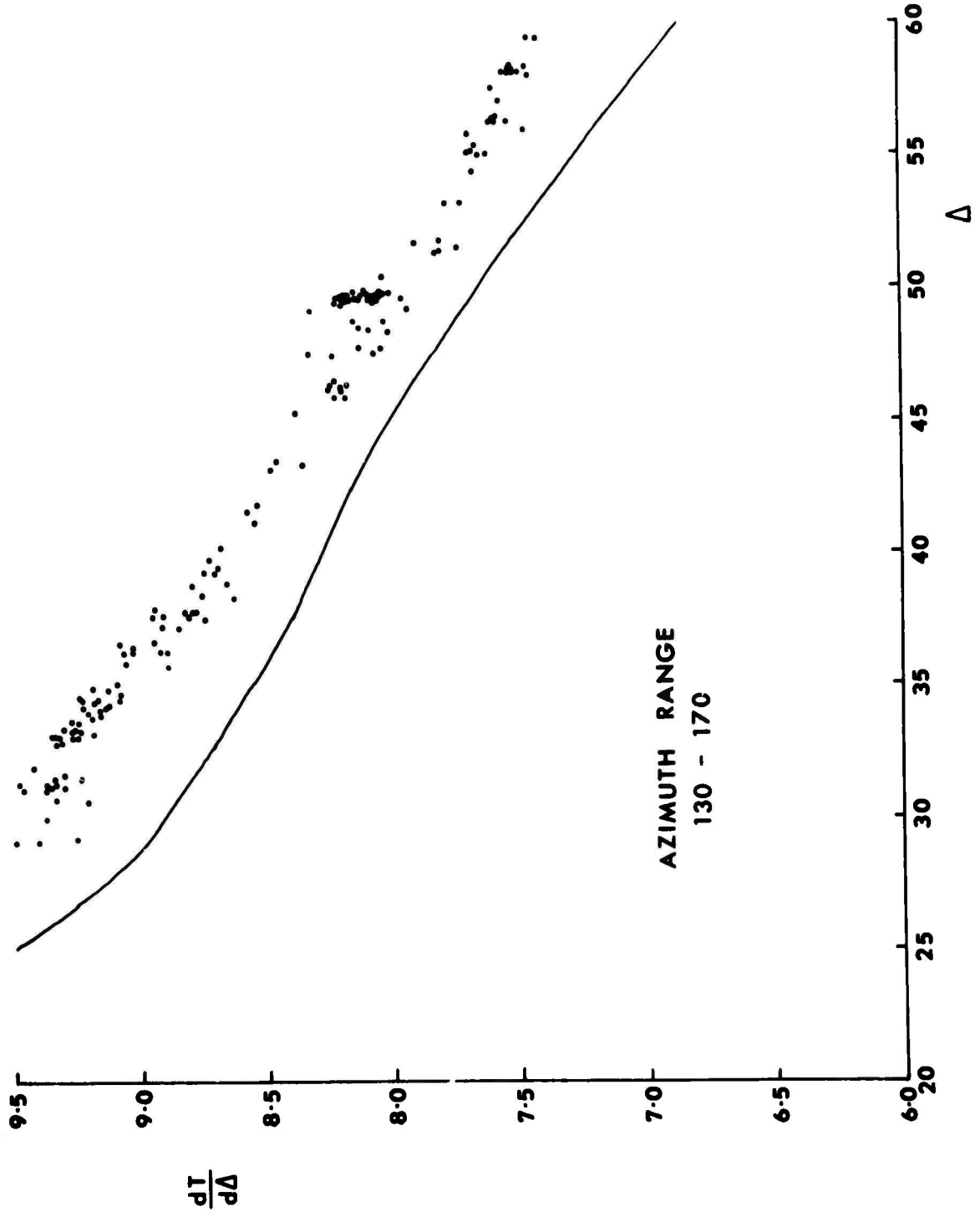
AZIMUTH RANGE
130 - 170
dT/dΔ
Δ
9·5
9·0
8·5
8·0
7·5
7·0
6·5
6·0
20
25
30
35
40
45
50
55
60

Fig. 11

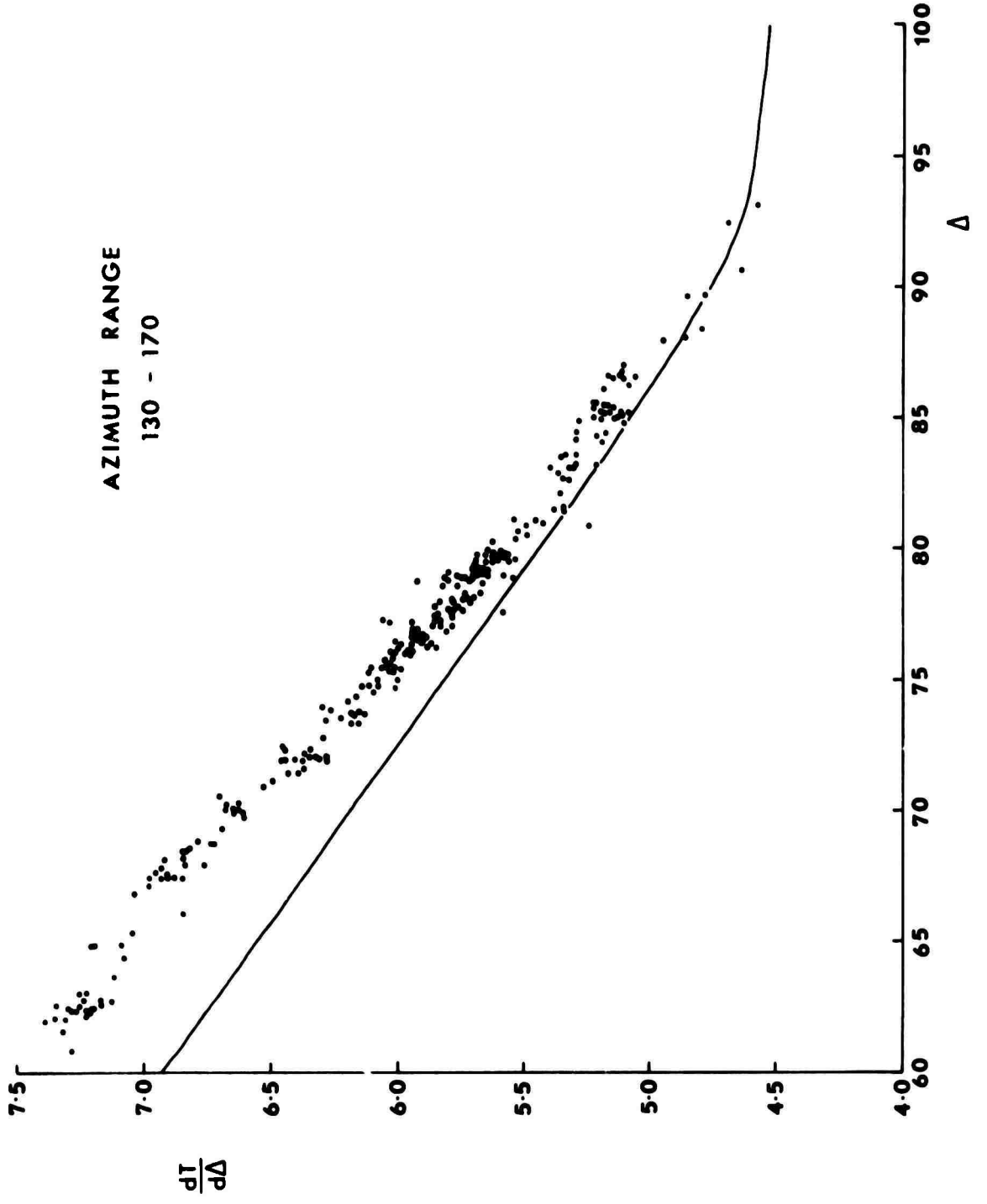
AZIMUTH RANGE
130 - 170
$\frac{\nabla p}{\nabla T}$
7·5
7·0
6·5
6·0
5·5
5·0
4·5
4·0
60
65
70
75
80
85
90
95
100
Δ

Fig. 12

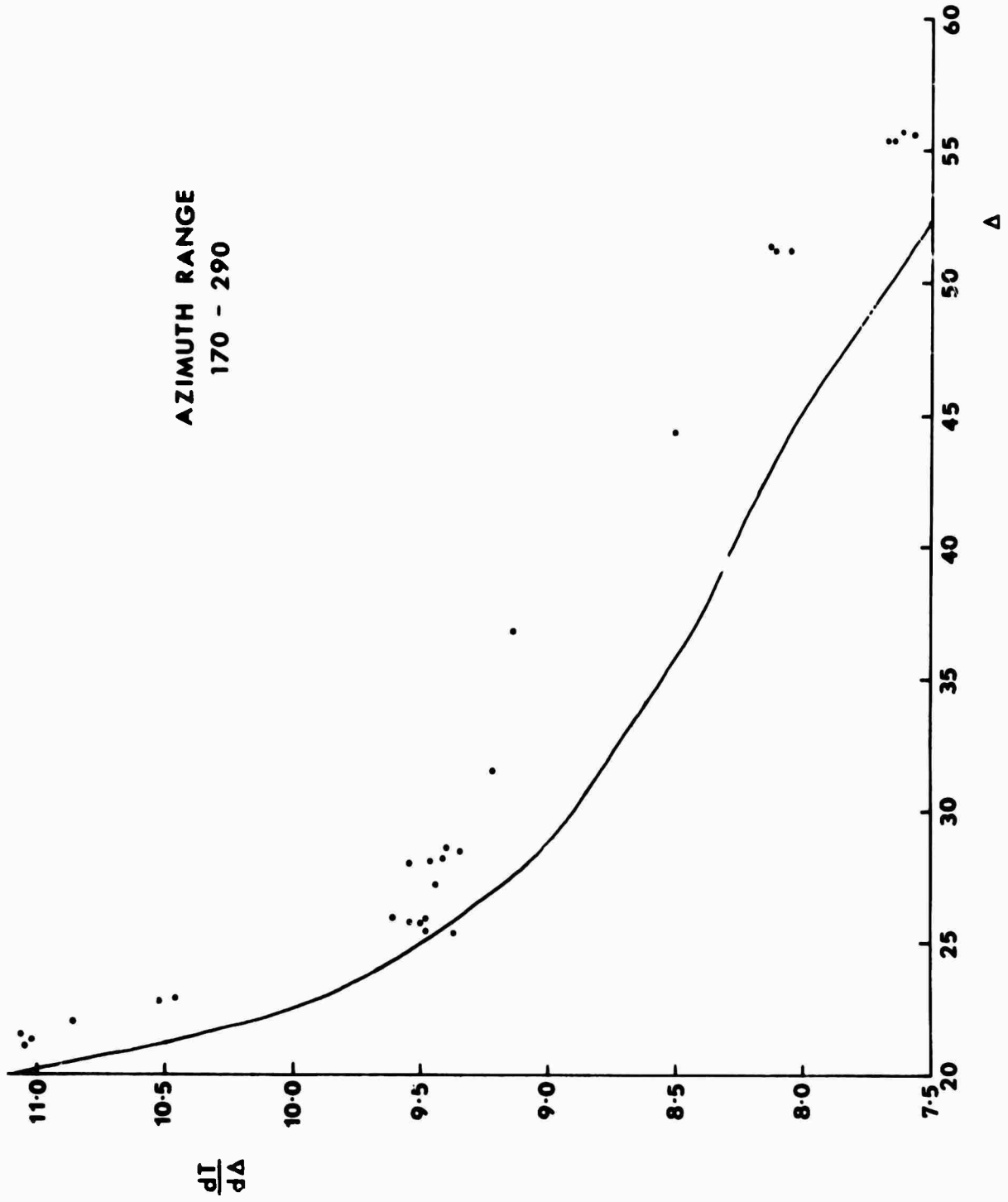
AZIMUTH RANGE
170 - 290
dT/dΔ
Δ
11·0
10·5
10·0
9·5
9·0
8·5
8·0
7·5
20
25
30
35
40
45
50
55
60

Fig. 13

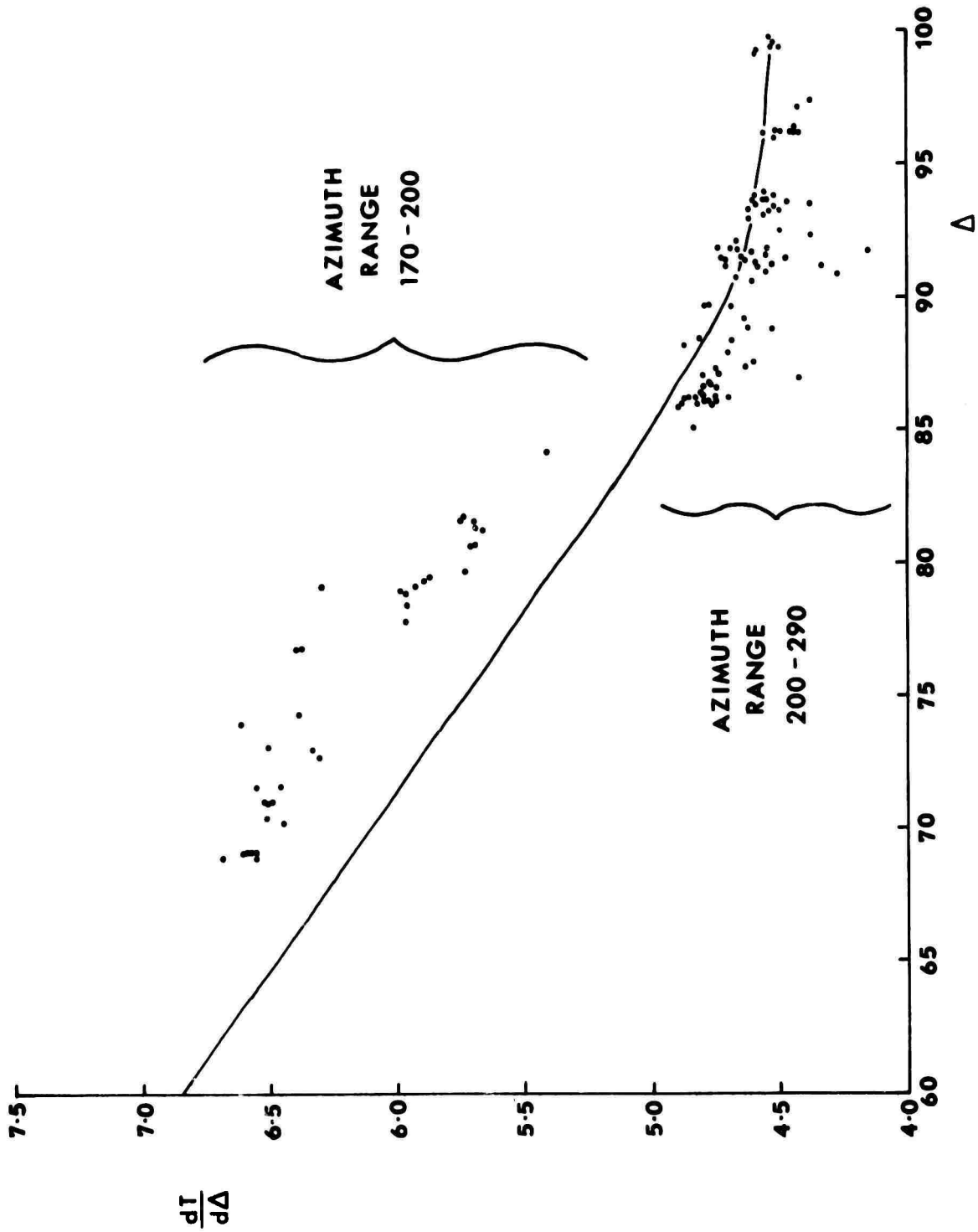
AZIMUTH
RANGE
170 - 200
AZIMUTH
RANGE
200 - 290
dT/dΔ
Δ
7·5
7·0
6·5
6·0
5·5
5·0
4·5
4·0
60
65
70
75
80
85
90
95
100

Fig. 14

IV. OBSERVATIONS OF $d^2T/d\Delta^2$

The second derivative of the travel time curve can easily be determined from the analysis outlined in section I, and is included in the printed output for each event (Figure 2b). This is easiest seen if the time T_i at the ith station is related to the distance δ_i of the ith station from AO along the event azimuth by a Taylor expansion

$$T_i = T_o + \left(\frac{dT}{d\Delta}\right)\delta_i + \frac{1}{2}\left(\frac{d^2T}{d\Delta^2}\right)\delta_i^2 + \cdots \qquad (5)$$

Estimates of $\frac{d^2T}{d\Delta^2}$ may therefore be obtained from the coefficients d and f in equations 3 and 4.

This is the first time that an attempt has been made to directly measure the second derivative of the travel time curve using an array (Chinnery 1968a, 1968b). The results are shown, for the two principal azimuth ranges, in Figures 15-18.

It is clear that the scatter in these data is large, and this is primarily due to the timing accuracy. The absolute value of $d^2T/d\Delta^2$ is quite unreliable, since station corrections have not been applied, and because these corrections could not be estimated accurately enough anyway for the present purpose. However, there is one feature of interest in these curves, for in the vicinity of a cusp or triplication of the travel time curve the magnitude of the second derivative should become large. Some indication of possible cusps may be obtained at those distance ranges where the scatter of these graphs becomes large. These are noted below:

a. Azimuth Range 290-330 (Figures 15 and 16)

Unusually large or small values of $d^2T/d\Delta^2$ are noted in the distance ranges 26-27°, 36-37° (only two points), 60-65°, 68-69°, 75-76°, 86-90° and 96-97°. There is a high correlation between these anomalous regions and those selected on the basis of the $dT/d\Delta$ data (section 7). This suggests that there is some useful information in the $d^2T/d\Delta^2$ data, though the present scatter makes any interpretation of the second derivative data alone quite meaningless.

b. Azimuth Range 130-170 (Figures 17 and 18)

Anomalous distance ranges are 32-34°, 49-50°, 65-67° and 81-83°. The poor correlation of these with the 290-330 azimuth range is striking. We shall see later that the $dT/d\Delta$ data for these two azimuth ranges also show little correlation (section 8).

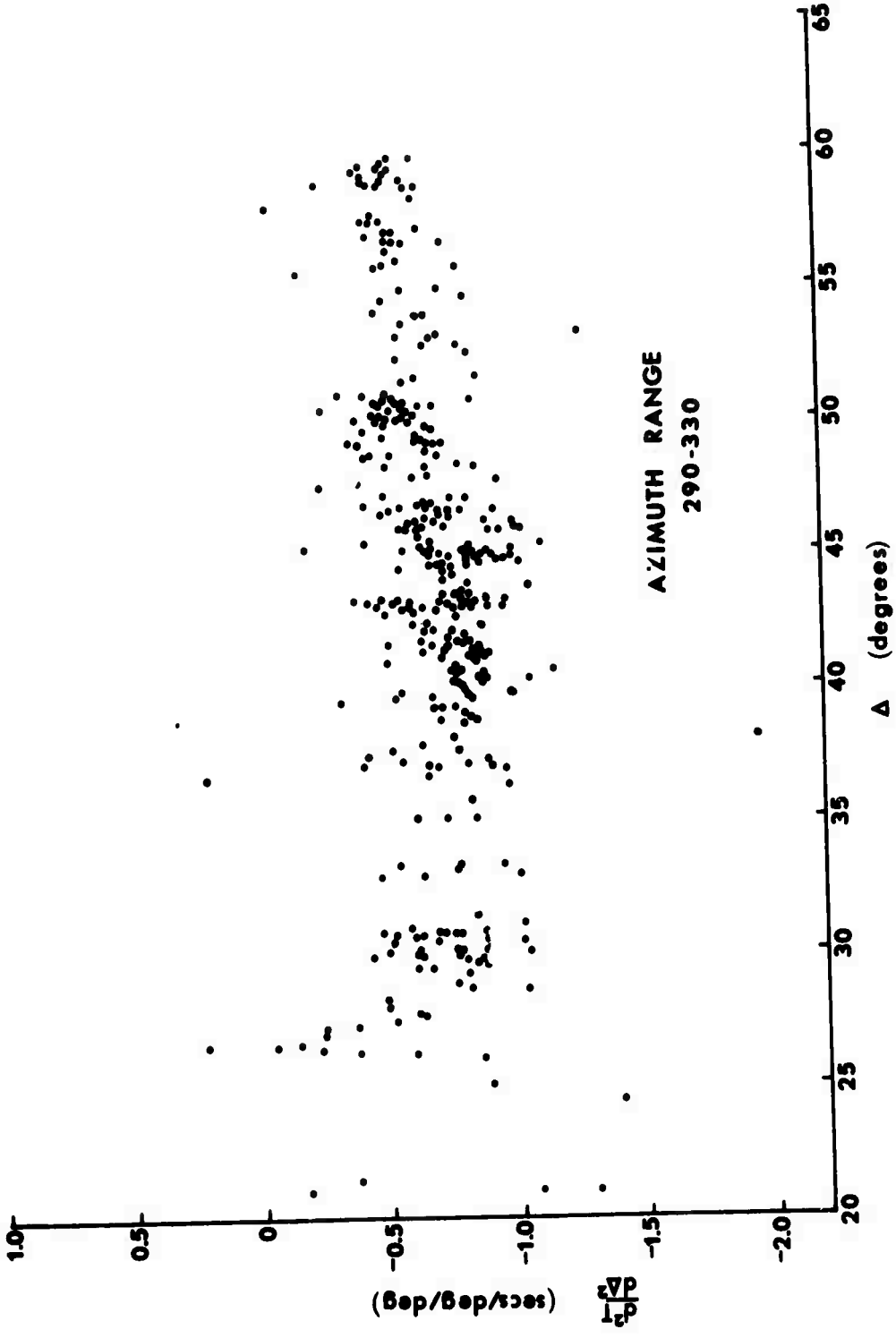
AZIMUTH RANGE
290-330
Δ (degrees)
(sec²/deg²/deg)
1.0
0.5
0
-0.5
-1.0
-1.5
-2.0
20
25
30
35
40
45
50
55
60
65

Fig. 15

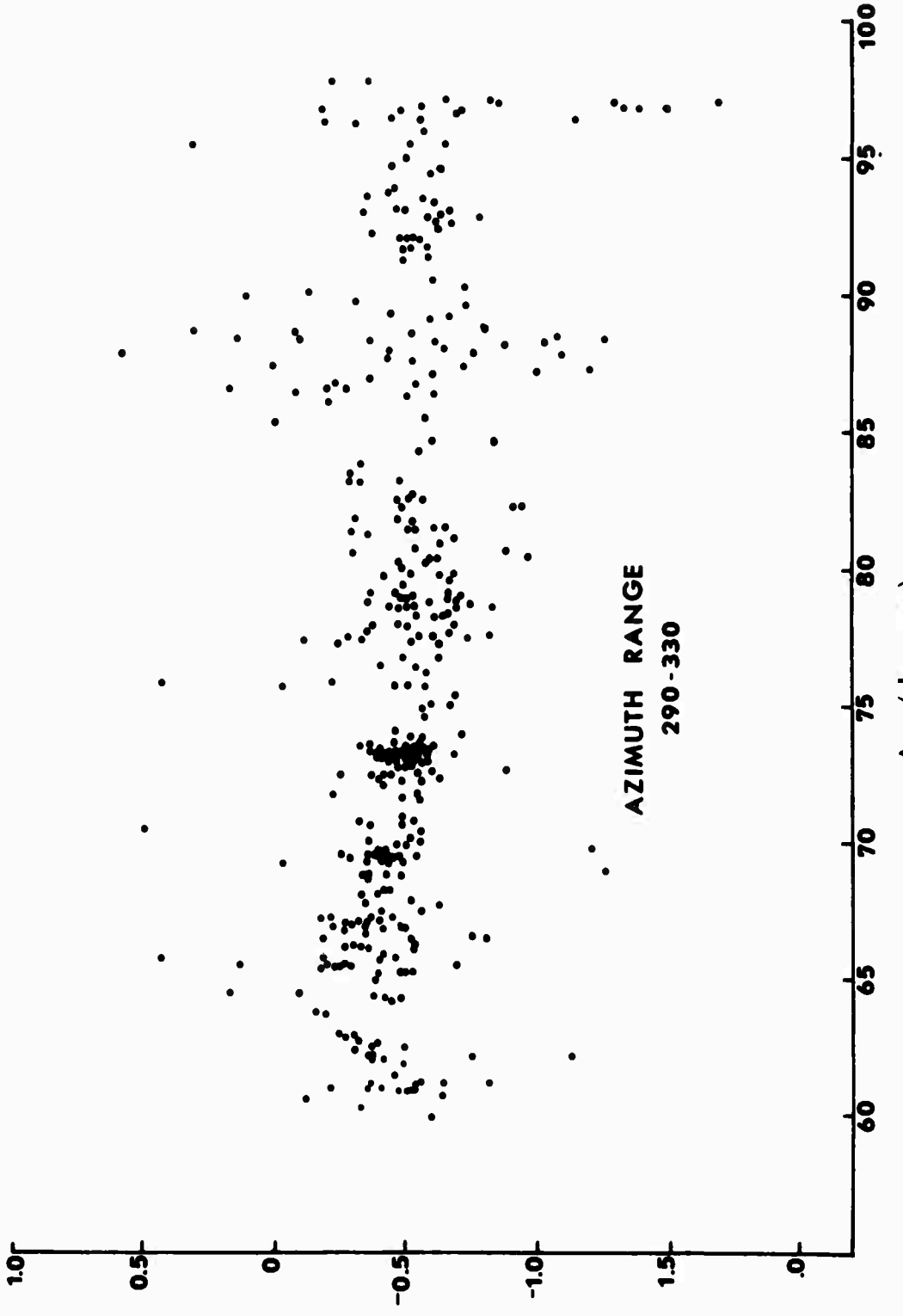
AZIMUTH RANGE
290-330
Δ (degrees)
60
65
70
75
80
85
90
95
100
1.0
0.5
0
-0.5
-1.0
1.5
.0

Fig. 16

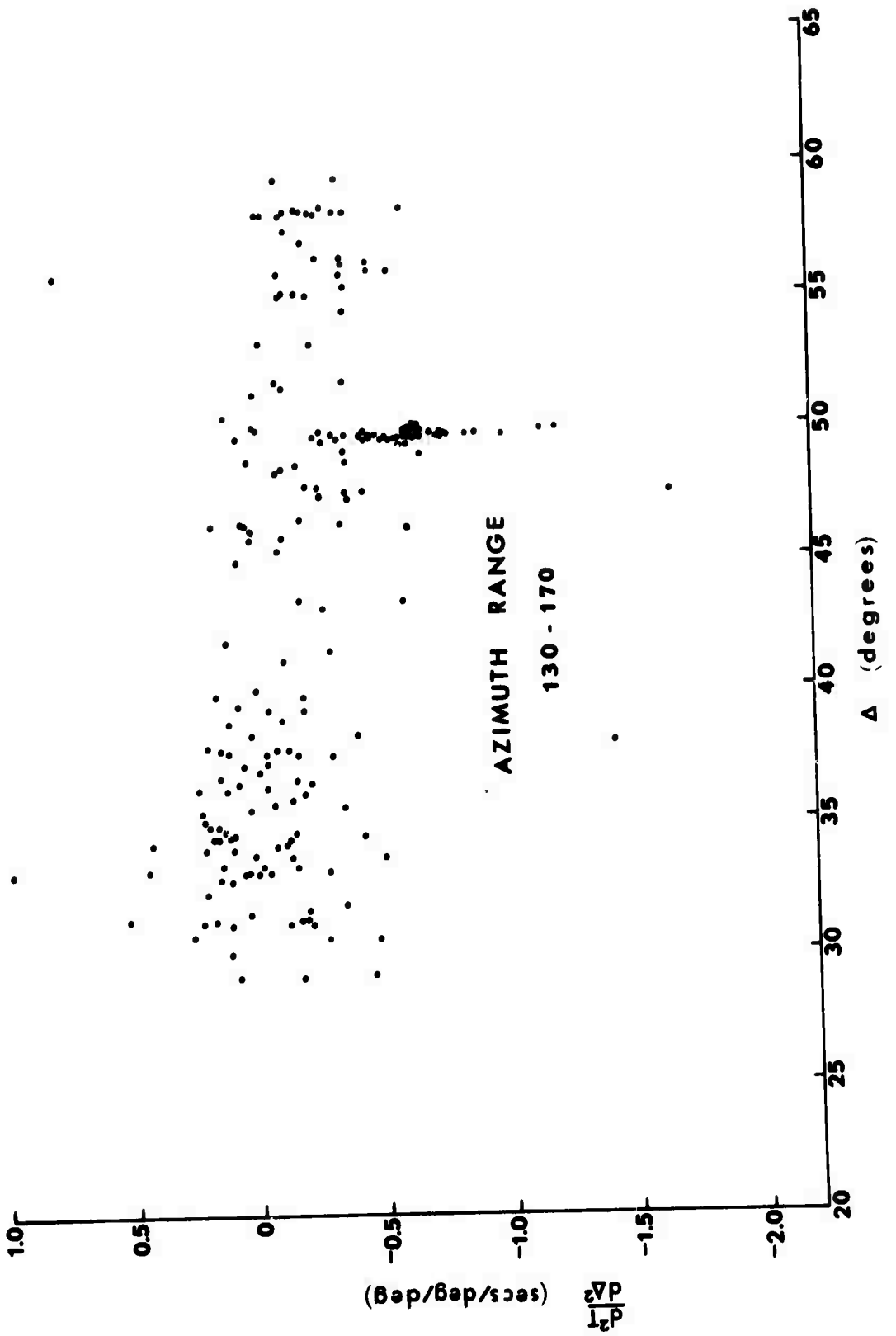
AZIMUTH RANGE
130 - 170
Δ (degrees)
$\frac{d^2T}{d\Delta^2}$ (secs/deg/deg)
1.0
0.5
0
-0.5
-1.0
-1.5
-2.0
20
25
30
35
40
45
50
55
60
65

Fig. 17

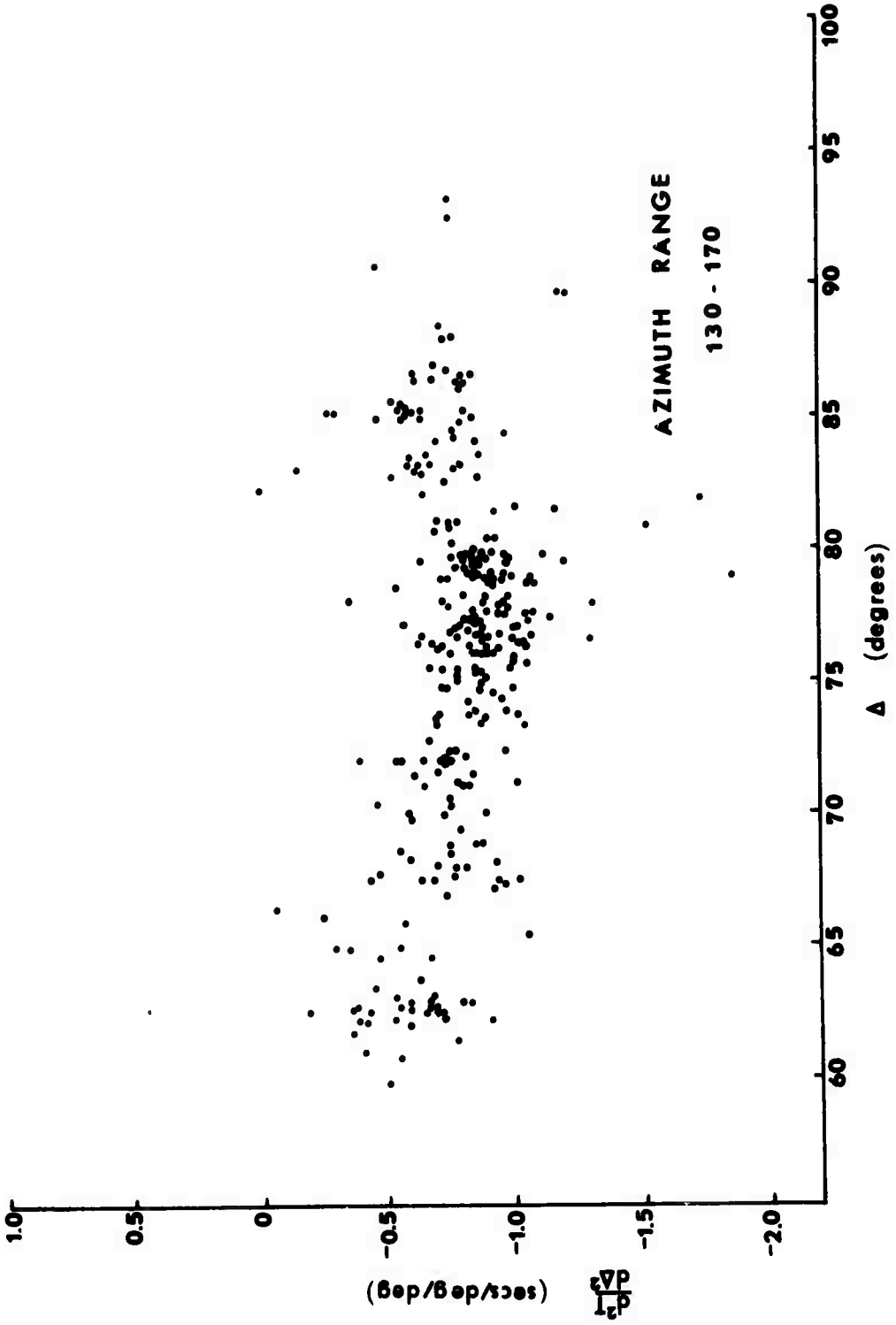
AZIMUTH RANGE
130 - 170
Δ (degrees)
60
65
70
75
80
85
90
95
100
1.0
0.5
0
-0.5
-1.0
-1.5
-2.0
(sec/deg/deg)

Fig. 18

V. OBSERVATIONS OF AZIMUTH ERROR

Two estimates of the azimuth to an event may be obtained. The "true" azimuth may be obtained from the published USCGS epicenter for each event. The error in this azimuth from its real value is likely to vary from place to place, and may contain systematic components which may create apparent variations with azimuth and/or distance. However, the error in the "true" azimuth is likely to be small. Most events should be located to within 1° or less of their true epicenters, and the corresponding error in azimuth should be much less than this.

A second estimate, the "observed" azimuth, may be obtained from the coefficients a and b in equation 1. The difference between the true and observed azimuths is a measure of the bending of the ray path out of the vertical plane containing the source and the array. However, where this bending occurs is harder to say. It may be due to source structure, a lateral variation in mantle structure, or local structure under the array.

Figure 19 shows the variation of true minus observed azimuth with distance for events to the Northwest of the array. Clearly there is a strong but apparently continuous variation of this quantity. The continuity suggests that the variation is not due to source structure, though this cannot be proved. The large errors for events at distances greater than 100° is very interesting, since these rays should traverse crustal structure almost vertically, and they should therefore be least affected by the crustal structure.

Figure 20 shows similar data from the Southeast events. The trend of the observations shows a marked similarity with Figure 19 in the distance range 50-90°, but is very different outside this range.

One possible reason for an azimuth error is crustal structure beneath the array. If this structure may be approximated by a dipping interface, the graph of azimuth error against azimuth should be a sine function (Niazi, 1966). Figures 21 and 22 show such graphs, for events in the distance ranges 20-55° and 75-95° respectively. No clear sinusoidal terms are apparent, and in fact there are significant differences between the two sets of data.

It has not proved possible, as yet, to interpret these observations of azimuth error.

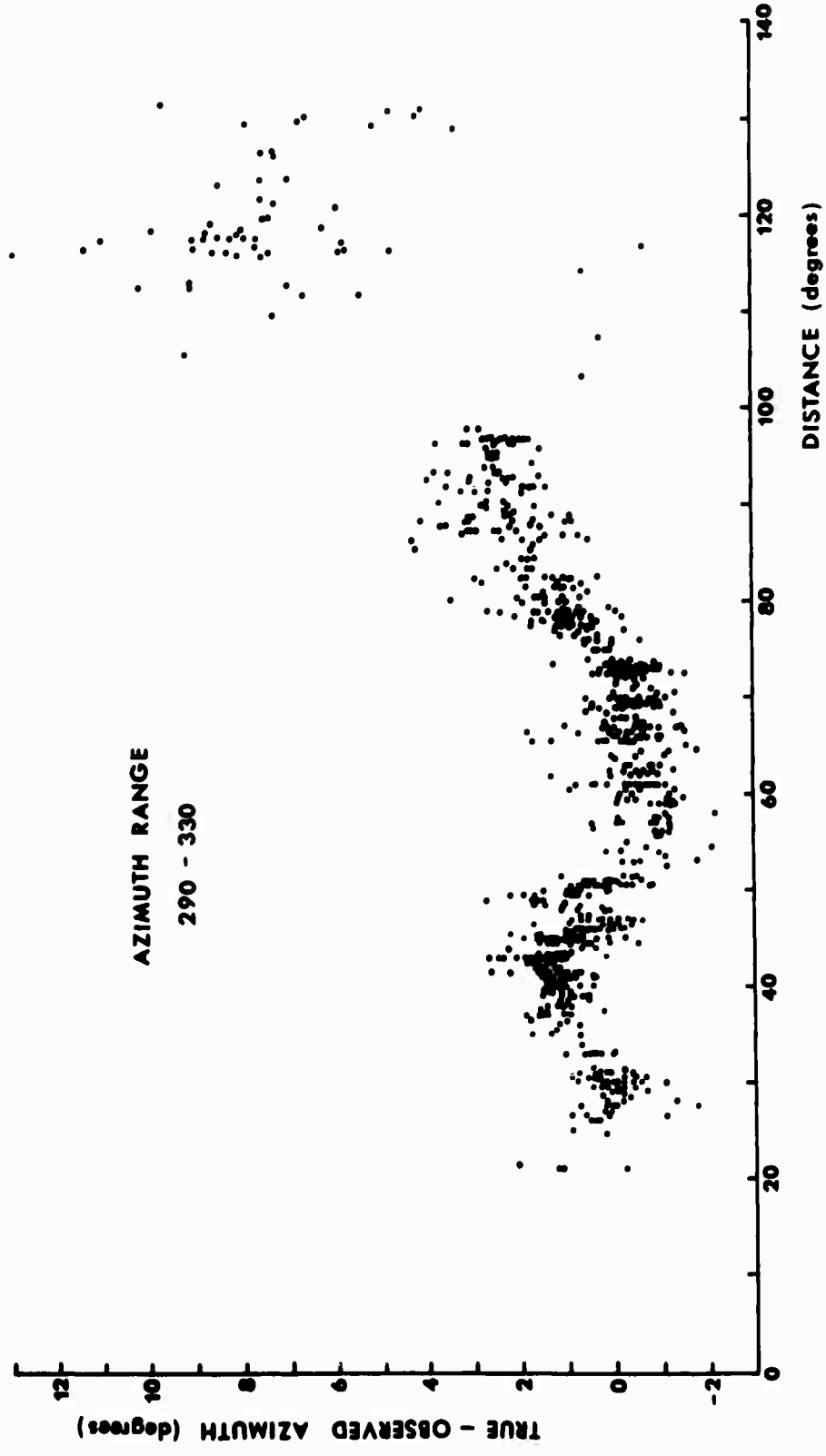
AZIMUTH RANGE
290 - 330
TRUE - OBSERVED AZIMUTH (degrees)
DISTANCE (degrees)
12
10
8
6
4
2
0
-2
0
20
40
60
80
100
120
140

Fig. 19

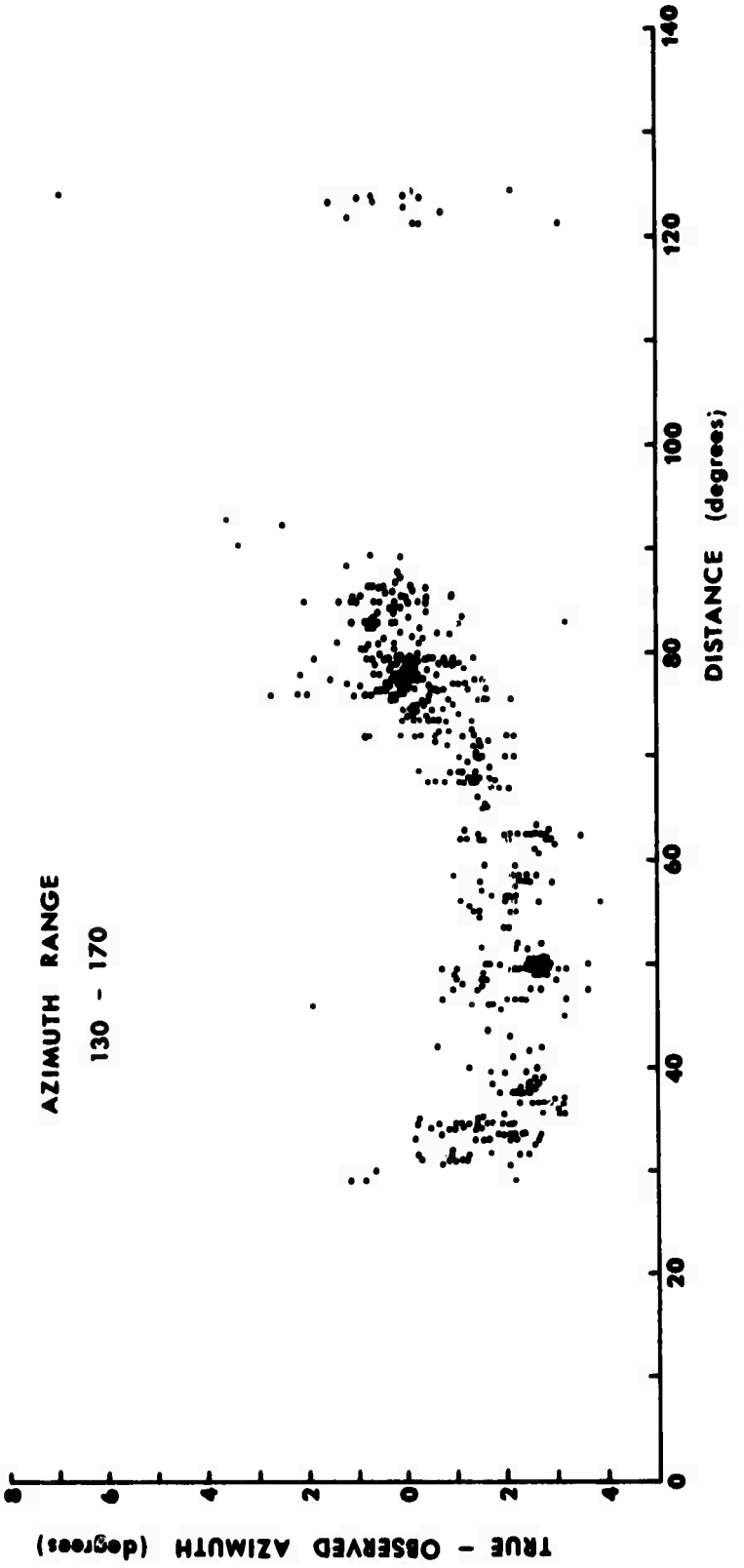
AZIMUTH RANGE
130 - 170
TRUE - OBSERVED AZIMUTH (degrees)
8
6
4
2
0
2
4
0
20
40
60
80
100
120
140
DISTANCE (degrees)

Fig. 20

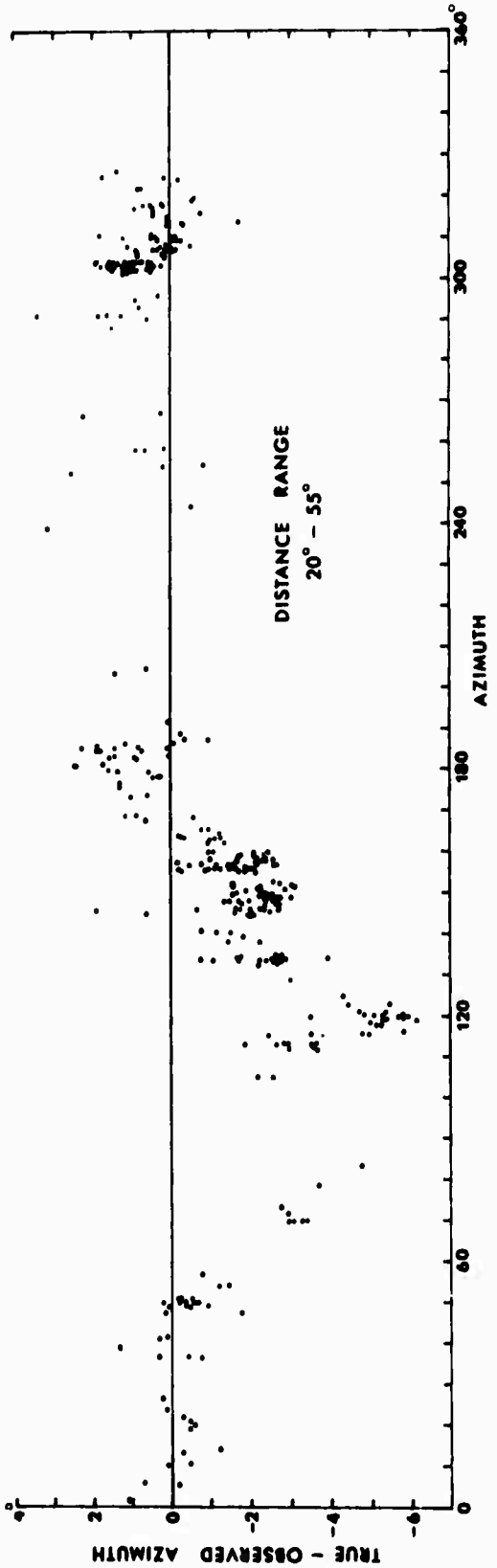
DISTANCE RANGE
20° – 55°
AZIMUTH
0
60
120
180
240
300
360°
TRUE – OBSERVED AZIMUTH
4
2
0
-2
-4
-6

Fig. 21

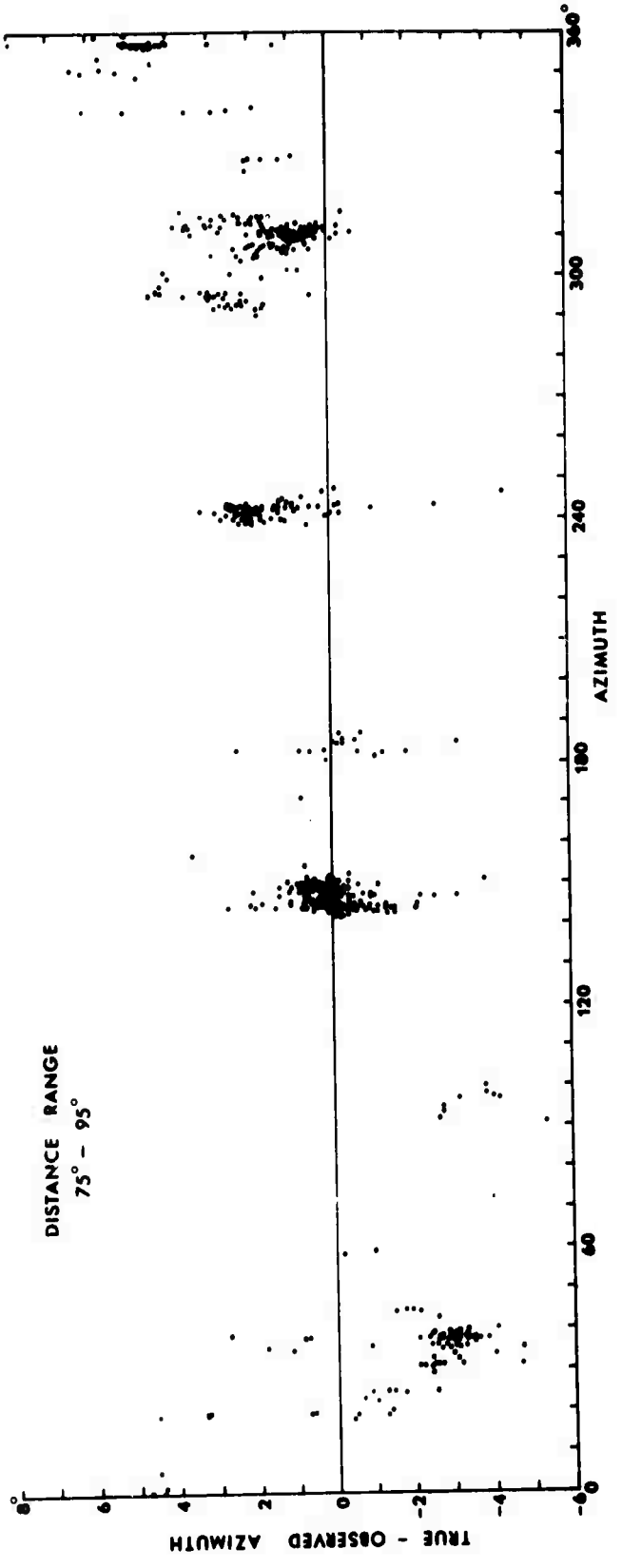
DISTANCE RANGE
75° - 95°
AZIMUTH
0
60
120
180
240
300
360°
TRUE - OBSERVED AZIMUTH
8°
6
4
2
0
-2
-4
-6°

Fig. 22

VI. OBSERVATIONS OF TRAVEL-TIME ANOMALIES

There is no doubt that the relative arrival times of P-waves across LASA show a surprising complexity. Many studies (e.g., Chiburis, 1966) have confirmed this, and there is little doubt that this complexity is, at least in part, due to structure beneath the array. However, attempts to use this complexity to determine the structure have met with little success.

At least part of the reason for this lies in the problem of defining the nature of the travel time anomalies at each sub-array. There are two basic ways to define these anomalies. First, the arrival times at the sub-arrays can be compared with those predicted by a standard travel-time curve. Second, the arrivals themselves may be fitted with a straight line or a curve, and the residuals from the fit defined as travel time anomalies. Each of these definitions has advantages and disadvantages, and may be applied to the data in various ways. They are discussed below:

(i) Departure from Standard Travel Times.

If the distance of an earthquake from the array is known, then any standard travel time table may be used to estimate the relative arrival times at the various sub-arrays. Many authors have used the Jeffreys-Bullen Tables for this purpose (e.g., Chiburis, 1966, Lincoln Laboratories Report LL-6, 1967, Greenfield and Sheppard, 1968). Other possiblities may include the Herrin Tables or any velocity model for the earth's interior, such as the model A of Chinnery (1969) (see section 7).

It would be nice if we could define the travel time anomaly at the ith station by

$$\Delta t_i = T_i^P - T_i^O \tag{6}$$

where T_i^P is the predicted time and T_i^O is the observed time. We cannot do this, of course, since (because of origin time errors) the absolute value of T_i^O is not known. We are forced therefore to select some reference time against which to measure the T_i^O. The simplest way to do this is to choose the arrival at one sub-array as a reference, and write

$$\Delta t_i - \Delta t_0 = (T_i^P - T_0^P) - (T_i^O - T_0^O) \tag{7}$$

The right hand side of this equation may be determined easily from the observations, and many authors have defined the "travel time anomaly" at the ith station as this quantity (Chiburis, 1966, Lincoln Laboratories Report LL-6, 1967, etc.). This definition may be satisfactory for calibrating the array, but is quite inadequate for studies of the crustal structure at the array, for two reasons.

In the first place, this definition includes only the difference between the structural contributions at the ith station and the reference station. This is particularly important if the station AO is chosen as reference, since AO is one of the more complex sites. Secondly, this definition of travel time anomaly attributes any difference between the standard model and

the true travel time curve to an effect at the sub-arrays. There is much evidence that any world-wide average travel time table may depart significantly from measurements along an individual profile on the earth's surface, and this is particularly true of the rather out-dated Jeffreys-Bullen Table. Each "travel time anomaly" will therefore be contaminated both by structure at the reference site and structure in the earth's interior.

The second of these problems can be minimized by using a set of travel times determined directly from the LASA data. As an example, Figure 23 shows the travel-time anomalies for sub-array F1 calculated using equation 7, with A0 as a reference sub-array, and predicted travel time differences according to model A (Chinnery, 1969; section 7 of this report). The anomalies for events to the Northwest of the array are plotted as a function of epicentral distance, and show a strong variation with distance.

The contribution from A0 can be reduced or removed by choosing some other reference for measuring time differences. If the arrival time at the ith station is T_i, referred to an arbitrary origin, then we may fit a curve to the data (as in equation 3) of the form

$$T_i - T_o + b\delta_i + c\delta_i^2 = 0 \qquad (8)$$

where, as before, δ_i is the distance from A0 along the azimuth to the event. T_o may be determined from the least squares fit and used as a reference time. The travel time anomalies with

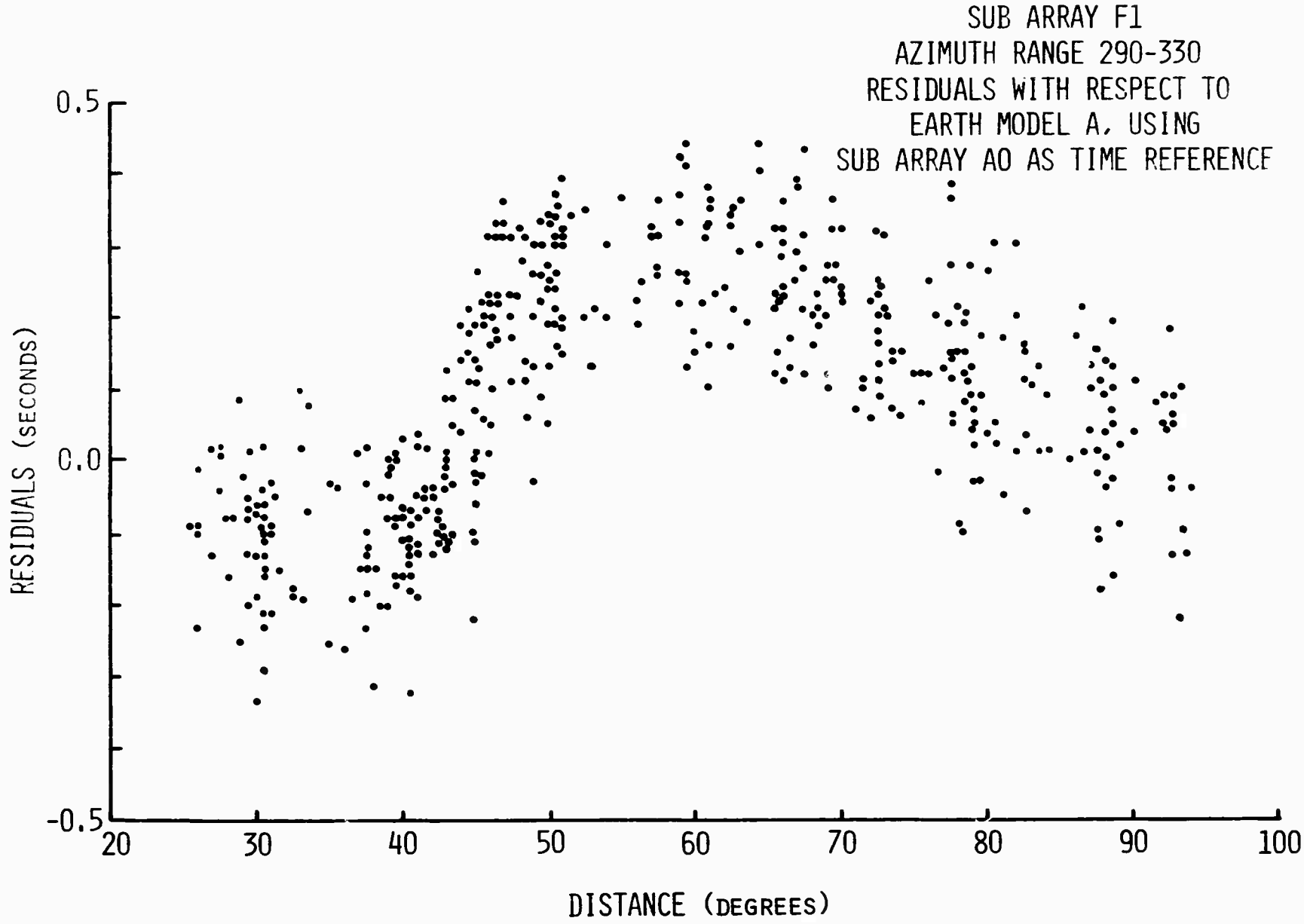
SUB ARRAY F1
AZIMUTH RANGE 290-330
RESIDUALS WITH RESPECT TO
EARTH MODEL A, USING
SUB ARRAY AO AS TIME REFERENCE
0.5
0.0
-0.5
RESIDUALS (SECONDS)
20
30
40
50
60
70
80
90
100
DISTANCE (DEGREES)

Fig. 23

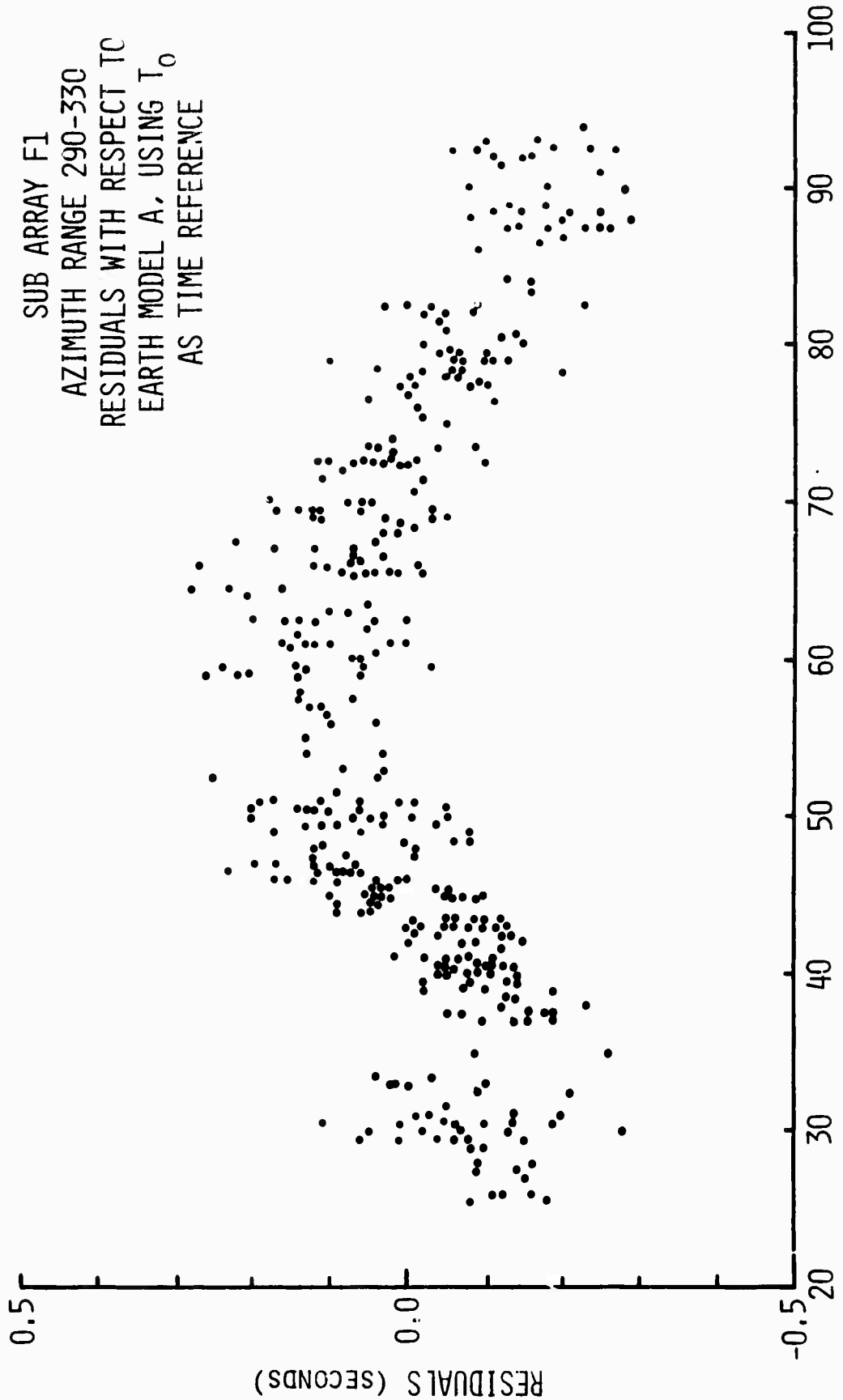
SUB ARRAY F1
AZIMUTH RANGE 290-330
RESIDUALS WITH RESPECT TO
EARTH MODEL A, USING T_0
AS TIME REFERENCE
0.5
0.0
-0.5
RESIDUALS (SECONDS)
20
30
40
50
60
70
80
90
100
DISTANCE (DEGREES)

Fig. 24

respect to this reference for sub-array F1 and velocity model A are shown in Figure 24. There is a considerable difference between this graph and Figure 23. Presumably at least part of the AO contribution has been removed.

Both of the techniques mentioned above may be criticized. The reality of model A is still questionable, and determination of T_o depends on all of the arrivals at the array and may be influenced by large-scale structure. However, these techniques should produce some improvement in the travel-time anomalies.

(ii) Residuals from Curve-Fitting.

Having fitted equation 8 to the data, the residuals at the sub-arrays may be regarded as travel-time anomalies. This definition of travel-time anomalies has the advantage that no assumptions about mantle structure are necessary. It has the same disadvantage as before, that the meaning of a fit such as this is not clear, and it may be influenced by large scale structure beneath the array.

Iyer and Healy (1971) proposed a similar definition for travel time anomalies, though they fitted a first degree equation (essentially equation 2). It turns out that there are only small differences between the 1st degree and 2nd degree residuals. Iyer and Healy then averaged the residuals from 9 events at various azimuths and distances, and used the variation of the average residual across the array to make conclusions about the crustal structure.

Since these residuals have not been studied in detail, the 2nd degree residuals for the 9 sub-arrays used in this study are shown in Figures 25-33. Clearly there are strong variations of the residuals with epicentral distance, at some of the sub-arrays. Similar complex variations occur as a function of azimuth. These variations are of the same order of magnitude as those found by Chiburis (1966), but have a different form since they are defined differently. The apparently small residuals at sub-arrays F2 and F4 are an inevitable result of any fitting process to events at this azimuth, since δ_i is largest for these sub-arrays. The magnitude of the variations throws some doubt on the averaging method of Iyer and Healy.

The 2nd degree residual for sub-array F1 (Figure 30) is very similar to the anomalies with respect to model A (Figures 24). This is hardly surprising, since model A was determined from the present data. However, this points out the underlying assumption of using least square residuals as travel time anomalies. A velocity structure very like model A is implied to be valid.

These residuals may be contoured across the array, in the same way that the authors mentioned have contoured travel time anomalies. Figure 34 shows an outline of the array, and Figures 35-38 show the mean residuals at distances of 40, 55, 70 and 90°, at the same scale. The contours, though schematic, have several interesting features. The values at 90° indicate a Northeast-Southwest trend which is similar to the conclusions

of others (e.g., Greenfield and Sheppard, 1968). At closer distances there appears to be evidence for a superimposed Northwest-Southeast trend. The reality of this trend and its interpretation are not clear at present. However, the variation in the contours with distance is significant, and has been disregarded in previous studies.

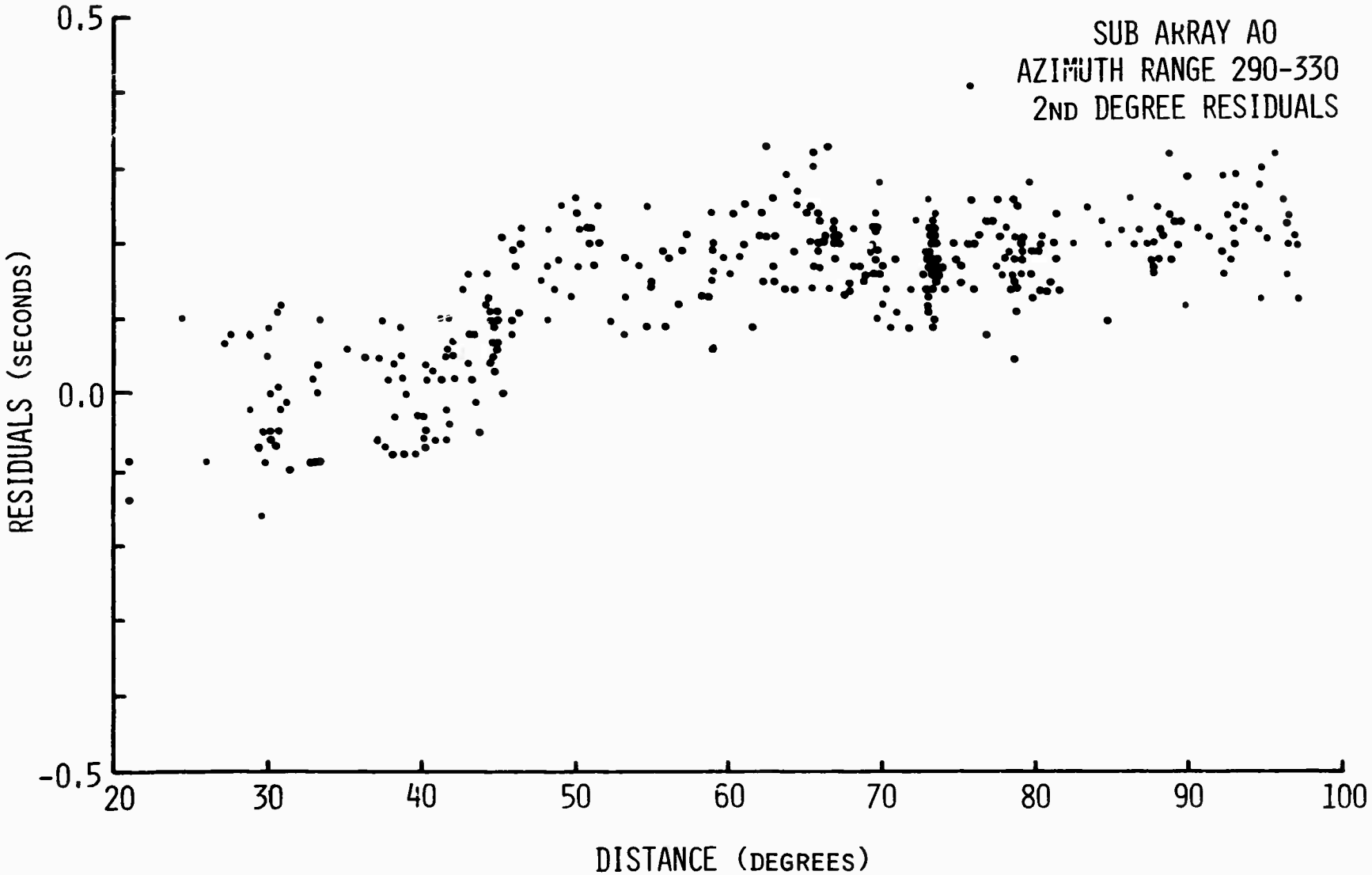
SUB ARRAY A0
AZIMUTH RANGE 290-330
2ND DEGREE RESIDUALS
RESIDUALS (SECONDS)
0.5
0.0
-0.5
20
30
40
50
60
70
80
90
100
DISTANCE (DEGREES)

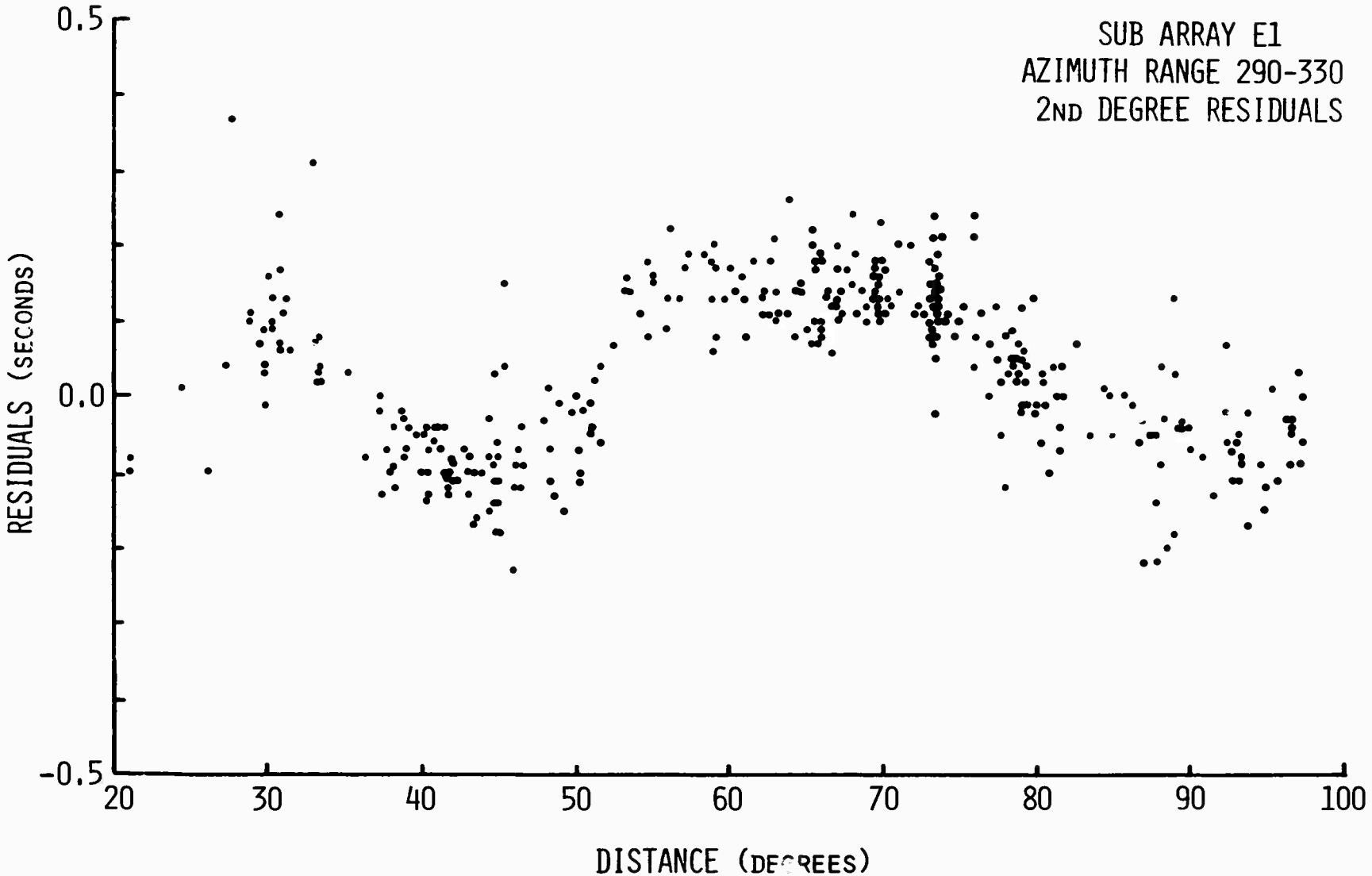
SUB ARRAY E1
AZIMUTH RANGE 290-330
2ND DEGREE RESIDUALS
RESIDUALS (SECONDS)
0.5
0.0
-0.5
20
30
40
50
60
70
80
90
100
DISTANCE (DEGREES)

Fig. 26

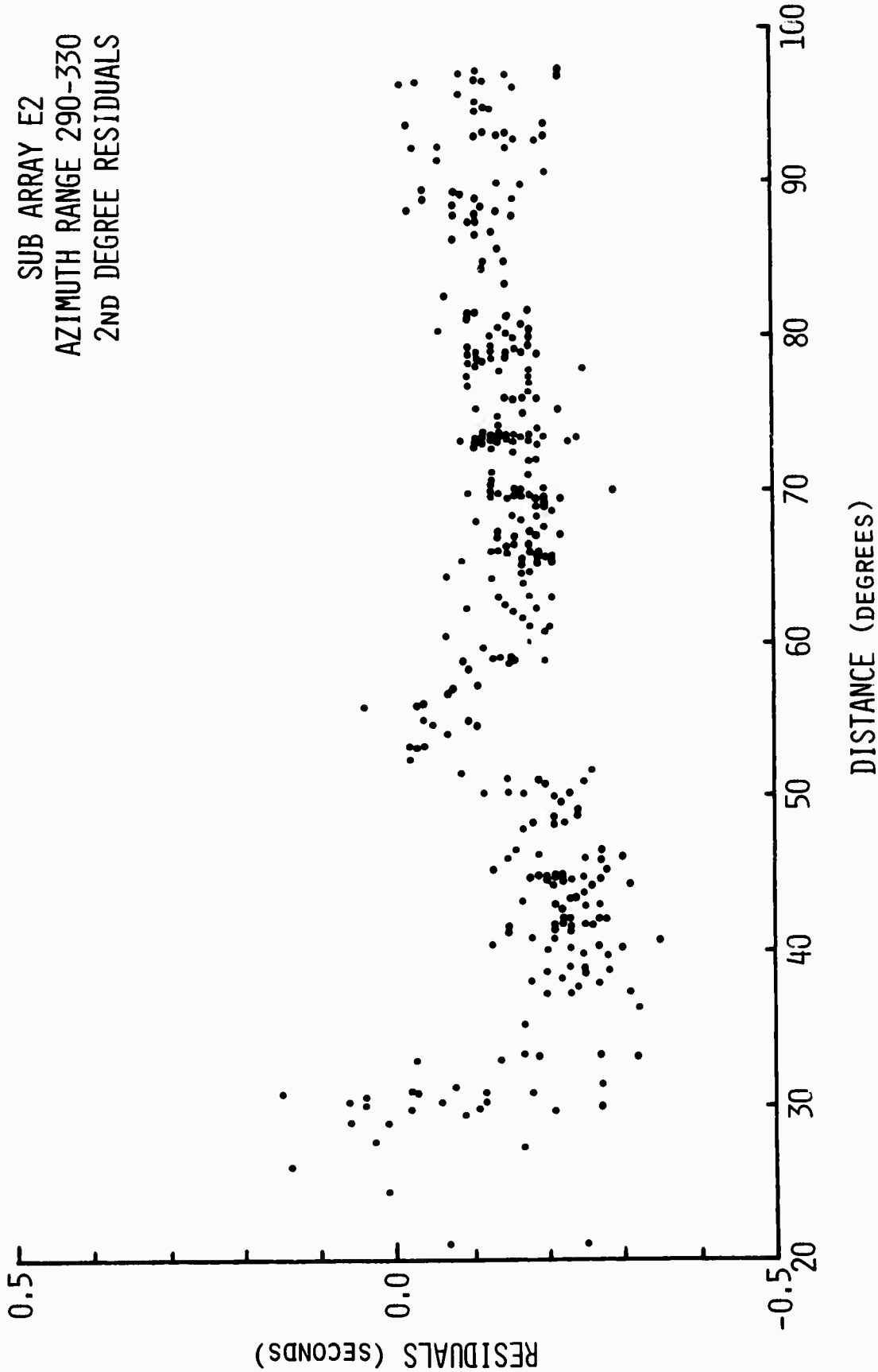
SUB ARRAY E2
AZIMUTH RANGE 290-330
2ND DEGREE RESIDUALS
RESIDUALS (SECONDS)
0.5
0.0
-0.5
20
30
40
50
60
70
80
90
100
DISTANCE (DEGREES)

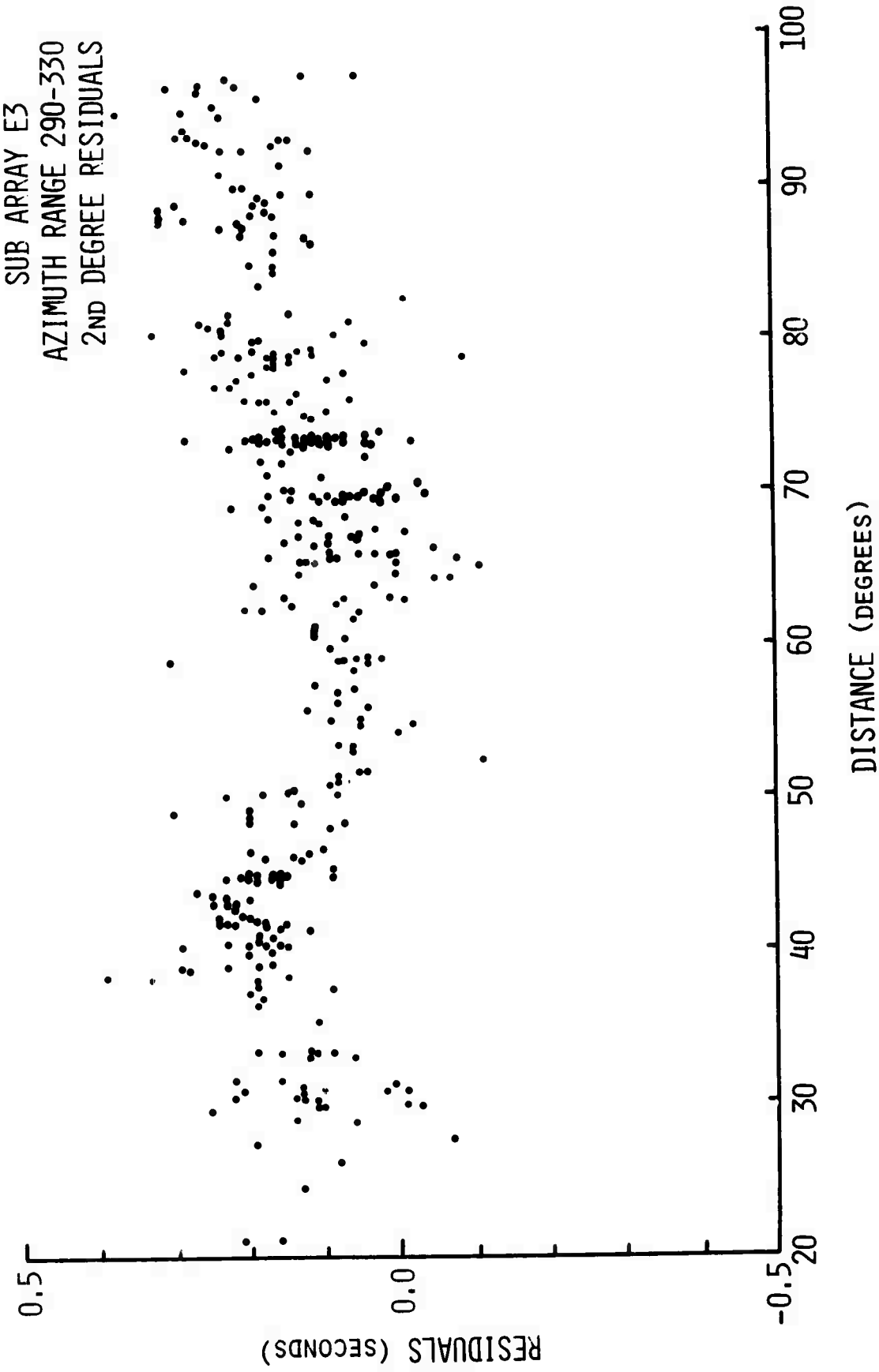
SUB ARRAY E3
AZIMUTH RANGE 290-330
2ND DEGREE RESIDUALS
0.5
0.0
-0.5
RESIDUALS (SECONDS)
20
30
40
50
60
70
80
90
100
DISTANCE (DEGREES)

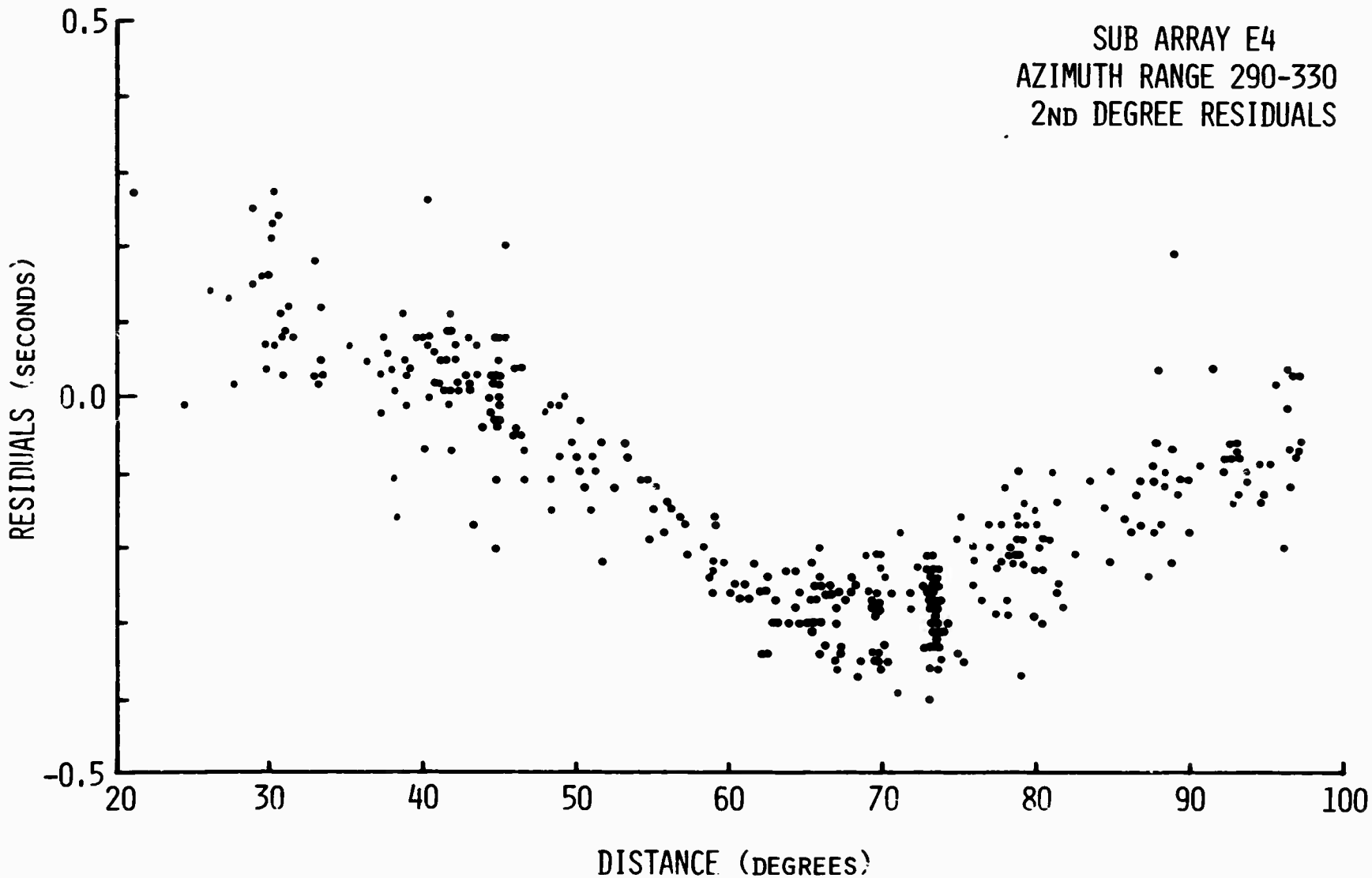
SUB ARRAY E4
AZIMUTH RANGE 290-330
2ND DEGREE RESIDUALS
RESIDUALS (SECONDS)
0.5
0.0
-0.5
20
30
40
50
60
70
80
90
100
DISTANCE (DEGREES)

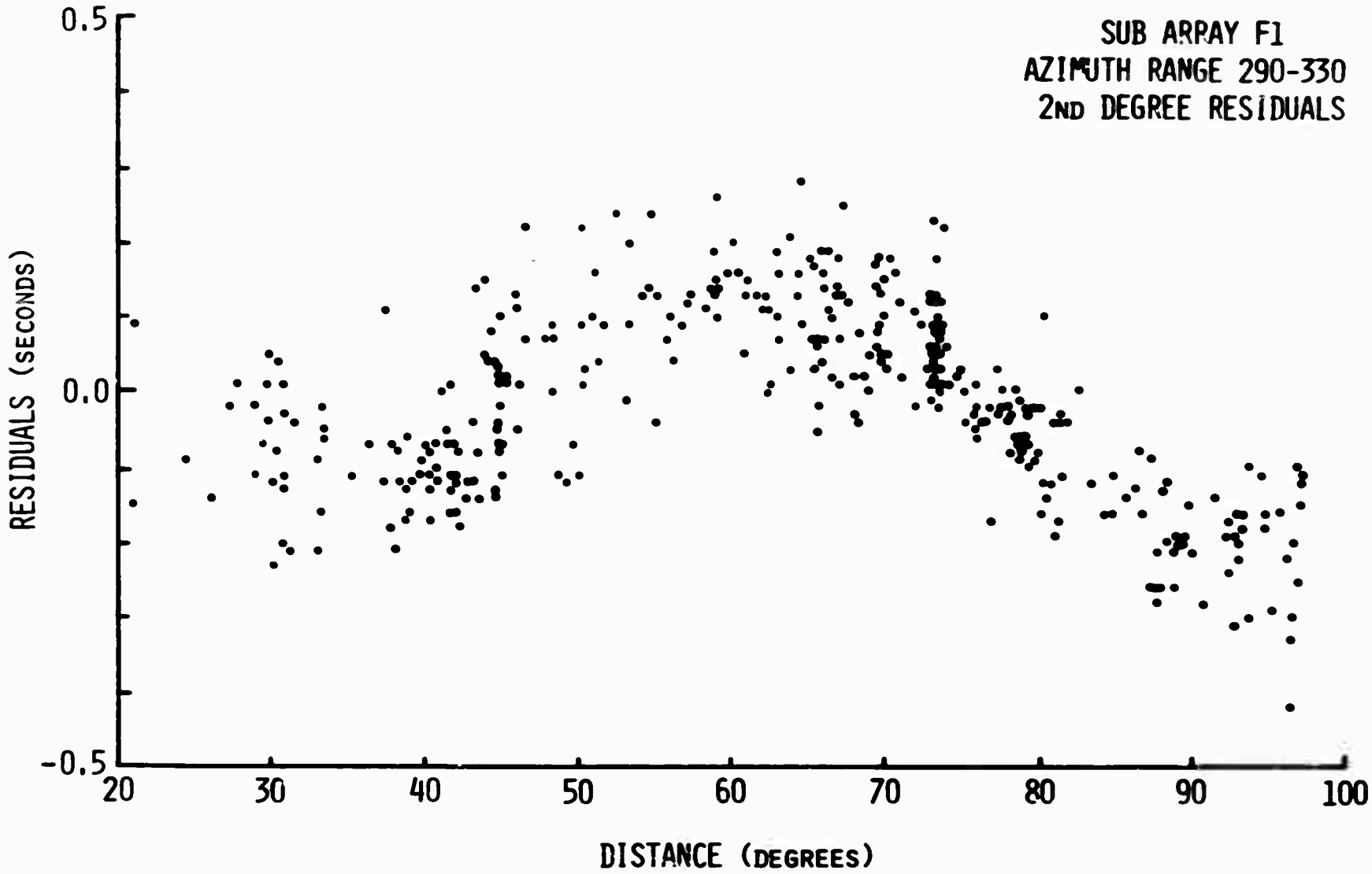
SUB ARRAY F1
AZIMUTH RANGE 290-330
2ND DEGREE RESIDUALS
RESIDUALS (SECONDS)
0.5
0.0
-0.5
20
30
40
50
60
70
80
90
100
DISTANCE (DEGREES)

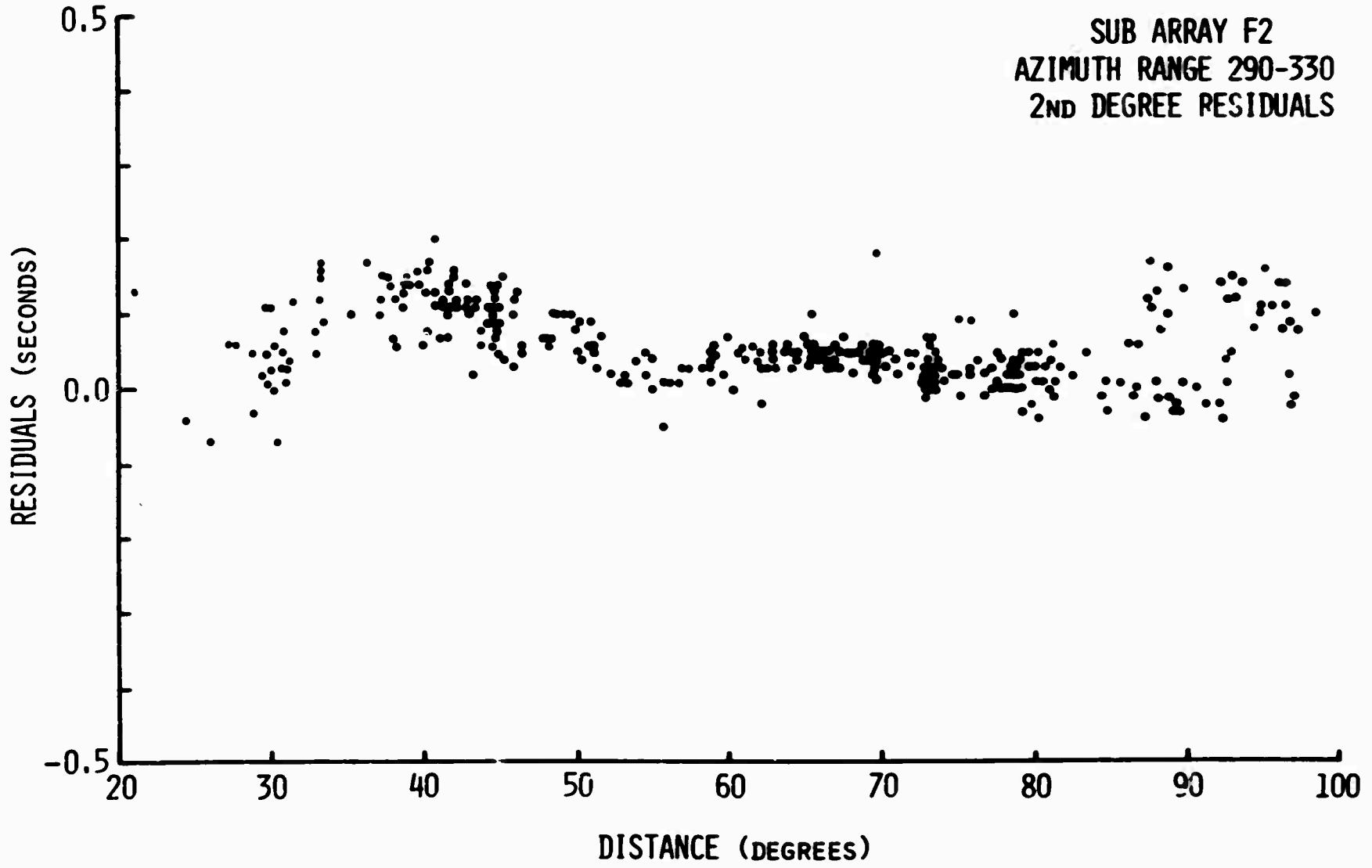
SUB ARRAY F2
AZIMUTH RANGE 290-330
2ND DEGREE RESIDUALS
RESIDUALS (SECONDS)
0.5
0.0
-0.5
20
30
40
50
60
70
80
90
100
DISTANCE (DEGREES)

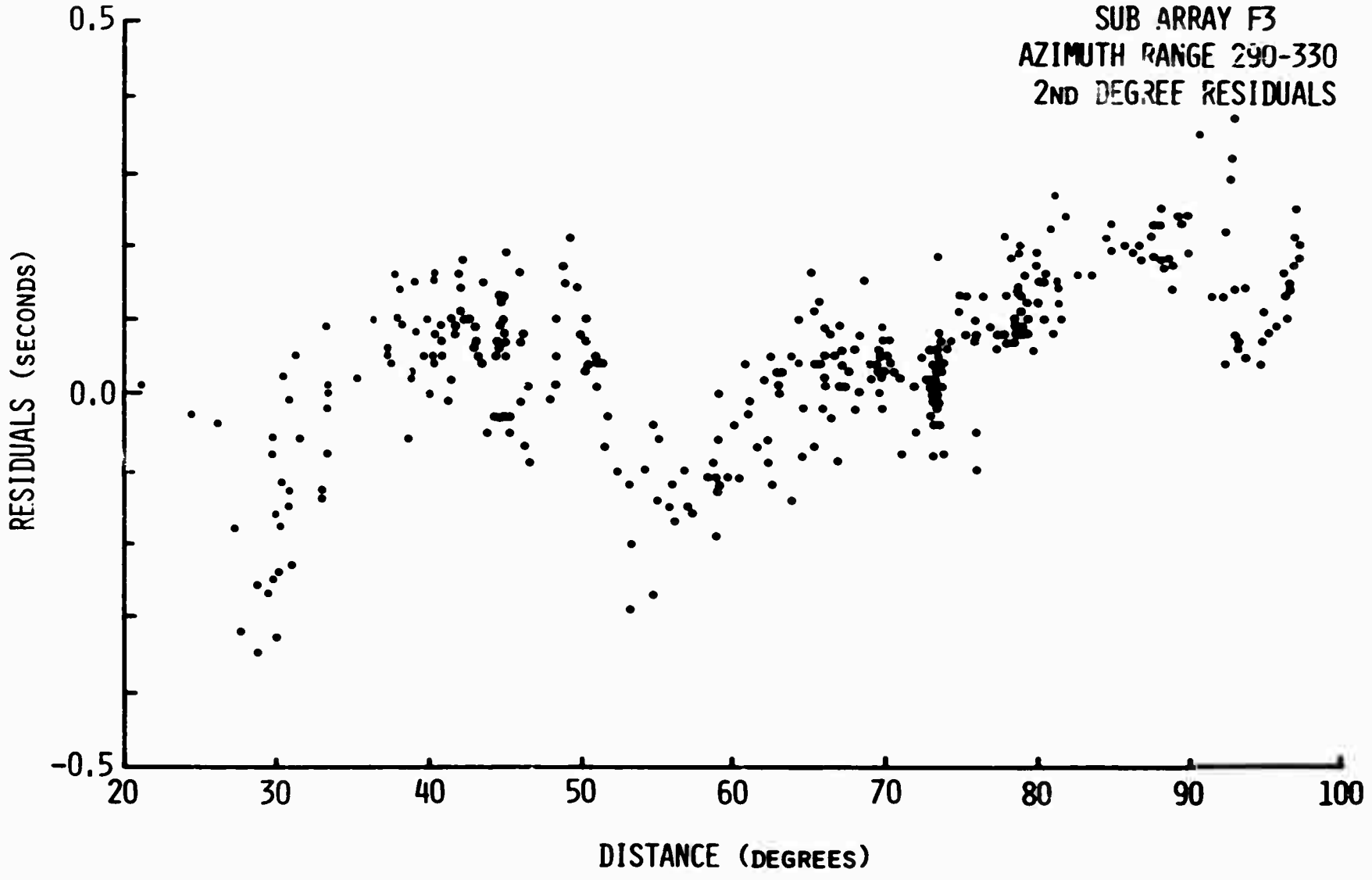
SUB ARRAY F3
AZIMUTH RANGE 290-330
2ND DEGREE RESIDUALS
0.5
0.0
-0.5
RESIDUALS (SECONDS)
20
30
40
50
60
70
80
90
100
DISTANCE (DEGREES)

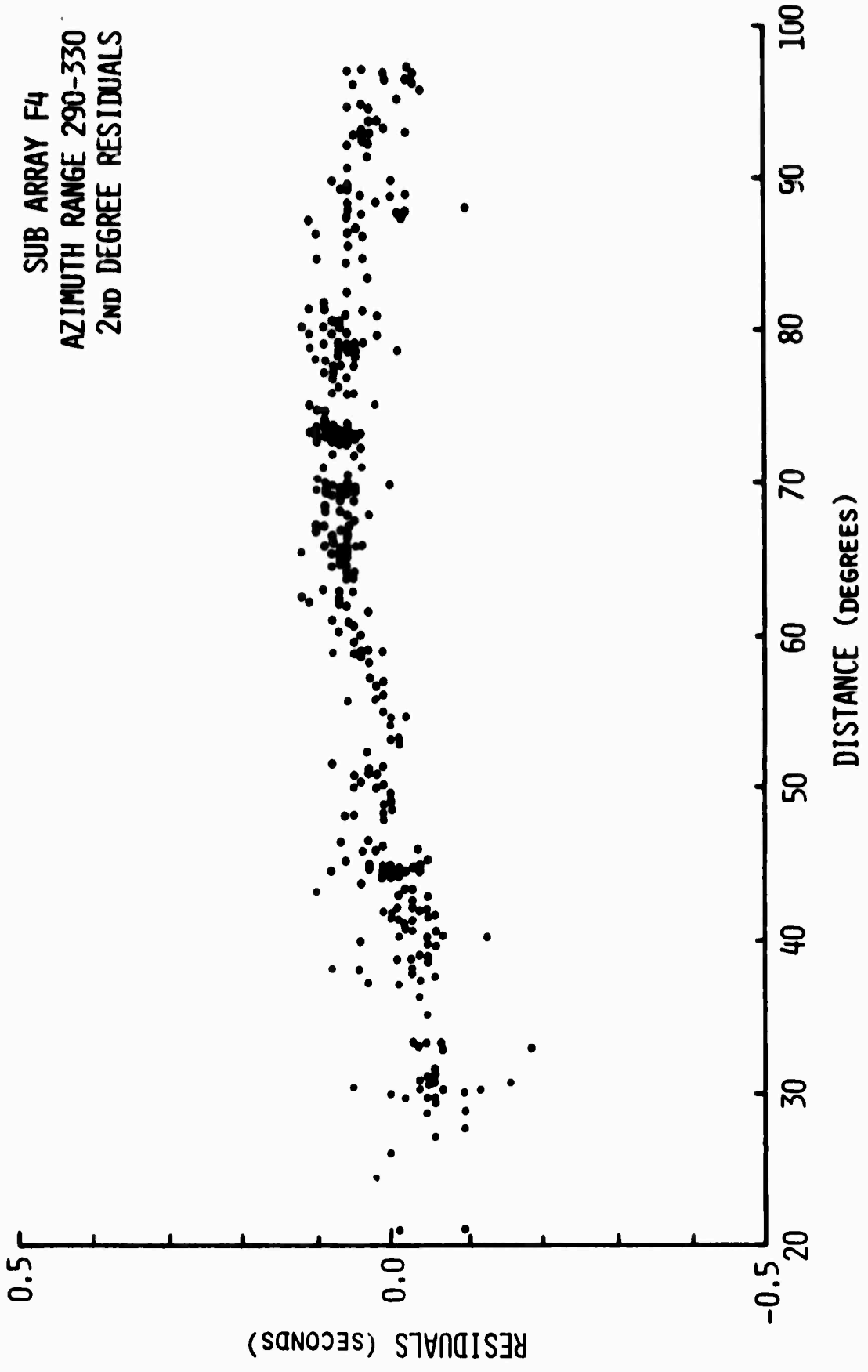
SUB ARRAY F4
AZIMUTH RANGE 290-330
2ND DEGREE RESIDUALS
RESIDUALS (SECONDS)
0.5
0.0
-0.5
20
30
40
50
60
70
80
90
100
DISTANCE (DEGREES)

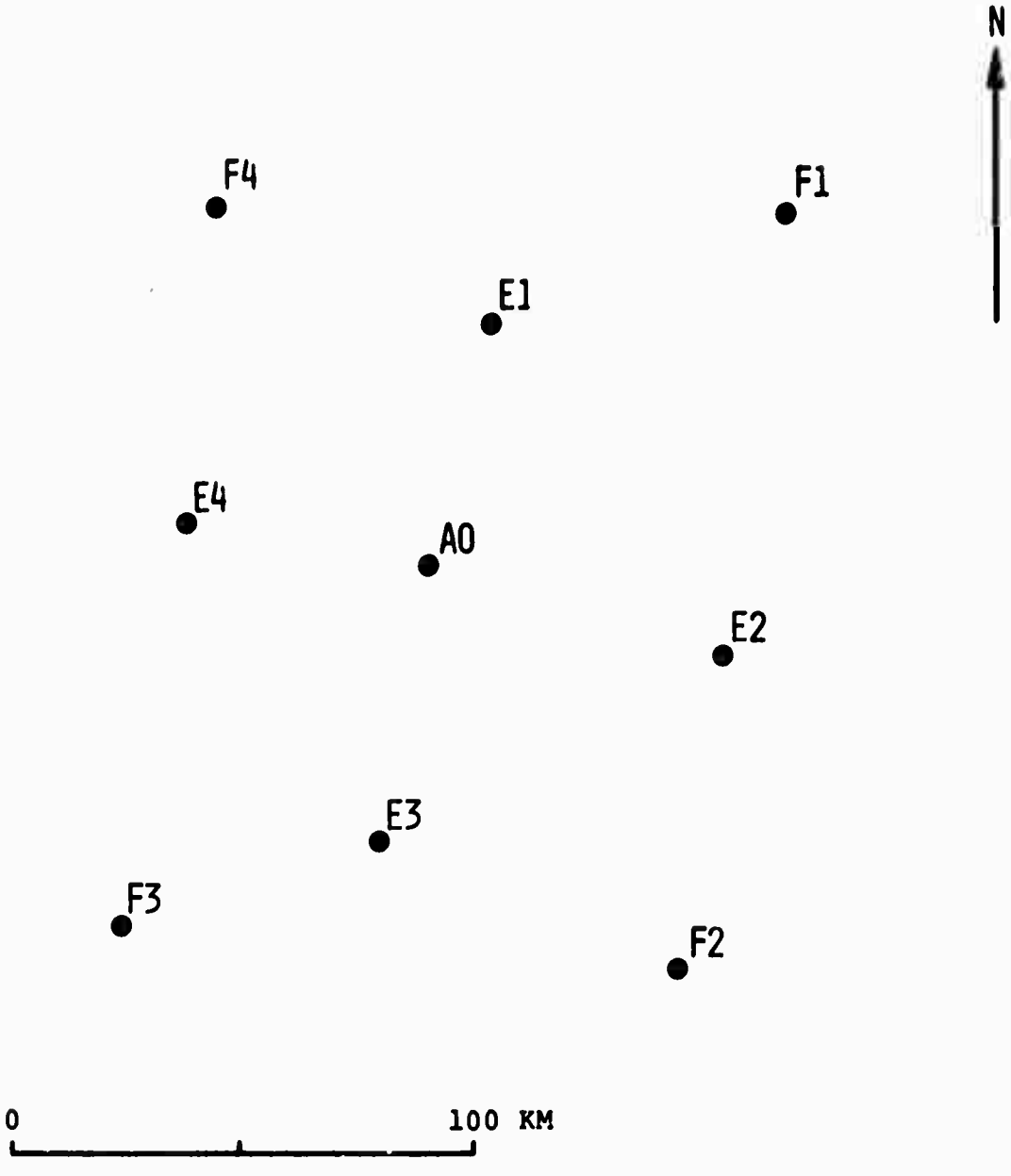

FIG. 34: ARRAY GEOMETRY, AT SAME SCALE AS FIGURES 35-38.

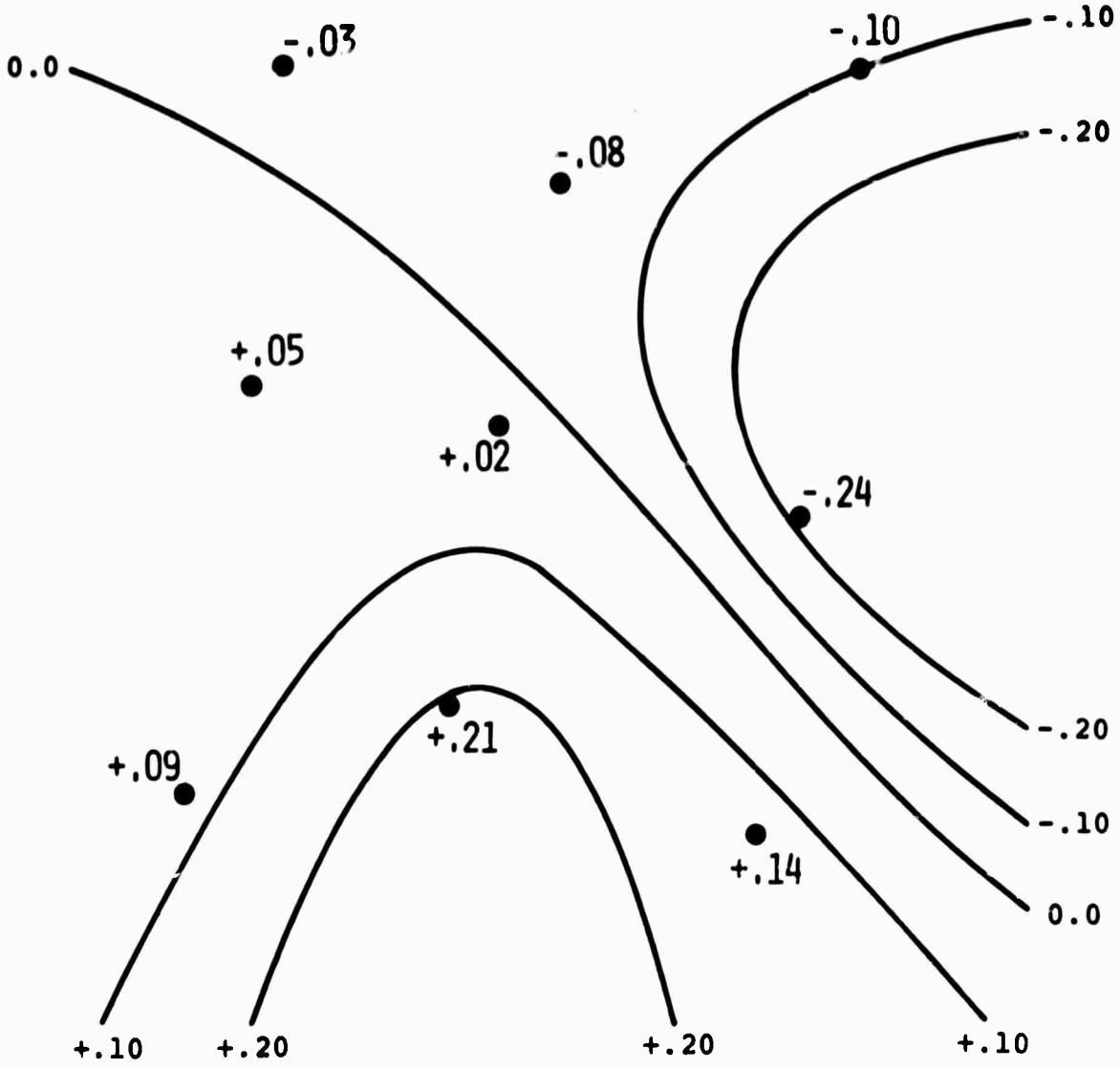

FIG. 35: CONTOURED 2ND DEGREE RESIDUALS (IN SECONDS) FOR EVENTS IN AZIMUTH RANGE 290-330, AT AN EPICENTRAL DISTANCE OF 40^{o}. FOR SCALE SEE FIGURE 34.

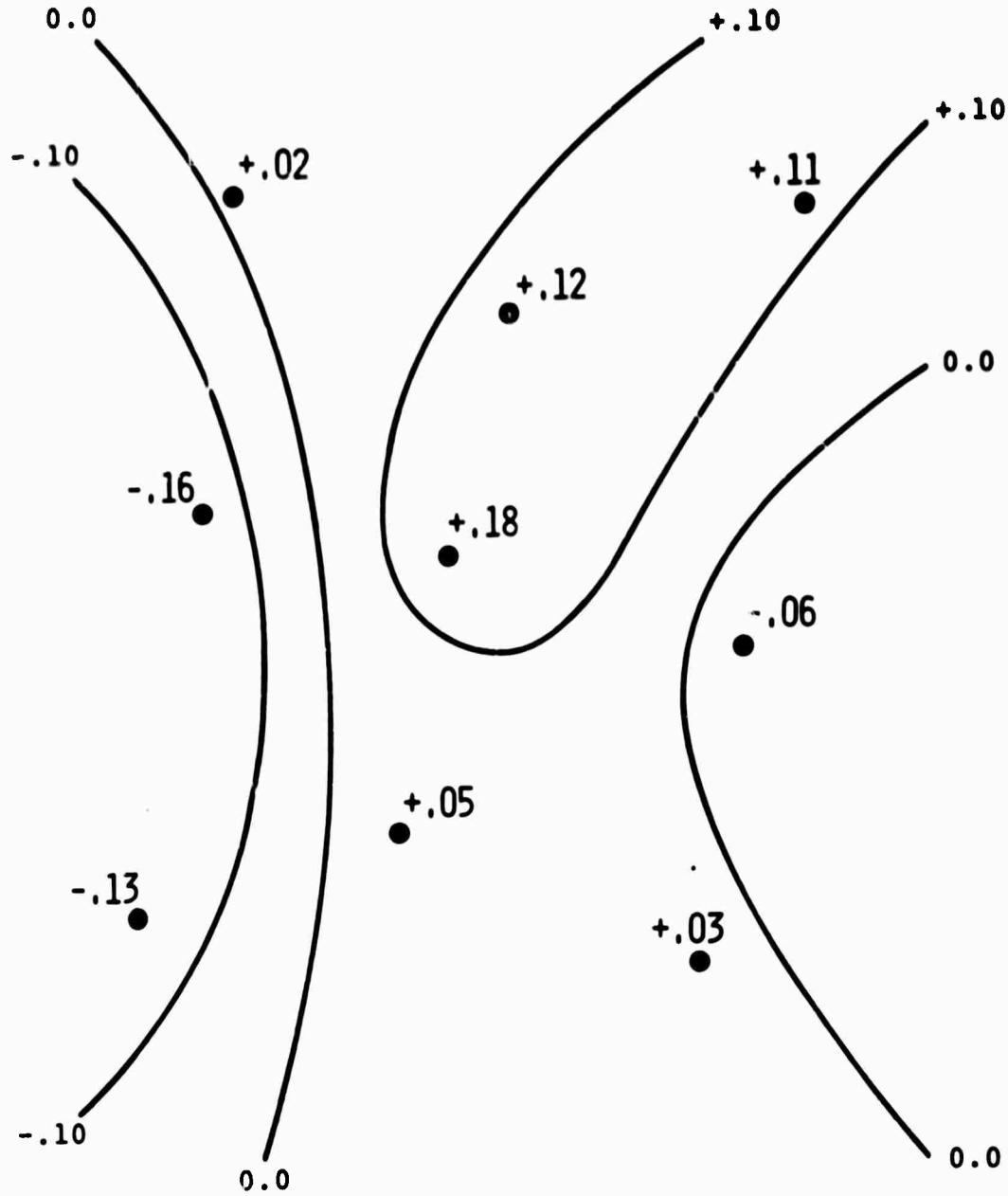

FIG. 36: CONTOURED 2ND DEGREE RESIDUALS (IN SECONDS) FOR EVENTS IN AZIMUTH RANGE 290-330, AT AN EPICENTRAL DISTANCE OF 55^{0}, FOR SCALE SEE FIGURE 34.

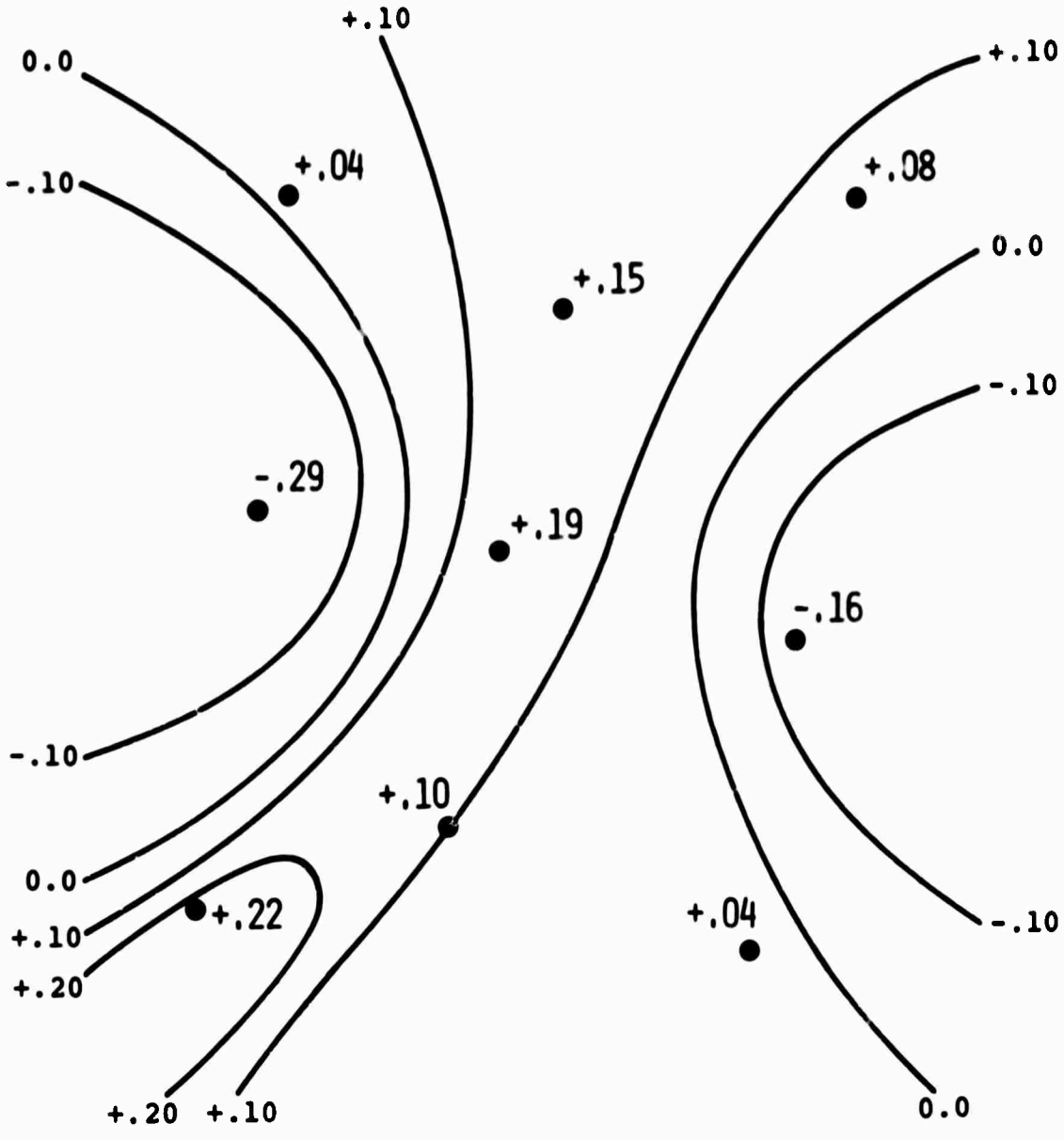

FIG. 37: CONTOURED 2ND DEGREE RESIDUALS (IN SECONDS) FOR EVENTS IN AZIMUTH RANGE 290-330, AT AN EPICENTRAL DISTANCE OF 70°. FOR SCALE SEE FIGURE 34.

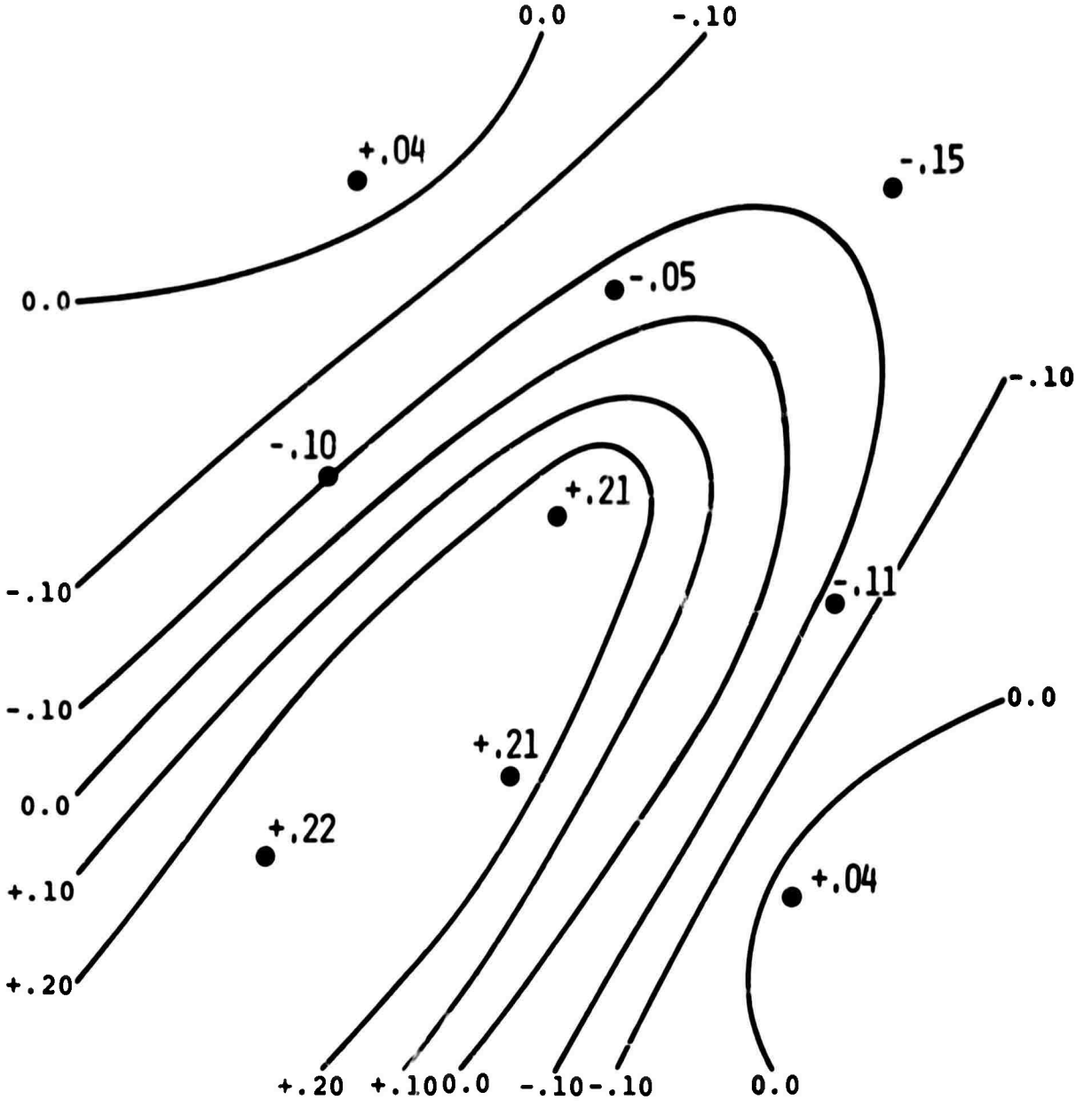

FIG. 38: CONTOURED 2ND DEGREE RESIDUALS (IN SECONDS) FOR EVENTS IN AZIMUTH RANGE 290-330, AT AN EPICENTRAL DISTANCE OF 90^{0}. FOR SCALE SEE FIGURE 34.

VII. INTERPRETATION OF dT/dΔ VERSUS DISTANCE (AZIMUTH RANGE 290-330)

An interpretation of the measurements of dT/dΔ shown in Figures 5 and 6, for the azimuth range 290-330, has been given in Chinnery (1969). The inferred velocity structures are shown in Figures 39-42. The velocity structures were obtained by a two-stage process. First, a curve was fitted visually to the dT/dΔ data, and then this was inverted into a velocity structure using the well-known Weichert-Herglotz technique. The resulting velocity structure was then used to recalculate dT/dΔ as a function of distance, and it is this curve that is shown through the data points. This technique largely overcomes any uniqueness problems in the Weichert-Herglotz method, except those introduced by scatter in the data. The additional data points shown in Figures 5 and 6 have not made any significant change to this interpretation.

There are several points about this interpretation that deserve consideration here, in the light of data obtained since the paper was published. First, some doubts were thrown on the interpretation because station corrections at the array were not included. The reason for this given in the paper was that the addition of station corrections will modify the shape of the curve of dT/dΔ against distance, and so change the travel time residuals of the curve with respect to the Jeffreys-Bullen table. (These residuals are simply the cumulative area between the two curves.) The nature of the modification will depend on the structure assumed in the calculation of the station corrections.

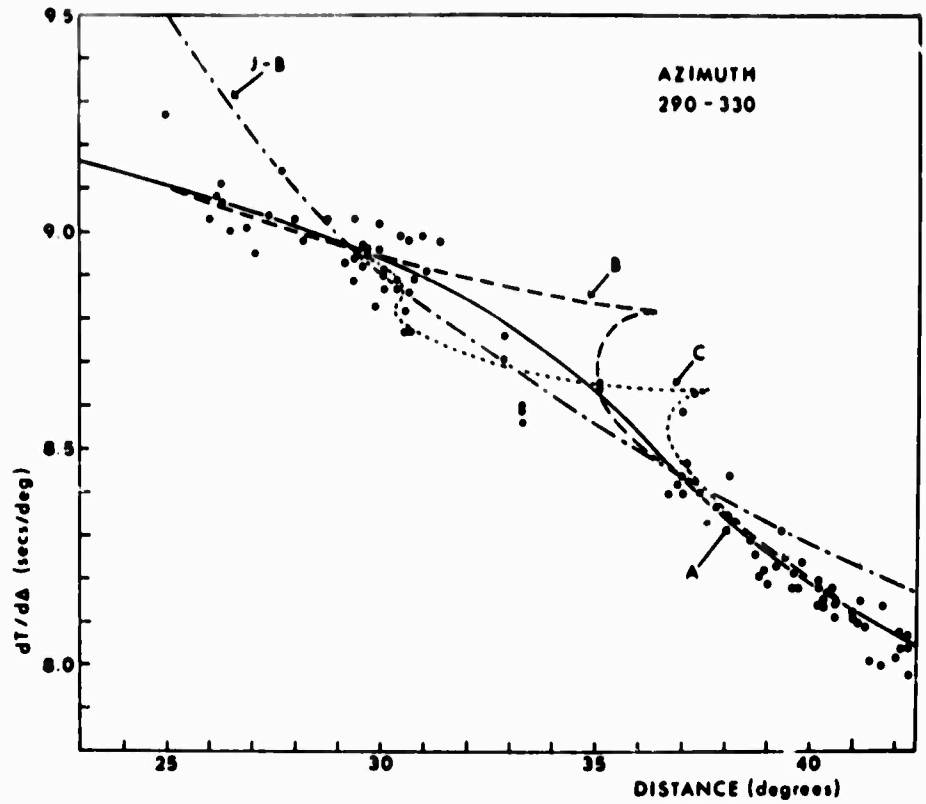

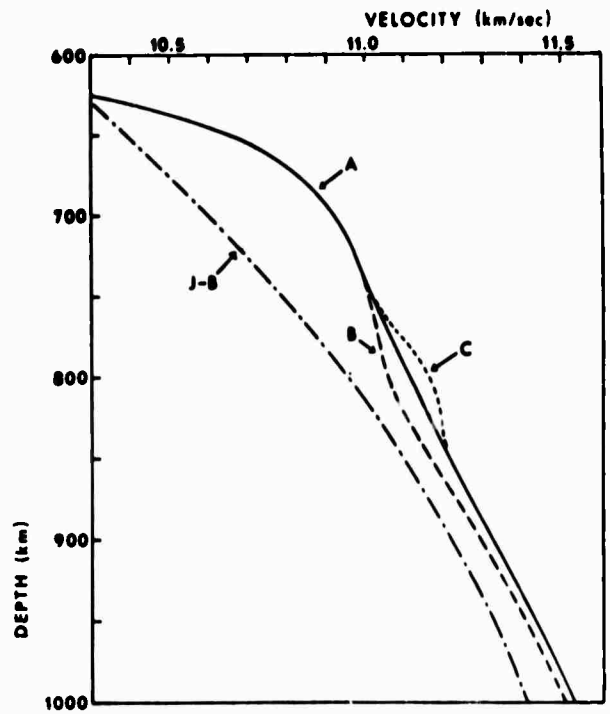

Fig. 39: (After Chinnery, 1969)

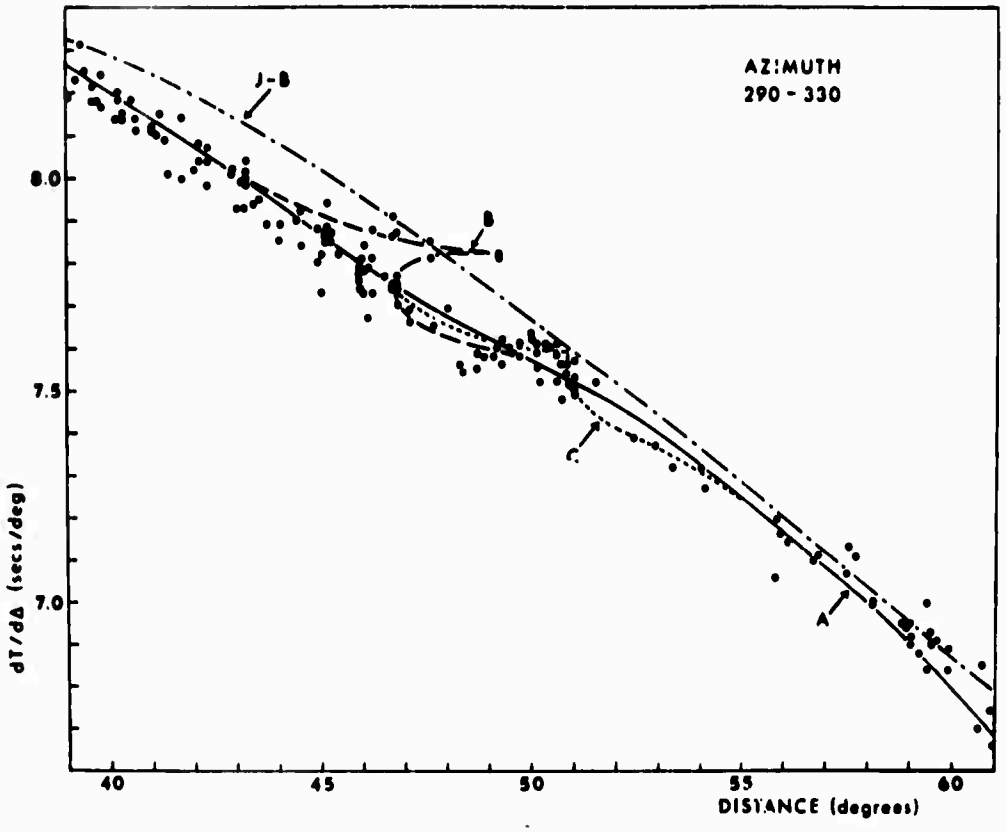

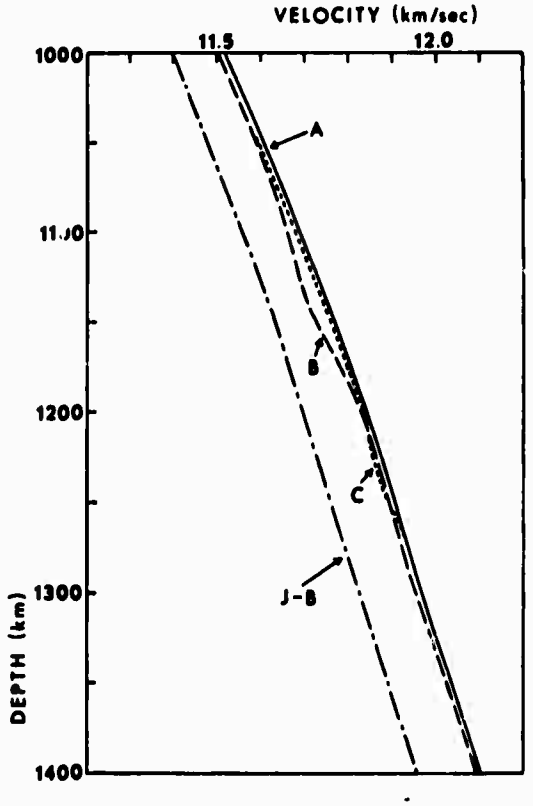

Fig. 40: (After Chinnery, 1969)

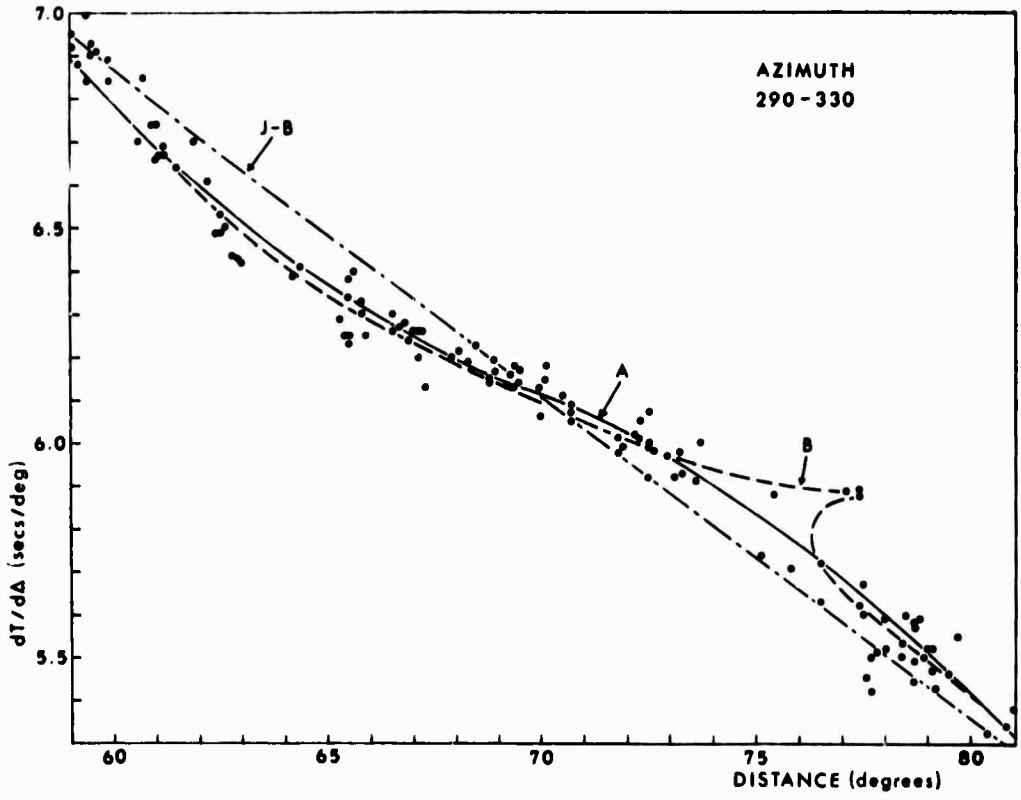

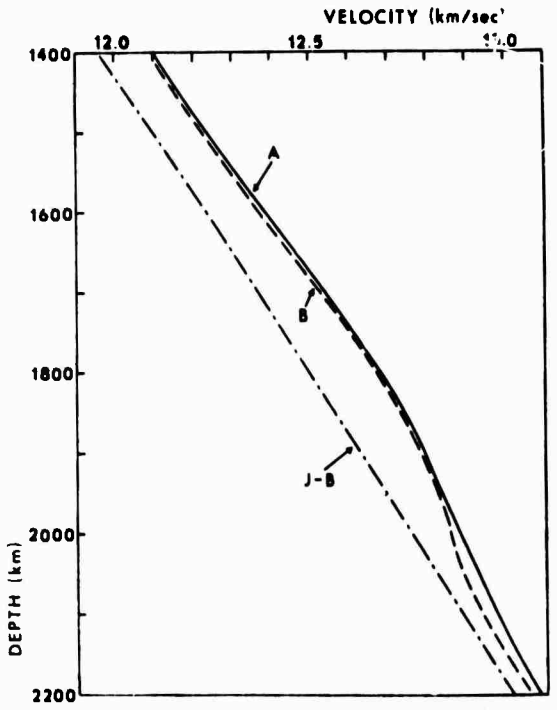

Fig. 41: (After Chinnery, 1969)

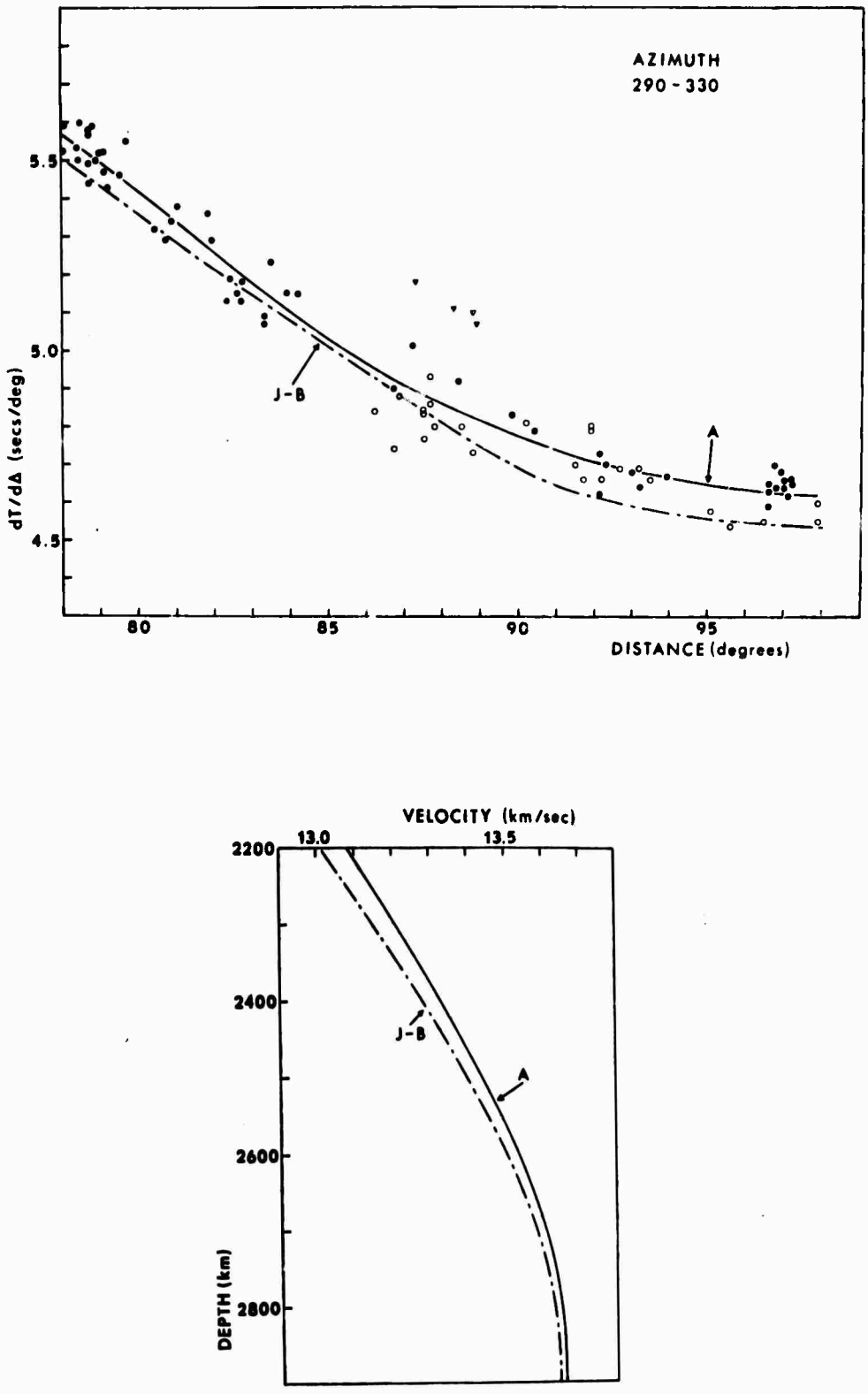

Fig. 42: (After Chinnery, 1969)

A simple dipping interface will raise or lower the observations with respect to the Jeffreys-Bullen curve. More complicated structures will distort the curve. However, the T-JB residuals of the uncorrected observations agree surprisingly well with the T-JB residuals at North American stations from the Longshot nuclear event, in the Aleutian Islands (Figure 43). The travel paths for this event were very similar to those involved in this study. It is therefore concluded that station corrections for the azimuth range 290-330^{o} must be very small, and may to a first approximation be neglected.

More recently a number of other arrays have been used to determine $dT/d\Delta$. Figure 44 shows that results of Johnson (1969), who used the TFSO array, and Corbishley (1970), who combined the data from four arrays. Figure 45 shows the results obtained by Wright (1971) using the Warramunga array in Australia. Although none of these newer studies have the resolution (small scatter) and amount of data contained in Figures 5 and 6, the similarities between the results are striking. Again, this strongly argues that the data in the present study should not be distorted by the addition of station corrections.

Further evidence on this point is obtained from amplitude studies, since the amplitude of an arrival depends strongly on the second derivative $d^2T/d\Delta^2$. Figure 46 shows how the logarithm of the slope of the $dT/d\Delta$ graph varies with distance, compared with the amplitude observations of Carpenter et al. (1967), using an arbitrary zero. Again a remarkable agreement is seen.

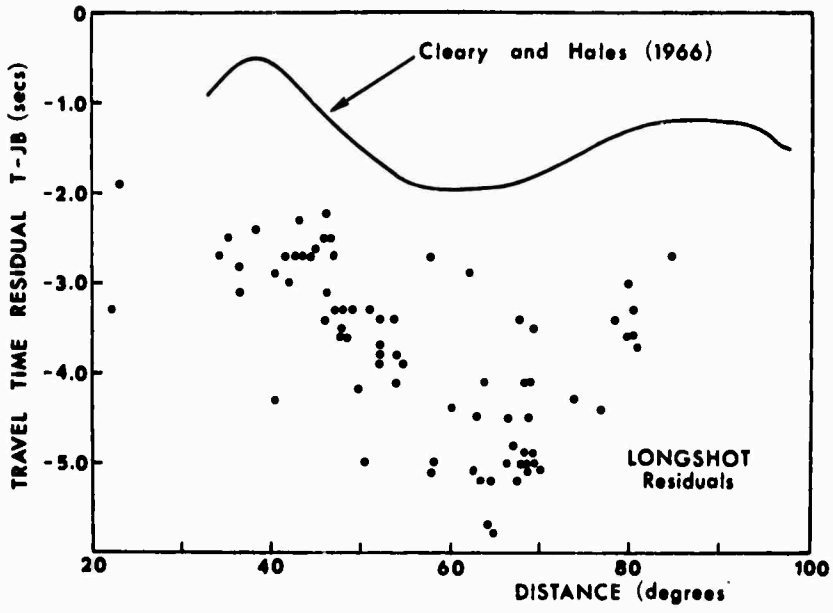

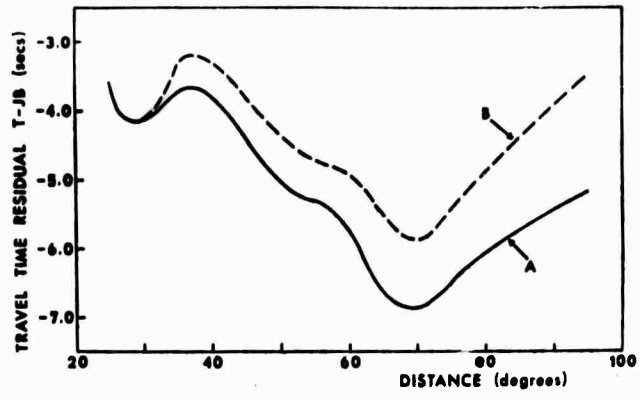

Fig. 43: Travel time residuals with respect to the Jeffreys-Bullen Tables; above, observations of the LONGSHOT test, below, corresponding to models A and B in figures 39-42. (After Chinnery, 1969)

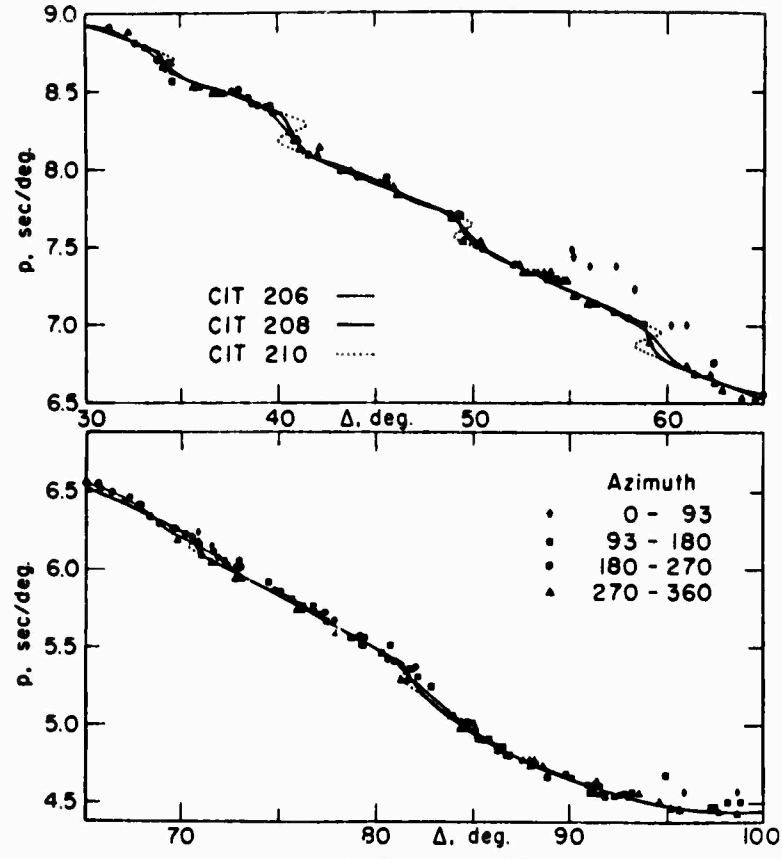

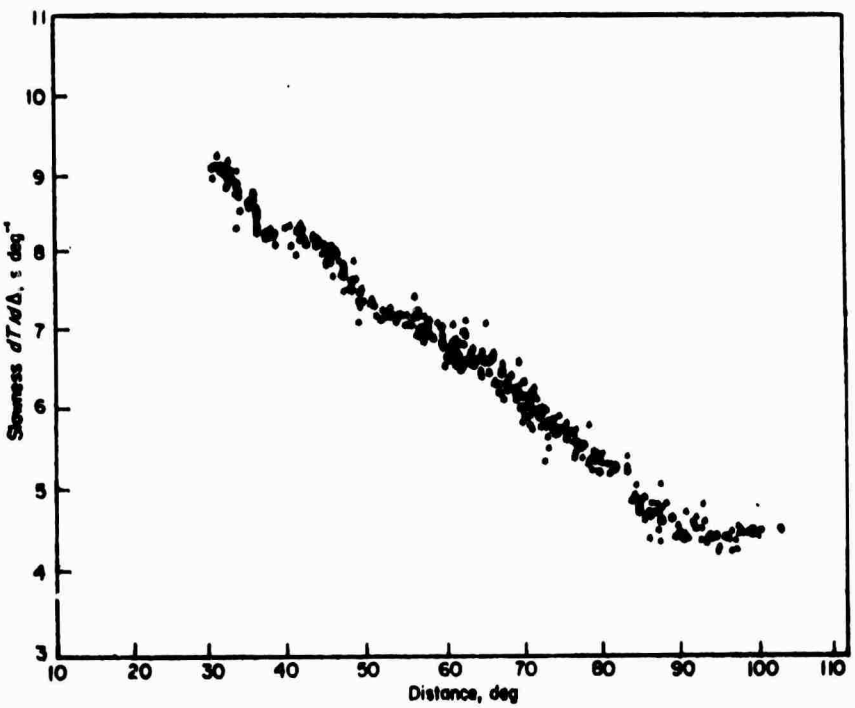

Fig. 44: Other observations of dT/dΔ; above, from Johnson (1969), below, from Corbishley (1970).

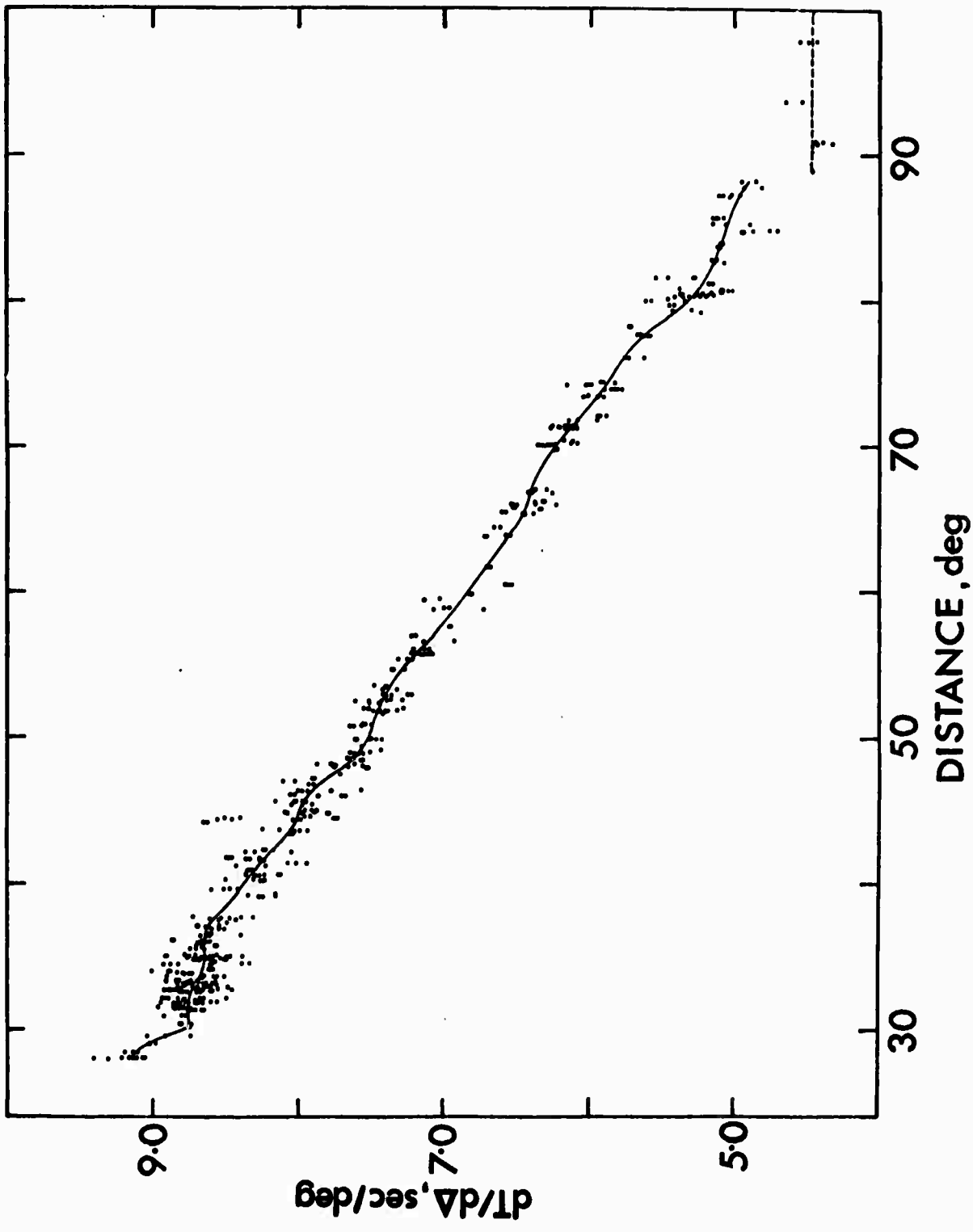

Fig. 45: Observations of dT/dΔ by Wright (1971).

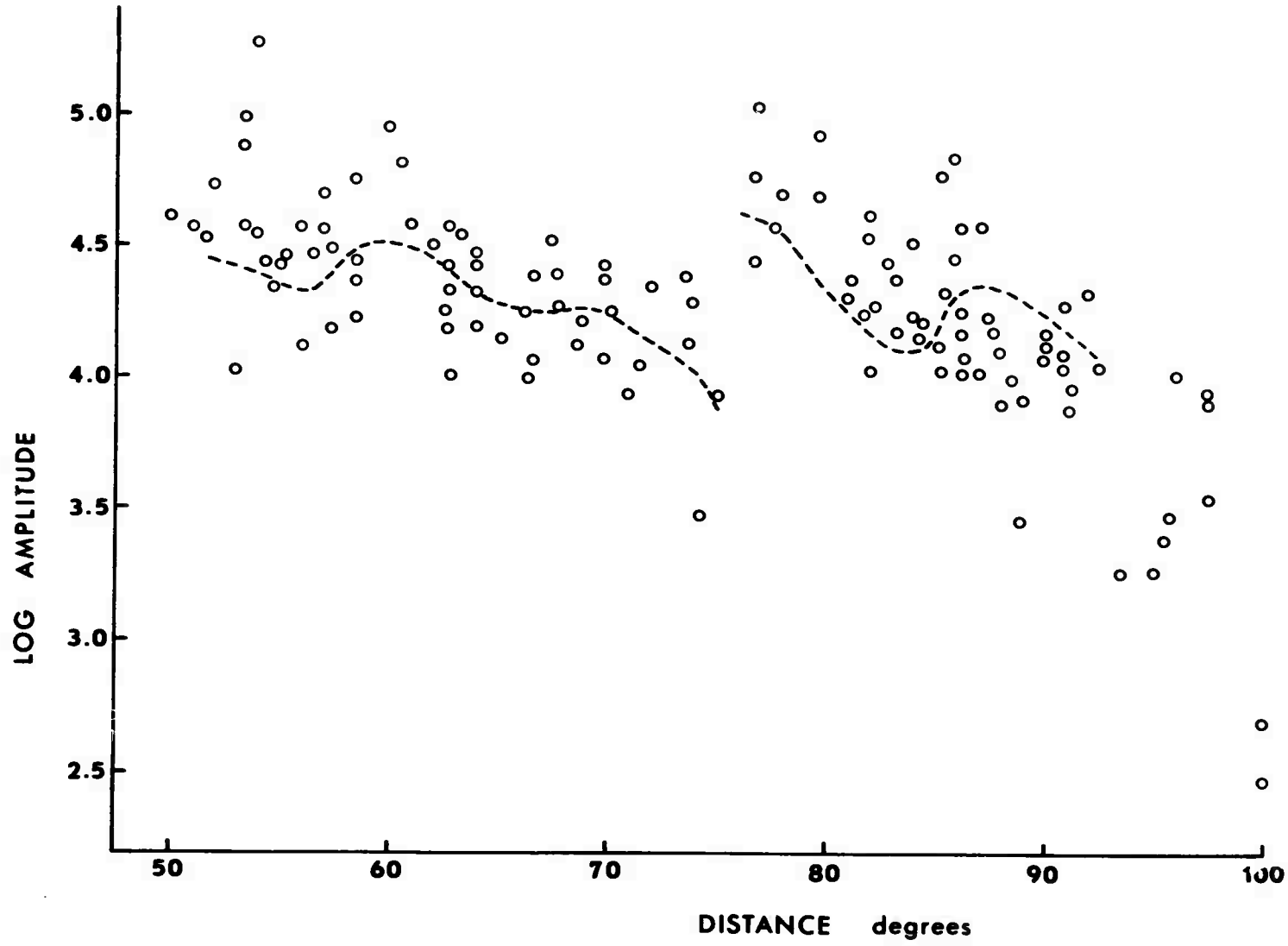

Fig. 46: Comparison of the amplitude-distance measurements of Carpenter et al (1967) with the logarithm of $d^2T/d\Delta^2$ for model B (figures 39-42) using an arbitrary origin.

We conclude that the smooth model A or the less smooth model B, shown in Figures 39-42, are reliable structures for the paths concerned in this study.

We may also return to our earlier comment that the scatter of the $dT/d\Delta$ observations is unusually large in two distance ranges, 32-37° and 83-88°. The latter will be discussed in the next section. The former has become interesting because of a suggestion, by Wright (1968, 1971), that a triplication may occur in the vicinity of 35°, as the result of a low velocity layer in the mantle at a depth of about 850 km. Wright's $dT/d\Delta$ data were obtained using the Warramunga array, and show a very similar structure to those in Figure 5 at this distance. It is very likely, therefore, that this effect is real. A possible interpretation of the present data, in terms of a low velocity layer, is shown in Figure 47. A variety of models are possible, since data in the vicinity of 35° is sparse, but the model AN shown is representative. Further studies of this feature are continuing.

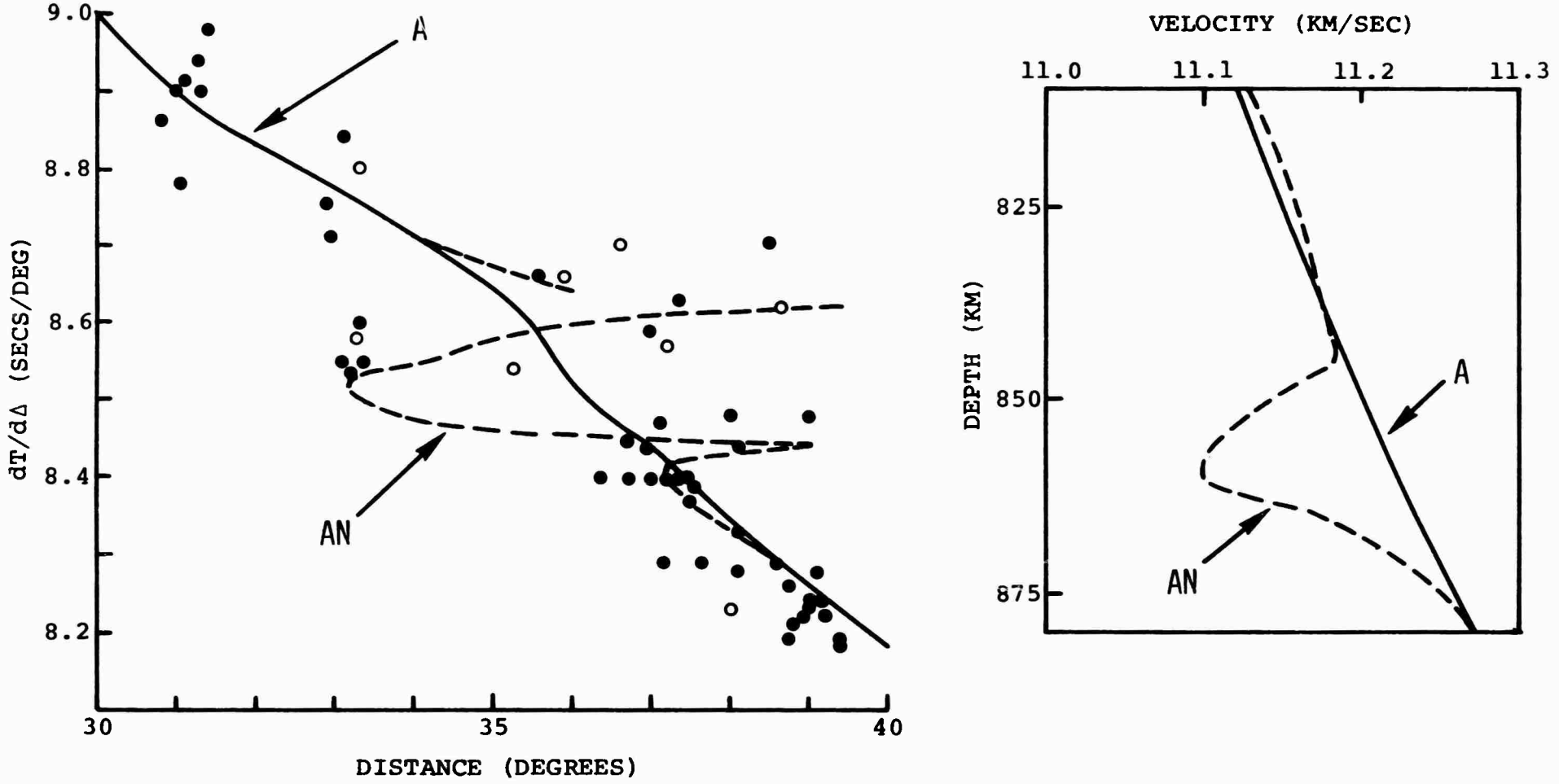

Fig. 47: An alternative interpretation of the scatter of observations in the distance range 33-39°, suggested by the work of Wright (1968). The data points marked by open circles are less reliable than the rest.

VIII. AZIMUTHAL VARIATIONS

Having established an apparently self-consistent interpretation for the data from the azimuth range 290-330, it is natural to attempt the same process for data from other azimuths. It is at this point that the differences between the observations at different azimuths become most apparent.

Fairly complete information as a function of distance is available for events in the azimuth range 130-170 (Figures 11 and 12). In order to make a direct comparison with the 290-330 data, a visual fit to the data in Figures 11 and 12 is shown, together with model A (see previous section) and the Jeffreys-Bullen curve, in Figure 48. The differences between the two sets of data are extreme. This may be a common feature of array measurements; certainly similar differences were observed at the Warramunga array by Wright (1971), as is shown in Figure 49.

There are three possible ways in which these differences may occur; they may be due to crustal effects at the array, or to lateral variations in mantle structure, or to effects in the vicinity of the source (or, most likely, to some combination of all three). These possibilities are discussed separately below.

(i) Effects of Crustal Structure.

Crustal structure at the array must be a major contributor to the differences between the data from these two azimuth ranges. However, the separation of this contribution from the other two possibilities is not easy.

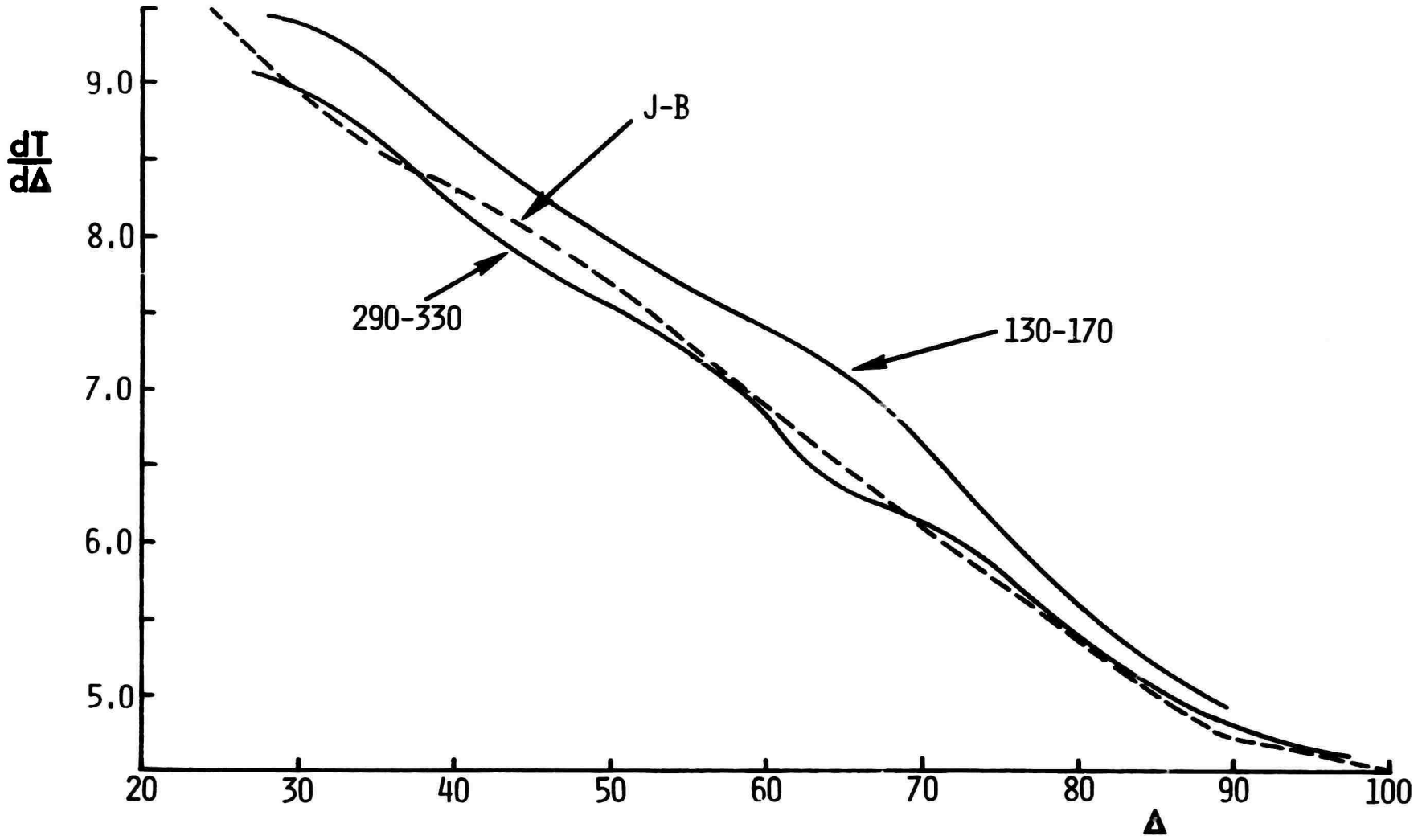

Fig. 48: Comparison of the data in the azimuth ranges 130-170 and 290-330; the Jeffreys-Bullen curve is also shown.

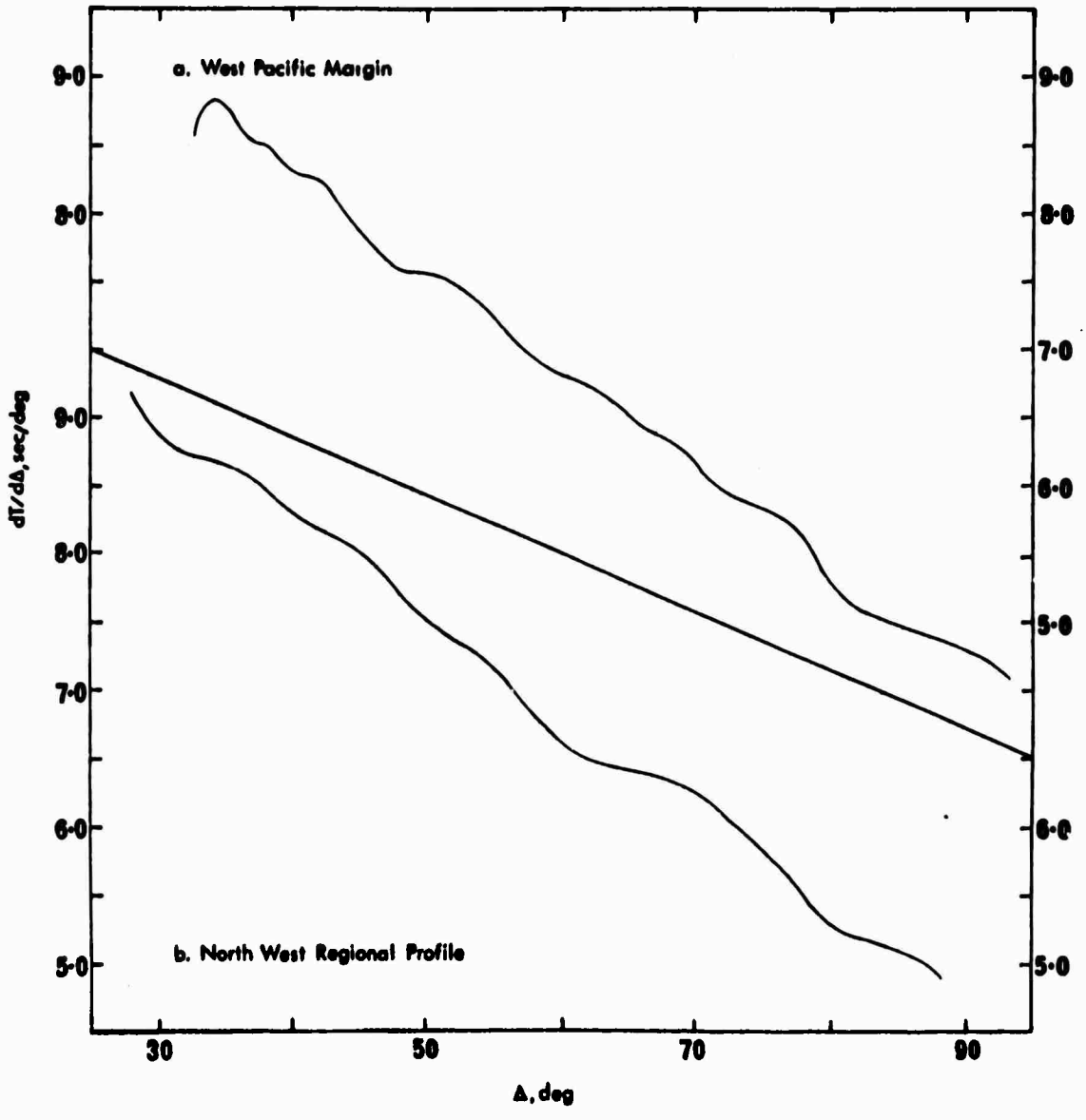

Fig. 49: Comparison of the data observed in two directions from the Warramunga array (after Wright, 1971).

If the paths from 130-170 traversed a simple dipping structure in the vicinity of the array, the $dT/d\Delta$ curve would be displaced parallel to the $dT/d\Delta$ axis. It is interesting to note that the curves from the two azimuth ranges are quite parallel in the distance range 30-55°, with the 130-170° data displaced upward by 0.5 seconds/degree. This is a substantial offset, and indicates a comparatively steeping dipping interface with considerable velocity contrast (Niazi, 1966).

The parallelism disappears at distances greater than about 55°, and it becomes much more difficult (though presumably not impossible) to relate the differences to a specific crustal model.

(ii) Lateral Variations in Mantle Structure.

The problem is compounded when these curves are studied in detail. There are a number of anomalous regions in the 290-330° curve that appear to be due to inhomogeneities in the mantle (Toksöz et al., 1967). None of these, including the feature shown in Figure 47, are apparent in the 130-170° data. This is supported by the $d^2T/d\Delta^2$ observations given in section 4 of this report. On the other hand, there is a variety of evidence to suggest that the interpretation of the 290-330° data is reasonable (see preceding section). We are therefore reluctantly led to the conclusion that the seismic paths from the South American earthquakes traverse a highly anomalous section of the mantle (Chinnery, 1967).

The degree of anomaly implied by these data is very large. The flattened portion of the 290-330° $dT/d\Delta$ curve at about 70° suggests the presence of a phase transition at a depth of about 2000 km in the mantle (Chinnery, 1969b). The continuity of the 130-170° data in this region appears to preclude the presence of such a feature anywhere in the depth range 1500-2500 km. On the other hand, the data from the vicinity of Easter Island (azimuth range 170-200°, Figure 14) do appear to indicate the presence of this feature.

It is not clear whether lateral variations in deep mantle structure of this magnitude are permissible. Certain types of convective flow in the mantle might lead to variations like this, but the present data have sufficient ambiguity that they cannot prove the existence of such features. It is even possible that the presence of the phase transitions is obscured in the 130-170° data by a complex array structure, though this seems unlikely.

One is led to the following conclusions. If the interpretation of the 290-330° data is valid, then seismic rays from this direction see a very simple structure at the array (on the average). Then, the 130-170° data imply either an enormously complicated crustal structure at the array for paths from this azimuth, or major lateral variations in mantle velocity structure. Neither of the possibilities are very desirable. The only alternative is that the crustal structure at the array is so complex that a "noise" is added to the observations at all

azimuths. In this case it is surprising that the interpretation of the 290-330° data agrees so well with other studies.

(iii) Source Structure.

The possibility of contamination of $dT/d\Delta$ data by structure close to the source has received little attention in the past. This is not surprising, since the angular separation of the rays that will ultimately arrive at the extremes of the array is very small at the source (much less than 1° for any mantle structure). Only an extraordinary structure could introduce a significant time difference into two rays so close together. However, there is at least one instance in the present data where this appears to have occurred.

Figure 50 shows an enlarged view of the scattered data at distances of 80-90°, in the azimuth range 290-330° (Figure 6). The data have been studied carefully, and all doubtful information removed. At about 80° from the array, the distribution of earthquakes bifurcates at the well-known junction just south of Japan. The data marked by solid circles and triangles are from events in Southern Honshu, Kyushu, and the Ryukyu Islands. Those marked by open circles and triangles are from events in the Bonin and Mariana Islands. The $dT/d\Delta$ values from these two regions, at the same distance, differ by as much as 0.3 seconds/degree. Since the azimuths concerned are so similar, it is unlikely that this could be produced by array structure, and this is substantiated by the agreement between the sets of data at distances less than 80° and greater than 90°.

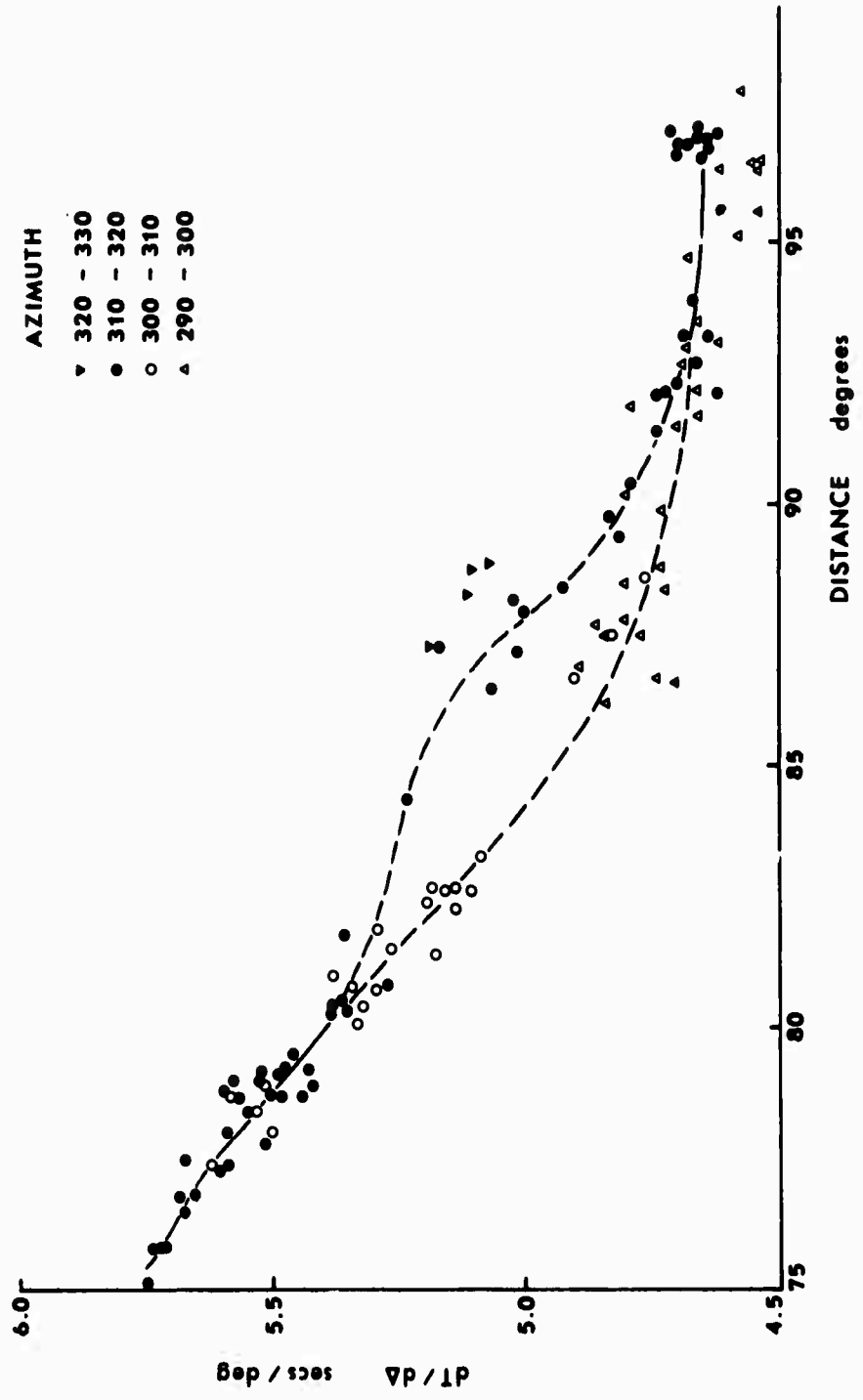

Fig. 50: Enlargement of a portion of figure 6.

At first sight, it is likely that this difference is the result of source structure. The azimuth to the array from events in the Ryukyu Islands is parallel to the oceanic trench. However, the azimuth to the array lies at a large angle to the island arc marked by the Bonin and Mariana Islands. However, on closer study, it is not easy to account for the observed differences in terms of normal island arc structures, for the dip of the Benioff zone is away from the direction toward the array. This means that the difference must arise either in the lithosphere (all the events are shallow, focal depths less than 100 km), or in the upper mantle on the ocean side of the downgoing slab. Since focal depth appears to have no significant influence on the measured value of $dT/d\Delta$, it is not clear that the former possibility is reasonable. However, if mantle structure is the cause, large lateral variations in velocity are implied. Until more is known about the structure of the mantle in the vicinity of a downgoing slab, it does not seem possible to produce a consistent interpretation of these data.

It appears, then, that array structure, lateral variations in mantle structure, and source structure, may each at times contribute significantly to contamination of $dT/d\Delta$ measurements. There are severe problems in attempting to separate out anyone of the three for individual study.

CONCLUDING REMARKS

The data set that has resulted from this study consists of the following:

(i) P-wave arrival time information at the 9 subarrays described for the more than 3000 events studied. These are punched on one card for each event, and included are an event code, and the USCGS latitude, longitude and depth of the event.

(ii) A one page computer print-out, as shown in Figure 2b, for each event.

The following programs have been written in Fortran IV for the IBM 360 computer:

(i) EVENTS: a versatile program for the analysis of the travel time data, giving the output shown in Figure 2b.

(ii) TIMDIS: a program that will accept any velocity-depth model, interpolate between data points to improve continuity, and then calculate, for a given value of $dT/d\Delta$, a variety of travel time information. This includes travel time, distance, depth of lowest point of ray path, residual from the Jeffreys-Bullen travel time table, the second derivative of the travel time curve, PcP times, etc.

(iii) WIEHER: a program for the inversion of $dT/d\Delta$ data to obtain a velocity-depth model, using the Wiechert-Herglotz method.

The graphs shown in this report are only a small fraction of those that could be drawn using the existing information.

REFERENCES

Carpenter, E. W., P. D. Marshall and A. Douglas, The amplitude-distance curve for short period teleseismic P-waves, Geophys. J., v. 13, p. 61-70, 1967.

Chiburis, E. F., LASA travel-time anomalies for various epicentral regions, Seismic Data Laboratory Report No. 159, Teledyne Inc., 1966.

Chinnery, M. A., Evidence for lateral variations in the lower mantle (abstract), Trans. Am. Geophys. Union, v. 48, p. 194, 1967.

_____, Measurement of the first and second derivatives of the travel-time curve using LASA (abstract), Geol. Soc. Am., Special Paper 101, p. 294, 1968.

_____, Direct measurement of the second derivative of the travel-time curve (abstract), Geol. Soc. Am., Special Paper 115, p. 315, 1968.

_____, Velocity anomalies in the lower mantle, Phys. Earth & Plan. Int., v. 2, p. 1-10, 1969.

_____, The velocity anomaly at 2000 km depth (abstract), Trans. Am. Geophys. Union, v. 50, p. 244, 1969.

_____, and M. N. Toksöz, P-wave velocites in the mantle below 700 km, Bull. Seism. Soc. Am., v. 57, p. 199-226, 1967.

Corbishley, D. J., Multiple array measurements of the P-wave travel-time derivative, Geophys. J., v. 19, p. 1-14, 1970.

Greenfield, R. J., and R. M. Sheppard, The Moho depth variations under the LASA and their effect on dT/d measurements, Bull. Seism. Soc. Am., v. 59, p. 409-420, 1969.

Iyer, H. M., and J. H. Healy, Teleseismic residuals at the LASA-USGS extended array and their interpretation in terms of crust and upper mantle structure, manuscript in preparation, 1971.

Johnson, L. R., Array measurements of P velocities in the lower mantle, Bull. Seism. Soc. Am., v. 59, p. 973-1008, 1969.

Lincoln Laboratories, Travel-Time Anomalies at LASA, Report No. LL-6, 1967.

Niazi, M., Corrections to apparent azimuths and travel-time gradients for a dipping Mohorovicic discontinuity, Bull. Seism. Soc. Am., v. 56, p. 491-509, 1966.

Toksöz, M. N., and M. A. Chinnery, Seismic travel-times from LONGSHOT and structure of the mantle (abstract), Trans. Am. Geophys. Union, v. 47, p. 164, 1966.

_____, and D. L. Anderson, Inhomogeneities in the earth's mantle, Geophys. J., v. 13, p. 31-59, 1967.

Wright, C., Evidence for a low velocity layer for P-waves at a depth close to 800 km, Earth Plan. Sci. Letters, v. 5, p. 35-40, 1968.

_____, P-wave investigations of the Earth's structure using the Warramunga seismic array, Ph.D. thesis, Australian National University, 1970.

Department of Geological Sciences

Brown University

Providence, Rhode Island

Final Technical Report

August, 1971

Project: Seismology and Acoustic Gravity Waves

Period Ending: 31 July 1971

Contract No: F44620-68-C-0082

Amendment/Modification No: P002

ARPA Order No: 292-68, Amendment No. 49

Program Code No: 8F10

Contractor: Brown University

Data of Contract: 1 August 1968

Amount of Contract: $123,108

Project Scientist: Michael A. Chinnery
401/863-3338

FINAL REPORT

Contract F44620-68-C-0082

The results of research performed under this contract fall into the following categories:

1. Task A: Investigations of P-wave Arrivals at LASA.

This research is discussed fully in the attached technical report.

2. Task B: Research in Acoustic-Gravity Waves.

This research was carried out by Professor David G. Harkrider (now at California Institute of Technology). A final technical report of this research has been submitted separately.

3. Research During the Period 8/1/70 to 7/31/71.

A no-cost extension of the contract was granted for the period 8/1/70 to 7/31/71, under Amendment/Modification No: P002. Research carried out during this period is described below. Much of this research is still in progress.

Research Under Amendment/Modification No. P002

This research has been concentrated on "Continuing Research Objective #4" (see original proposal, page 9), which is concerned with the residual displacements that accompany earthquake sources. Portions of this research are described in three technical papers (one in press, and two in the late stages of preparation). Abstracts of these papers are given below:

1. On the Correlation between Earthquake Occurrence and Disturbances in the Path of the Rotation Pole, by M. A. Chinnery and F. J. Wells. (Given orally at the International Astronomical Union Symposium #48 on Rotation of the Earth, Morioka, Japan, May, 1971; paper will appear in the proceedings of the symposium.)

   The hypothesis that earthquakes may be the principal excitation of the Chandler motion of the rotation pole is examined in the light of recent theoretical and observational developments. There is some doubt about the amount of excitation by a large earthquake necessary to maintain the Chandler Wobble, but it appears to be about 10 feet. Theoretical calculations for the Alaskan Earthquake (M = 8½) give available excitations in the range 1-5 feet, but there are considerable uncertainties in these calculations. Earthquakes may be able to provide all of the required excitation, or only a small portion (10% or less). The problem is confused by observational studies, which show differences between

various sets of data on polar motion which seem to be larger than the expected error in each set. The earthquake hypothesis, though reasonable, is still very much open to debate.

2. The Inertia Changes due to Faulting in a Homogeneous Sphere, by M. A. Chinnery and J. R. Rice (manuscript, in late stages of preparation).

A very simple and elegant theory for the changes in the inertia tensor due to slip over an arbitrary surface inside a homogeneous sphere is presented. Full expressions are given for the case of a point slip source, for the inertia changes ΔI_{13}, ΔI_{23} and ΔI_{33}. These results are compared with those of Ben-Menahem and co-workers, and Dahlen.

3. Two-Dimensional Faulting in a Layered Half-space, by M. A. Chinnery and D. B. Jovanovich. (Presented orally at the April, 1971 meetings of the American Geophysical Union, Washington, D. C.; manuscript in late stages of preparation).

The method of images is used to evaluate the displacement field due to a very long (2-dimensional) fault in two layers over a half space, with arbitrary rigidities. The model is used to investigate the effect on earthquake displacements of the lithosphere-asthenosphere boundary, the low velocity layer, and possible thin soft layers in the upper mantle. Each of these produce an amplification of the surface displacements over a uniform half-space

model. It is shown that thin layers of soft material may effectively decouple earthquake displacements from the earth's interior.

Continuing Research

Continuing research, which will be reported later, and which will acknowledge the support received under this contract, is described below.

Considerations such as those contained in reference #3 above have strengthened our interest in the far displacement fields of earthquakes. It is likely that these fields may contain significant information about source mechanism and earth structure, including some information not readily available from seismic wave studies.

It is impossible, at present, to detect these fields directly. Strain step observations permit an indirect method of detection, but relatively few strain meters are available, and the observations of strain steps are contaminated to an unknown extent by local structure and instrumental effects.

Astronomical observations of latitude variation are one possible way to detect the total mass redistribution associated with these displacement fields. In particular, it has been suggested that

(i) The total displacement field of a large earthquake may be sufficient to cause a reasonable change in the moments of inertia of the earth, and so excite the Chandler Wobble.

(ii) This excitation may precede the occurrence of the earthquake by several days.

(iii) A natural corollary to these is that information about large-scale motions in the earth (apart from earthquakes) may be obtained from a detailed study of the path of the rotation pole.

We have therefore been led to examine, in some detail, the astronomical observations of the path of the rotation pole. It turns out that these observations are extremely complex, and are probably much less reliable than has been reported in the literature.

The most serious problem appears to be the separation of the free Eulerian motion of the earth (14 month period) from a variety of effects with a 12 month period. The latter include the forced motion of the earth due to atmospheric motions, together with a series of local effects (local meteorology, star catalogue errors, operator changes, etc.) that each contribute substantially (and with variable phase) to the 12 month component. The separation of these two terms is essential to any study of the excitation of the free motion by earthquakes. However, examination of the published techniques used to carry out the separation has shown that they are quite inadequate. This arises partly because of the small separation between the two spectral peaks, and partly because of the variability of amplitude and phase of the 12 month component.

Present investigations are concentrating on the statistical characteristics of these data, and the extent to which separation

is possible. This in turn will lead to a more complete understanding of the validity of the hypotheses mentioned above. It is not expected that definitive answers to these questions can be obtained from the presently available data. However, within a few years it is expected that satellite data will become available that will permit much more accurate (by an order of magnitude) determinations of pole position. This study is expected to lay the groundwork for the analysis of this new data.